energies

MDPI

Review

Renewable Energy Potential and CO_2 Performance of Main Biomasses Used in Brazil

Elem Patricia Rocha Alves [1], Orlando Salcedo-Puerto [2], Jesús Nuncira [2], Samuel Emebu [3] and Clara Mendoza-Martinez [2,*]

[1] Department of Science and Technology, Federal University of Jequitinhonha and Mucuri Valleys (UFVJM), Janaúba 39440-000, MG, Brazil; elemprocha@gmail.com
[2] Department of Energy Technology, School of Energy Systems, Lappeenranta-Lahti University of Technology (LUT), 53850 Lappeenranta, Finland; orlando.salcedo.puerto@lut.fi (O.S.-P.); jesus.nuncira@lut.fi (J.N.)
[3] Department of Automatic Control and Informatics, Faculty of Applied Informatics, Tomas Bata University in Zlín, 760 05 Zlín, Czech Republic; emebu@utb.cz
* Correspondence: clara.mendoza.martinez@gmail.com

Abstract: This review investigates the effects of the Brazilian agriculture production and forestry sector on carbon dioxide (CO_2) emissions. Residual biomasses produced mainly in the agro-industrial and forestry sector as well as fast-growing plants were studied. Possibilities to minimize source-related emissions by sequestering part of carbon in soil and by producing biomass as a substitute for fossil fuel were extensively investigated. The lack of consistency among literature reports on residual biomass makes it difficult to compare CO_2 emission reductions between studies and sectors. Data on chemical composition, heating value, proximate and ultimate analysis of the biomasses were collected. Then, the carbon sequestration potential of the biomasses as well as their usability in renewable energy practices were studied. Over 779.6 million tons of agricultural residues were generated in Brazil between 2021 and 2022. This implies a 12.1 million PJ energy potential, while 4.95 million tons of forestry residues was generated in 2019. An estimated carbon content of 276 Tg from these residues could lead to the production of approximately 1014.2 Tg of CO_2. Brazilian biomasses, with a particular focus on agro-forest waste, can contribute to the development of sustainable alternative energy sources. Moreover, agro-waste can provide carbon credits for sustainable Brazilian agricultural development.

Keywords: biomass; renewable energy; carbon dioxide; thermochemical conversion; biofuels

Citation: Alves, E.P.R.; Salcedo-Puerto, O.; Nuncira, J.; Emebu, S.; Mendoza-Martinez, C. Renewable Energy Potential and CO_2 Performance of Main Biomasses Used in Brazil. *Energies* **2023**, *16*, 3959. https://doi.org/10.3390/en16093959

Academic Editor: Diego Luna

Received: 27 March 2023
Revised: 25 April 2023
Accepted: 2 May 2023
Published: 8 May 2023

1. Introduction

The utilization of fossil energy sources releases a large amount of carbon dioxide (CO_2) and other greenhouse gases (GHG) into the atmosphere, thus causing their excessive accumulation and intensifying global warming. From the CO_2 Emissions in 2022 report, the total energy-related greenhouse gas emissions increased to an all-time high of 41.3 Gt CO_2-eq in 2022, of which about 89% were related of CO_2 emissions from energy combustion and industrial processes [1]. To reduce GHG emissions, stop global warming and meet the energy requirements of modern civilizations, fossil fuels need to be replaced by renewable energy alternatives. Biomass fuels and chemicals derived from a wide variety of organic feedstock materials are expected to play a strategic role in the transformation of energy, industry and transport systems [2–4]. In this sense, the International Panel on Climate Change (IPCC) identified that bioenergy has significant potential to mitigate GHG emissions, providing sustainable resources and efficient energy systems [5]. In addition to climate change concerns, diverse demands on energy systems such as supply security, reduced reliance on imported fuels, affordable price, jobs creation and stimulation of local economy can also be addressed by the bioenergy sector [5].

Brazil is one of the global leaders in terms of energy generation from renewable sources such as biomass and hydropower. In April 2023, Brazil had more than 210,700 MW of installed power generation capacity, with around 85% coming from biomass (8.65%), hydro (57.31%), solar (4.38) and wind (13.19%) [6]. The Brazilian biomass energy potential was estimated by the Global Energy Network Institute (GENI) to be between 250 and 500 EJ. However, a conservative bioenergy potential of 11.69–13.93 PJ was also reported, based on the typical productivity of 20 to 80 tons of agricultural culture per hectare. Brazil is one of the countries with the largest GHG global emissions. The principal emissions are concentrated in agriculture, forestry and other forms of land use [7,8]. Brazil was the leading deforestation country in 2021, accounting for 41% of all primary forest loss [9]. According to data from MapBiomas, in less than five decades, the area used for agriculture grew from 1.8 million to 2.6 million square kilometers, corresponding to 30.97% of the national territory in 2020 [10]. In 2019, Brazil reported total emissions of about 411 Mt CO_2-eq, which was a visible CO_2 emission reduction from 2014 [1]. Nevertheless, Brazilian economic and political crises are delaying the progress on climate and energy policies.

2. Biomass Potential in Brazil

Lignocellulosic biomass is a complex fuel consisting of fibrous plant material containing extractives, cellulose, hemicelluloses and lignin polymers [11]. Any biomass used should be harvested without threatening habitats, food security and soil conservation. Several researchers worldwide are investigating the concept of biorefining to convert lignocellulosic biomass into biofuels and other potential value-added products such as organic acids, polyhydroxyalkanoates, biochemicals, bioplastics, among others, at competitive prices [12]. In Brazil, biorefinery allows diversification and decentralization, creating energy self-sufficiency in some industrial activities and micro-regions in the country. The effective utilization of biomass residues from industrial or agricultural processes reduces the amount of waste sent to landfills, increases the profitability of planting areas and avoids the competition with food crops [13,14].

The agro-forest industry is one of the major sectors of the Brazilian economy. In 2020, the agriculture sector shared that the Brazilian gross domestic product (GDP) was about 6% [15], while the forestry sector was represented by 1.2% GDP. The forestry industry is responsible for creating employment for 1.3 million individuals and providing work opportunities for 3.75 million people in various parts of Brazil [16]. About 9 million hectares of planted trees, with another 5.9 million hectares set aside for conservation, are available in over 1000 municipalities, of which *Eucalyptus* and *Pinus* represents the majority with 6.97 million and 1.64 million hectares, respectively [16]. The additional hectares are planted with other species such as acacia, teak, rubber, acacia and paricá. These areas have the combined potential to store 4.48 billion tons of CO_2-eq [16].

The Brazilian pulp and paper industry (PPI), which is a significant global producer, relies entirely on cultivated forests. According to the Brazilian PPI association (BRACELPA), the major focus of Brazil's timber production lies in the pulp and paper industry. Other related sectors include the manufacturing of wood panels, plywood, firewood, sawdust and coal-fired steel. A considerable amount of waste is usually produced during the different operational stages, from forest harvesting to the final product. In 2019, forest industry companies in Brazil produced around 52 million tons of solid waste, 71% of which came from forestry activities and 29% from further processing [17]. Due to the lack of well-developed markets, clear environmental policies and sustainable management information, these residues are wasted. This situation is primarily observed in Brazil's Amazon and Central areas, where high transportation costs and uncompetitive pricing prevent the bioeconomy from developing.

The latest survey of 2023 of the Brazilian Institute of Geography and Statistics reported an agricultural productive activity of 3.3%, 8.9%, 37.7%, 17.5% and 32.5% in the north, northeast, southeast, south and mid-west regions in Brazil, respectively [18]. An average growth of 6% was observed compared to the previous production census in 2022 [19]. In

Brazil, the main crops are sugarcane, corn, soybeans, rice, wheat and coffee, in addition to banana, coconut and orange fruits [20]. A large amount of residues are produced from them, mainly in the crop fields, as a result of harvesting activities. Brazil is the second largest generator of agricultural residues in the world after China, with annual agricultural waste of approximately 600 million tons [21]. Some of these residues are commonly used for energy production, soil applications, animal feed, medicine and fertilizers. However, Brazil does not use more than 200 million tons of agro-industrial residues and, currently, a significant part is burned in the crop fields.

The data related to crop production were obtained by consulting the agricultural statistics, the corresponding governing authorities such as the Ministry of Agriculture, the research institutes and the available literature. The gross annual potential of the main Brazilian agro-forestry residual biomasses was determined using the residue-to-product ratio (RPR) based on the model described in Equation (1) [22]:

$$CR_i = RPR_i \cdot PrC_i \quad (1)$$

where CR_i is the amount of agro-forestry residual biomass of $_i$th crop in ton, RPR_i the RPR of the $_i$th crop on dry mass basis and PrC_i is the amount of crop production in ton. Energy potential of crop residues was also determined by using Equation (2):

$$EP_i = \sum_{i=1}^{n} (P_i \cdot RPR_i \cdot LHV_i) \quad (2)$$

where EP_i is the gross annual energy potential of agricultural residues, P_i is the annual production of crop and LHV_i is the lower heating value of a given crop. For Eucalyptus and Pinus, the energy potential was calculated by multiplying the productivity by LHV_i. From it, over 784 million tons of agro-forestry residues were generated in the latest harvesting reports as shown in Table 1.

Table 1. Estimated Brazilian production of main biomasses and its residues.

Agro-Industrial Biomass								
Raw Material	**Planted Areas (Million ha)**	**Production 2021/2022 Harvest (Million Tons)**	**Type of Residue**	**RPR [%] [a] [19–21]**	**Amount of Residue (Million Tons)**	**LHV [MJ/kg]**	**EP (PJ/yr) [b]**	**Competitive Uses**
Soybean	40.95 [23]	124.05 [23]	Stalk and straw Husk	20 8	248.10 9.90	17.15 14.14	4254.92 140.37	– Human and animal feed [24]
Rice	1.62 [23]	10.80 [23]	Straw Husk	154 26	16.63 2.81	17.14 16.43	285.07 46.12	– Drying, power generation at rice mills, chicken bedding production. – Usually burned in harvested field [25,26]
Wheat	2.92 [23]	9.03 [23]	Straw	155	14.00	15.10	211.35	– Animal feeding, erosion control, artesanal utilization [27]
Corn	21.66 [23]	115.66 [23]	Leaves Corn cob	21 15	24.29 17.35	22.43 19.32	544.79 355.18	– Left in the field [26]
Coffee	1.84 [28]	3.21 [28]	Husk	33	1.06	18.20	19.25	– Left in the field and usually burned – Animal feeding [7]
Coconut	0.19 [29]	2.45 [29]	Husk Shell	70 10	1.71 0.24	19.91 15.94	34.05 3.83	– Agricultural fertilizer, composites, activated carbon
Sugarcane	8.21 [30]	596.01 [30]	Straw Bagasse	34 30	202.64 178.80	18.07 18.40	3661.77 3289.98	– Fired in steam boilers tfor energy production [25,26]
Banana	0.47 [31]	7.11 [31]	Leaves Stem	48 300	3.41 21.33	16.13 15.73	55.05 335.52	– Animal feed [32]
Orange	16.47 [31]	0.63 [31]	Bagasse	50	0.32	15.82	4.98	– Aromatizing and animal feeding [33]

Table 1. *Cont.*

Forestry Biomass								
	Planted Areas in 2019 (Million ha) [12]	**Productivity (m^3/ha yr) [12]**	**Type of Residue**	**RPR [%] [a] [34,35]**	**Amount of Residue (Million tons) [c]**	**LHV [MJ/kg]**	**EP (PJ/yr)**	**Competitive Uses**
Eucalyptus [d]	6.97	35.30	Bark	0.08	0.56	18.26	10.23	– Energetic valorization
			Branches	0.03	0.21	18.05	3.79	
			Leaves	0.02	0.14	16.05	2.25	
			Tips [e]	0.13	0.91	-	-	
Pinus [f]	1.64	31.30	Bark	0.10	0.69	16.81	11.60	– Energetic valorization
			Branches	0.30	2.09	18.08	37.79	
			Leaves	0.05	0.35	17.81	6.23	

[a] RPR = RT [-]·RA [%]; [b] $EP_i = \sum_{i=1}^{n}(P_i \cdot RPR_i \cdot LHV_i)$; [c] 1337 tree per hectare at cutting age; [d] *Eucalyptus urograndis*, age of 79 months; [e] Tips: wood with diameter lower than 3 cm; [f] *Pinus tadea*, age of 27 years. RPR—Residue to product ratio; RT—Ratio between total residues (dry basis) and mass of the harvest field moisture; RA—Ratio between waste available (dry basis) and the total mass of waste in [%]; EP—Energy potential; P—Annual production; n—Total number of residue categories; LHV—Low heating value.

In Brazil, both in terms of their production value and agrobusiness trade balance, rice and wheat are important crops for the agricultural landscape and livelihood. Rice and wheat are the most popular food crops in Asia, Latin America and Africa. Considering that 95% of rice is produced in developing countries, it is suggested that for each ton of rice grain produced, 1.5 tons of rice straw are generated in these countries [34]. Around 770 million tons of rice straw were produced in 2021/2022, whereas the global rice production was 513 million tons [35]. This equates to roughly 3666 MWh/year of energy if the rice straw is used as a fuel source. Currently, straw residues are not used efficiently from an energy perspective. Soybean (SB) is also an important commodity for the Brazilian economy. Currently, Brazil is the second largest producer of SB in the world (behind the United States (USA)), produced mainly for oil extraction. SB meal or cake are the main residues generated, i.e., solid waste traditionally consumed as a filler and protein diet in animal feed. Soybean is a rich source of nitrogen and phosphorus; as such, disposal of its waste without following the regulations deposits these elements into the environment, which could damage soil surface and water bodies, leading to eutrophication [36]. The interests in exploring SB waste potential for numerous applications are increasing due to its abundance. Among the various applications of SB waste, it is a worthy adsorbent for heavy metals removal, agent for soil amendment, precursor for bio-oil production and electrode material for supercapacitors.

Corn is also one of the major crops from a food production perspective. Between 2022 and 2023, the total annual production worldwide was 1151 million tons [37]. USA, China and Brazil are the major corn producers with a production of 349 million tons, 277 million tons and 125 million tons, respectively [37]. Approximately 50% of the corn plant is corn stover, which is an excellent substrate for the biomaterials production due to lignocellulosic composition. Cellulose fibers derived from the stalks and husks of corn plants were used in industrial applications such as textiles [38]. Corn and sugarcane are the primary sources of first-generation ethanol. However, the significant water consumption in the production and the use of food resources for fuel generation resulted in higher prices [39]. Corn stover can be utilized for second-generation biofuel, but pretreatment is required. This pretreatment may pose a challenge for cost-effective second-generation bioethanol production. Different studies summarized by Zao et al. [40] showed efficient pretreatment methods for bioethanol production from corn stover. Nevertheless, the production is in its early stages and more research focus on technology and composition, e.g., glucan/glucose and xylan/xylose, is needed.

Brazil was the largest producer in 2020 of sugar cane worldwide with 757 million tons, followed by India (377 million tons) and China (110 million tons) [19,41]. The National Fuel Alcohol Program (Proalcool) was the strategic policy of the Brazilian government launched in 1975 that made Brazil the world leader in the production of sugarcane ethanol—the first large scale alternative for substitution of fossil fuel in the transport sector [42]. The high

production of effluents and residues from the sugar cane industry are typically used as an energy source through direct combustion in boiler furnaces. However, several studies focused on transforming the residual material into fermentable sugar for second generation ethanol production. According to the Brazilian National Agency for Petroleum, Natural Gas and Biofuels (ANP), in 2021, about 29 million m^3 of anhydrous and hydrate ethanol were produced in the country [43]. Brazil also tops the list of coffee producers worldwide with 3.7 million tons in 2022/2023. In coffee crops, a large amount of residues are obtained from the cherries and shrub. Recent studies proved the high potential of coffee residues for energy generation through different conversion processes [7,44].

More than 675 million tons of fruits are produced annually worldwide. Brazil is a significant contributor with an output of 43.6 million tons annually [45]. The most abundant fruits produced in Brazil are oranges (17.7 million tons in 2020), bananas (6.6 million tons in 2020) and coconuts (2.4 million tons in 2020) [19], which are essential to the country's economy and produce a vast amount of waste. Brazilian southeast region alone is responsible for over 80% of the country's orange production and the northeast region is the largest producer of coconuts and bananas [19]. According to The Brazilian Agricultural Research Corporation (EMBRAPA), almost half of the harvested bananas do not meet the consumption standards and are unused. Although most bananas are consumed fresh, industrialization accounts for 2.5–3.0% of national production [46]. Banana residues are primarily used in Brazil as a natural fertilizer. Moreover, banana residues also demonstrated high potential of producing biopolymers [47], hydrogen, methane [48], bioethanol [49] and as a material for heavy metals removal from wastewater sources [50]. Similarly, orange and coconut residues are highly used in the country commonly for animal feed or as a natural fertilizer. Several researchers demonstrated the potential of coconut and orange residues to produce essential oils [51,52], pectin [53] and biofuels [54,55].

3. Biomass Composition and Properties

Over time, the practice of genetically modifying crops became more common, which may cause changes in its composition that are not just related to their use as food, but also for other applications [56]. Conducting a thorough literature review and continuously updating agro-forestry data is highly important to evaluate the potential of the biomass for value-added purposes. In this study, an extended review of agro-forest biomasses was conducted to extend and improve knowledge on alternative residues utilization.

The major components of biomass are water, organic and inorganic components. Biomass from various types of plants contain different proportions of cellulose, hemicellulose, lignin, extractives, sugars, starch and proteins. This leads to differences in quantities of biomass carbon (C), hydrogen (H), oxygen (O), nitrogen (N) and sulfur (S) content, which impacts its energy potential. The inorganic content of biomass is defined as the residual mass remaining after its combustion (ashes). Table 2 summarizes the proximate analysis (volatile matter, fixed carbon and ash content), ultimate analysis (C, H, O, N and S) and heating values of the selected biomasses.

Table 2. Heating value, proximate analysis and ultimate analysis of evaluated biomasses.

Resource	Residue	Proximate Analysis [wt%]				Ultimate Analysis [wt%]					LHVdaf	HHVdaf	Ref
		MC	VM	FC	AC	C	H	O	N	S	MJ/kg	MJ/kg	
Agro-Industrial Biomass													
Soybean	Straw	5.20	81.30	8.90	4.60	41.98	5.05	47.46	0.46	0.45	-	16.40	[57]
	Straw	7.98	70.03	13.78	8.21	41.34	4.23	45.26	0.85	0.11	-	-	[58]
	Straw	-	85.50	10.60	3.90	44.30	5.80	45.20	0.70	0.10	-	16.10	[59]
	Stalk	-	-	-	8.87	41.05	5.52	41.39	2.90	0.28	-	16.39	[60]
	Straw	7.60–10.90	-	-	2.6–5.9	-	-	-	-	-	15.92	-	[61]
	Straw	-	-	-	-	-	-	-	-	-	15.92	-	[62]
	Stalk	-	-	-	-	-	-	-	-	-	16.99	-	[63]
	Husk (gordana)	13.93	68.18	8.15	5.81	49.54	4.72	52.73	2.51	0.18	15.71	16.17	[64]
	Husk (sivka)	14.85	66.91	9.41	4.74	48.41	4.28	54.77	2.21	0.11	16.18	17.12	[64]
	Husk (slavonka)	16.25	66.24	10.08	4.00	49.33	5.14	53.42	2.11	0.14	15.34	16.46	[64]

Table 2. *Cont.*

Resource	Residue	Proximate Analysis [wt%]				Ultimate Analysis [wt%]					LHVdaf	HHVdaf	Ref
		MC	VM	FC	AC	C	H	O	N	S	MJ/kg	MJ/kg	
	Husk	6.80	82.20	6.80	94.00	-	-	-	-	-	-	-	[65]
	Husk	-	70.60	24.50	4.90	-	-	-	-	-	-	-	[66]
Rice	Straw	5.46	88.78	1.43	9.82	46.24	6.21	46.23	1.32	-	-	16.16	[67]
	Straw	4.91	71.82	8.07	4.91	46.11	6.83	46.03	1.03	-	-	16.14	[68]
	Straw	4.35	74.86	11.56	9.23	42.57	5.84	49.33	2.13	0.13	-	-	[69]
	Straw	8.08	69.99	13.40	8.79	39.61	5.83	43.80	1.21	-	14.21	-	[70]
	Straw	-	-	-	-	-	-	-	-	-	15.54	-	[63]
	Husk	7.73	64.20	15.50	12.57	38.62	5.67	41.38	0.48	-	15.39	-	[70]
	Husk	-	68.70	16.30	15.00	40.80	5.30	38.20	0.60	0.10	-	15.30	[59]
	Husk	-	70.70	15.40	13.90	40.10	-	39.70	-	-	-	16.79	[71]
	Husk	-	-	-	-	-	-	-	-	-	15.54	-	[63]
	Husk	-	-	-	-	-	-	-	-	-	12.80	-	[72]
Wheat	Straw	7.10	76.70	7.10	9.20	45.50	5.70	47.90	1.00	-	-	16.50	[73]
	Straw	6.46	77.03	19.47	3.50	44.00	5.76	48.92	0.94	0.38	-	17.52	[74]
	Straw	10.11	68.92	12.74	8.23	38.96	5.27	55.27	0.50	-	-	13.37	[75]
	Straw	12.81	83.08	10.29	6.63	38.34	5.47	55.59	0.60	0.37	-	16.68	[76]
	Stalk	10–20	-	-	2.6–9.6	-	-	-	-	-	17.20	-	[61]
	Stalk	-	-	-	-	-	-	-	-	-	17.15	-	[63]
	Husk	3.37	72.78	13.70	12.14	38.70	5.50	54.73	0.66	0.41	-	13.64	[77]
	Husk	13.31	69.53	13.20	3.96	52.84	6.10	15.12	2.55		-	22.91	[78]
	Husk	8.13	80.54	15.73	3.43	45.97	6.81	52.62	1.41	0.11	17.11	18.59	[79]
	Husk	7.00	71.40	19.30	2.30	42.00	6.30	47.40	1.90	0.10		17.80	[80]
Corn	Straw	26.00	67.60	17.80	14.60	41.90	5.76	35.75	-	-	-	16.30	[81]
	Straw	6.18	71.21	16.12	6.49	45.84	5.11	34.89	1.28	0.21	-	16.80	[82]
	Stalk	-	78.12	17.99	3.89	44.36	5.73	45.35	0.67	-	-	-	[83]
	Stalk	-	75.38	17.95	6.67	42.53	6.17	43.59	0.93	0.11		16.59	[84]
	Stalk	15–45	-	-	3.50–9.00	-	-	-	-	-	8–17.	-	[61]
	Stalk	-	-	-	-	-	-	-	-	-	13.70	-	[62]
	Cob	7.83	69.24	17.29	5.64	48.51	5.90	39.14	0.29	0.52	14.94	17.05	[85]
	Cob	9.60	71.60	17.20	1.60	44.40	6.50	48.80	0.30	0.00	-	16.80	[86]
	Cob	11.00	70.00	9.20	9.80	36.40	6.20	47.10	0.50	0.05	-	15.40	[87]
	Cob	-	83.10	13.78	3.12	43.40	6.55	48.88	0.65	0.49	-	-	[88]
Coffee	Husk	9.95	84.20	14.30	1.50	48.98	5.32	44.92	0.78	0.29	-	18.04	[44]
	Husk	9.06	77.09	19.36	3.55	46.41	6.33	44.51	2.66	0.09	-	18.50	[89]
	Husk	2.70	77.70	17.90	1.70	48.50	5.90	40.60	2.80	0.60	-	18.30	[90]
	Husk	8.33	78.44	18.93	5.63	44.41	5.78	49.80	-	-	-	18.26	[91]
Banana	Leaves	8.40	73.05	11.29	7.26	43.28	6.68	48.31	1.28	0.30	-	17.80	[92]
	Leaves	-	77.79	11.31	10.90	44.85	6.23	48.17	0.58	0.17	14.69	15.90	[93]
	Leaves	-	72.60	18.00	9.10	41.40	5.40	41.40	2.50	0.29	16.10	16.30	[94]
	Leaves	-	70.14	14.51	15.35	-	-	-	-	-	-	-	[95]
	Stem	10.20	80.60	6.90	12.50	33.60	7.30	36.90	22.1	0.20	10.8	12.40	[96]
	Stem	12.56	80.27	9.96	8.00	39.00	5.44	54.84	0.82	-	-	16.13	[97]
	Stem	-	-	-	-	38.44	5.03	43.10	1.24	0.09	-	-	[98]
	Stem	-	73.98	17.94	8.08	-	-	-	-	-	-	14.09	[99]
Orange	Bagasse	7.62	76.45	23.55	7.62	44.93	7.10	46.31	1.42	0.14	14.31	15.86	[100]
	Bagasse	9.23	73.20	20.60	6.20	46.40	5.54	40.15	1.17	0.01	17.03	18.16	[101]
	Bagasse	6.15	70.33	20.86	2.66	43.57	4.40	51.78	0.17	0.09	-	17.26	[102]
	Bagasse	1.50	74.10	23.60	2.30	42.70	6.40	47.60	1.00	-	-	19.40	[103]
	Bagasse	2.71	81.84	11.44	6.71	44.33	6.09	48.46	1.64	-	-	17.61	[104]
Coconut	Husk	8.50	61.50	33.11	5.39	49.59	5.30	36.87	0.38	0.01	18.22	19.31	[105]
	Husk	6.70	61.78	31.52	6.70	49.03	5.37	38.36	0.41	0.13	-	19.33	[106]
	Husk	9.96	72.60	15.21	2.23	48.95	5.40	43.10	0.40	-	-	-	[107]
	Husk	-	82.94	16.14	0.92	47.00	6.07	46.60	0.21	0.12	-	15.44	[77]
	Husk	-	73.38	22.95	4.66	-	-	-	-	-	-	16.75	[108]
	Shell	8.83	92.16	7.35	0.49	47.70	5.44	46.25	0.06	0.03	-	24.29	[109]
	Shell	5.67	73.89	19.55	8.89	48.35	6.21	45.25	0.18	0.01	-	17.17	[110]
	Shell	3.29	73.80	19.40	6.78	46.77	5.61	46.83	0.79	-	-	18.64	[111]
	Shell	15.98	72.90	19.40	0.80	46.60	7.10	41.80	0.32	-	-	14.10	[112]
	Shell	7.82	79.91	12.04	0.23	39.20	4.50	55.90	0.20	-	-	-	[107]
	Shell	-	-	-	-	49.50	6.10	40.10	0.80	0.06	-	18.90	[113]
Sugarcane	Straw	16.80	80.50	19.50	20.10	50.60	6.40	44.60	2.60	0.28	-	19.00	[114]
	Straw	9.54	-	-	-	45.69	5.80	48.38	0.13	-	-	17.38	[115]
	Straw	3.12	87.61	3.22	9.17	41.88	5.87	41.72	0.47	-	-	16.42	[116]
	Straw	8.30	71.10	14.60	6.00	42.60	5.29	43.40	0.51	0.14	-	-	[117]
	Bagasse	2.80	80.32	10.14	6.75	47.40	6.14	46.18	0.28	0.10	-	18.51	[118]
	Bagasse	-	79.01	16.09	4.90	32.50	5.01	61.55	0.38	0.56	-	16.53	[119]
	Bagasse	-	83.46	14.26	2.17	46.37	6.29	46.79	0.55	0.11	-	14.33	[120]
	Bagasse	-	-	-	-	42.52	5.92	50.38	1.18	-	-	-	[121]
	Bagasse	-	-	-	-	-	-	-	-	-	20.00	-	[63]

Table 2. *Cont.*

Resource	Residue	Proximate Analysis [wt%]				Ultimate Analysis [wt%]					LHVdaf	HHVdaf	Ref
		MC	VM	FC	AC	C	H	O	N	S	MJ/kg	MJ/kg	
Forestry Biomass													
	Leaves	48.40 (in nature)	80.10	16.60	3.20	54.70	6.00	34.70	1.20	0.20	-	21.10	[122]
	Bark	61.70 (in nature)	80.40	15.10	4.50	48.10	5.50	41.70	0.10	0.10	-	20.47	[122]
Eucalyptus	Wood	13.18	75.21	11.00	0.10	49.29	5.91	44.68	0.09	0.03	-	18.10	[123]
	Wood	7.60	87.95	11.59	0.46	46.13	5.90	47.83	0.14	-	-	20.25	[124]
	Wood	12.00	83.10	16.70	0.30	-	-	-	-	-	-	19.48	[125]
	Wood	12.00	85.49	14.16	0.34	-	-	-	-	-	15.50	19.32	[126]
	Wood	-	81.60	18.20	0.21	48.60	6.10	44.60	0.49	-	17.89	19.28	[126]
	Wood	-	87.00	12.80	0.30	52.30	5.90	41.40	0.00	0.10	-	19.10	[122]
	Wood	-	88.30	9.80	1.90	50.30	6.90	40.80	0.10	-	-	18.50	[59]
	Wood	-	82.40	16.43	1.17	52.80	6.10	40.50	0.50	0.09	-	20.80	[127]
Pinus	Wood	6.28	83.43	16.32	0.26	-	-	-	-	-	-	-	[128]
	Wood	-	87.40	11.00	1.55	-	-	-	-	-	-	-	[129]
	Wood	67.00 (in nature)	-	-	-	-	-	-	-	-	18.08	19.44	[130]

daf: dry ash free basis; MC: moisture content; VM: volatile matter; FC: fixed carbon; AC: ash content; LHV: lower heating value; HHV: higher heating value.

Moisture content is a significant concern in many processes where biomass is used as an energy source. If the biomass is too wet, it requires extra energy to evaporate the water before conventional technologies of biomass treatment conversion can be applied. This can increase the cost of energy generation and increased storage space for the fuel [131,132]. Some types of agro-forest biomass have high moisture content at harvest (40–70%) [133–135] but can be dried to a more suitable level for energy conversion. Most agro-industrial residues have a low enough moisture content for conversion (<11%), except for orange bagasse and banana residues which have higher moisture contents [97,136]. However, these materials should not be dismissed since they are waste and can still be used for energy. Sustainable alternatives to treat wet biomass are hydrothermal carbonization and hydrothermal liquefaction [132,137,138]. Moreover, the presence of water in biomass affects its vulnerability to microbial colonization, which leads to the consumption of its nutrients causing economic material losses. When the moisture content falls below the fiber saturation point, there is limited possibility for microbial breakdown, and it is entirely prevented at lower moisture levels [139].

Volatile matter (VM) comprises components of a solid fuel, apart from moisture, which are driven off as gases when temperature increases in the absence of an oxidative agent (typically 900 °C for 7 min). The organic material that remains following such treatment is referred to as fixed carbon. Understanding the VM help evaluate the practical aspect of combustion of the biomass and the potential for liquid and char generation in thermal process such as pyrolysis [123,129]. The highest values were found for most agro-industrial residues, sugarcane residues, wheat straw and forest biomass (74–94%). Volatile compounds are responsible for the initial ignition and flame propagation of the biomass material. Biomass with higher VM tent to ignite more easily and burn more rapidly.

The ultimate analysis showed high oxygen content (47–55%) in residues from corn, banana, rice, sugarcane and orange. High oxygen concentrations decrease the biomass heating value, which makes them not desirable for fuel application [44]. The highest values for carbon content were observed in the residues from soybean, coconut and wood-base (47–53%), indicating higher energy density per unit of biomass. N and S contents are an indication of the amount of undesirable emissions, i.e., N generates NOx when biomass is combusted and S generates SOx during gasification and may contaminate catalysts. For solid biofuels, problematic emissions can be expected for biomasses with S concentrations above 0.2% and N concentrations above 0.6% [140]. In this study, the highest N content was found for residues from coffee, banana, soybean and corn. For S content, relatively low values were found for most biomasses. Therefore, the elemental composition of biomasses may affect their thermal utilization. Management and emissions control measures, such flue gas cleaning technologies, are required.

The average lower heating value on dry ash free basis (LHVdaf) of the evaluated biomasses ranged from 14 MJ/kg to 19 MJ/kg. The highest values were reported for forest residues. LHV indicates the highest amount of energy possible to recover from a biomass source and is considered an important parameter for assessing and modeling energy potential in biomass conversion technologies [141].

The main organic components of biomass are cellulose, hemicelluloses, lignin and extractives in addition to pectin, sugars, proteins and starches. The content can vary significantly from one biomass to another. Table 3 summarized the structural chemical composition of the selected biomasses.

Table 3. Chemical composition (wt.% dry) of evaluated biomasses.

Resource	Residue	Extractive [wt.%]	Lignin [wt.%]	Cellulose [wt.%]	Hemicelluloses [wt.%]	Ref.
Agro-Industrial Residues						
Soybean	Straw	15.50	15.20	37.60	27.80	[59]
	Straw	-	21.80	35.30	16.90	[142]
	Straw	-	24.12	22.69	17.73	[143]
	Straw	-	21.60	34.10	16.10	[57]
	Stalks	-	19.80	34.50	24.80	[144]
	Husk	4.80	7.80	40.60	33.80	[145]
	Husk	-	2.10	32.90	3.10	[146]
	Husk	-	3.70	52.30	18.50	[147]
	Husk	-	2.10	5.10	19.40	[148]
Rice	Straw	1.62	25.79	42.32	19.50	[67]
	Straw	-	18.70	47.20	31.80	[149]
	Straw	-	8.3–9.9	19.6–36.2	19.0–50.4	[144]
	Straw	-	14–28	32–40	24.00	[150]
	Husk	-	21.10	38.57	21.30	[70]
	Husk	-	26.00	33.00	7.00	[142]
	Husk	-	22.00	40.00	21.00	[148]
Wheat	Husk	20.00	16.00	36.00	18.00	[151]
	Husk	2.40	16.40	30.50	28.90	[152]
	Husk	-	14.00	23.00	21.00	[153]
	Husk	-	16.00	39.00	30.00	[154]
	Straw	20.10	20.20	34.00	23.15	[150]
	Straw	-	16.00	30.00	26.00	[149]
	Straw	-	8.9–22.1	32.9–49.8	23.7–25.0	[144]
Corn	Straw	-	7.02	32.72	33.35	[155]
	Straw	-	6.87	24.58	25.97	[155]
	Stalks	-	7.0–7.3 (db)	35.0–39.0	16.8–42.0	[144]
	Stalks	-	17.18	49.22	25.57	[149]
	Husk	19.60	15.50	32.50	30.40	[150]
	Husk	-	14.30	31.00	34.00	[148]
	Cob	14.25	18.50	35.75	30.70	[150]
	Cob	-	9.40	27.71	38.78	[142]
	Cob	-	6.10	33.70	31.90	[144]
Coffee	Husk	38.00	24.30	31.50	43.80	[44]
	Husk	-	27.57	41.60	21.90	[91]
	Husk	20.53	24.15	47.29 (hollocellulose)		[89]
Banana	Leaves	7.32	15.00	43.34	34.34	[92]
	leaves	7.59	25.25	35.20	20.28	[95]
	stem	7.60	22.30	55.50	5.40	[156]
	stem	4.90	15.30	69.40	8.80	[157]
	Stem	-	6.08	27.79	30.08	[98]

Table 3. *Cont.*

Resource	Residue	Extractive [wt.%]	Lignin [wt.%]	Cellulose [wt.%]	Hemicelluloses [wt.%]	Ref.
Orange	Baggase	35.30	28.70	17.10	16.60	[158]
	Bagasse	21.96	29.04	40.33	8.66	[101]
	Bagasse	29.80	9.52	28.98	31.70	[102]
	Bagasse	-	8.50	12.40	7.50	[159]
Coconut	Husk	-	26.69	31.60	26.33	[160]
	husk	5.44	43.34	26.27	26.00	[106]
	Husk	-	46.36	21.26	17.33	[142]
	shell	4.20	29.70	29.58	23.80	[161]
	Shell	13.96	5.35	1.70	61.96	[109]
	Shell	2.71	33.15	30.47	25.42	[160]
Sugarcane	Straw	25.00	27.00	54.00	39.00	[114]
	Straw	15.31	18.21	33.13	26.25	[162]
	Straw	8.91	31.14	31.46	27.03	[115]
	Straw	4.30	19.60	37.20	30.60	[163]
	Straw	-	16.00	30.00	22.50	[164]
	Bagasse	12.70	19.20	36.90	26.30	[119]
	Bagasse	6.49	26.72	44.46	20.53	[121]
	Bagasse	4.80	19–25	35–45	25–32	[150]
	Bagasse	-	25.00	50.00	25.00	[142]
	Bagasse	-	20.30	41.60	25.10	[149]
	Bagasse	-	11.70	36.50	26.50	[164]
Forestry Biomass						
Eucalyptus	Wood	3.70	24.40	47.00	24.90	[165]
	Wood	1.81	23.24	42.83	43.42	[166]
	Wood	4.80	23.30	38.10	36.60	[167]
	Wood	-	14.58	48.54	28.36	[168]
	Wood	-	31.08	68.92 (hollocellulose)	-	[124]
Pinus	Wood	9.00	26.30	41.10	13.70	[59]
	Wood	3.06	31.56	37.20	22.88	[128]
	Wood	14.00	34.50	-	-	[169]
	Wood	3.20	28.00	45.50	23.10	[170]
	Wood	2.54	22.06	69.49 (hollocellulose)	-	[171]
	Wood	7.10	26.50	59.00	21.10	[172]
	Wood	-	36.10	37.80	26.10	[173]

db: dry basis. Holocellulose: Cellulose + Hemicellulose.

Cellulose content ranged from 15% (orange bagasse) to 45% (sugarcane residues), whereas hemicelluloses ranged from 10% (banana residues) to 60% (coconut shell). Coconut husk reported the maximum lignin content of 45% and the lowest was found for soybean, with a content of 2%. A high content of hemicelluloses is desirable for biochemical processes. Hemicelluloses are a mixture of polysaccharides including xylose, arabinose and mannose that can be converted into various chemicals and fuels such as ethanol through hydrolysis. Cellulose and lignin are more resistant to degradation and require more severe conditions than hemicelluloses. Lignin is a very rigid polymer desirable as an additive for pellets production. Cellulose can be hydrolyzed into glucose, which can be used to produce biofuels.

Ash Composition and Ash Fusibility Trends

The mineral content of ash produced during thermochemical process may result on several problems related to reactor operation or conversion technology efficiency such as slagging and fouling. Table 4 shows the correlation between indicator values and levels of slagging and fouling tendencies. According to Febreto et al. [174], the ash fusibility, sintering and slagging property of energy material can be determined by the ratio of

alkaline oxides content (CaO, Fe_2O_3, MgO, Na_2O, K_2O) and acidic oxides content (SiO_2, Al_2O_3, TiO_2), using Equation (3). This study used Equation (4) proposed by Pronobis [175], due to highest compatibility with the biomass composition since it considers the influence of several ash constituents.

$$B/A = \frac{(Fe_2O_3 + CaO + MgO + Na_2O + K_2O)}{(SiO_2 + Al_2O_3 + TiO_2)} \quad (3)$$

$$B/A_{+P} = \frac{(Fe_2O_3 + CaO + MgO + Na_2O + K_2O + P_2O_5)}{(SiO_2 + Al_2O_3 + TiO_2)} \quad (4)$$

Table 4. Correlation between indicator values and levels of slagging and fouling tendencies.

Index	Range	Slagging and Fouling Inclinations
B/A	<0.5	Low
	0.5–1.0	Medium
	1.0–1.75	High
	>1.75	Extremely High
Fu	<0.6	Low
	0.6–40	Medium
	>40	High
S_R	>72	Low
	65–72	Medium
	<65	High
SI	>0.6	Low
	0.6–2	Medium
	<2	High

The fouling index (F_u) [176], slag viscosity index (or slagging index) (S_R) [175–177] and the silica ratio (Si) were calculated using Equations (5)–(7), respectively.

$$F_u = (B/A)(Na_2O + K_2O) \quad (5)$$

$$S_R = \frac{(SiO_2)}{(SiO_2 + Fe_2O_3 + CaO + MgO)} \times 100 \quad (6)$$

$$Si = \frac{(CaO + MgO)}{(Na_2O + K_2O)} \quad (7)$$

Table 5 shows the composition of the ash samples, base-to-acid ratio (B/A), slagging index (S_R) and fouling index (Fu) of biomass ash.

Table 5. Ash composition and ash fusibility trends of evaluated biomasses.

Resource	Residue	Ash Composition									Ash Fusibility Trends					
		F_2O_3	CaO	MgO	Na_2O	K_2O	SiO_2	Al_2O_3	TiO_2	P_2O_5	B/A	B/A + P	F_u	S_R	SI	Ref
Agro-Industrial Residues																
Soybean	Stalk	0.83	33.20	9.83	0.91	18.80	30.40	2.15	0.05	2.62	1.95	2.03	38.43	40.94	2.18	[178]
	Husk	0.25	0.70	0.61	-	1.06	94.87	0.84	0.03	1.25	0.03	0.04	-	98.38	-	[100]
Rice	Straw	0.73	1.61	1.89	1.85	11.30	74.31	1.40	0.02	2.65	0.23	0.26	3.02	94.61	0.27	[179]
	Straw	0.46	5.92	3.61	2.08	22.92	51.02	0.23	0.04	2.83	0.68	0.74	17.05	83.63	0.38	[180]
	Husk	0.05	0.67	0.40	1.26	0.62	95.77	0.05	-	0.46	-	-	-	98.84	0.57	[181]
	Husk	0.21	0.91	0.26	0.13	2.42	94.26	0.29	0.02	0.55	0.04	0.05	0.11	98.56	0.46	[182]
Wheat	Straw	1.60	12.20	7.03	0.42	20.49	38.43	3.41	0.27	3.39	0.99	1.07	20.73	64.85	0.92	[183]
	Straw	0.49	6.11	4.95	0.31	25.08	25.08	1.05	0.07	1.81	1.41	1.48	35.80	68.47	0.44	[184]
	Husk	0.84	5.46	0.99	0.16	11.30	43.22	-	-	-	-	-	-	85.57	0.56	[185]
	Husk	0.08	1.20	0.80	-	0.70	95.56	0.14	-	0.80	-	-	-	97.87	-	[185]
Corn	Straw	1.31	21.66	15.96	0.90	20.24	26.79	1.73	0.18	2.75	2.09	2.19	44.25	40.76	1.78	[186]
	Cob	1.20	10.43	0.11	2.24	31.13	19.63	1.23	0.35	7.19	2.13	2.47	70.97	62.58	0.32	[85]
Coffee	Husk	2.06	13.05	4.32	0.66	52.45	14.65	1.07	0.27	4.94	4.54	4.85	240.94	42.99	0.33	[182]
	Husk	0.56	17.70	4.51	0.14	46.46	1.24	0.58	0.08	3.85	36.51	38.54	1701.39	5.16	0.48	[187]
Banana	Leaves	1.14	-	-	0.21	-	48.70	2.60	-	-	-	-	-	-	-	[188]
	Leaves	1.11	18.75	9.43	0.39	10.73	49.14	1.49	0.18	3.07	0.80	0.86	8.84	62.65	2.53	[189]
Orange	Bagasse	2.91	22.22	6.34	0.26	31.58	3.18	5.24	0.19	10.71	7.35	8.60	234.12	9.18	0.90	[100]
	Bagasse	0.09	29.47	4.78	1.98	30.90	0.29	0.33	0.02	8.34	-	-	3453.43	0.84	1.04	[158]
Coconut	Husk	11.90	2.33	2.19	4.82	27.50	31.60	3.00	0.30	1.60	1.40	1.44	45.14	65.81	0.14	[105]
	Shell	6.16	2.41	1.54	4.62	8.48	66.75	8.48	0.01	1.54	0.31	0.33	4.04	86.85	0.30	[182]
Sugarcane	Bagasse	5.55	9.60	2.36	1.18	2.08	53.09	6.94	0.57	0.25	0.34	0.35	1.12	75.20	3.67	[190]
	Bagasse	5.42	4.00	0.63	0.19	0.96	64.12	20.01	1.12	0.38	0.13	0.14	0.15	86.45	4.03	[182]
Forestry Biomass																
Eucalyptus	Wood	2.05	48.19	3.78	2.68	29.92	3.46	0.47	0.16	4.88	21.18	22.37	690.42	6.02	1.59	[182]
Pinus	Wood	5.93	20.04	4.55	1.42	9.76	45.23	10.6	0.64	1.29	0.74	0.76	8.26	59.71	2.20	[191]
	Wood	5.8	11.7	3.3	1.3	5.9	47.4	18.1	0.8	1.2	0.42	0.44	3.04	69.50	2.08	[192]

Pronobis [175] stated that values of B/A < 0.75 indicated low slagging. The average ash content of residues from coconut, rice and sugarcane residues are lower than 0.75, indicating a lower medium slagging potential, while residues with B/A over 0.75 may greatly increase the deposition tendency in combustion temperature. The S_R value showed a similar trend with B/A ratio. A low S_R value suggests low slagging tendency such as soybean husk residue (S_R < 0.6). High viscosities and, hence, low slagging inclination are correlated with high S_R values (>72) such as those found in residues from sugarcane, rice and coconut shell. The S_R average value (65 to 72) found for banana, wheat and coconut residues indicates medium slagging tendency [175]. High slagging with values <65 was found for soybean, corn, coffee and banana leaves residues. Except for rice husk, which demonstrated low fouling inclination (Fu 0.6), the majority of the studied biomasses have strong tendency to sintering of deposits [18]. Co-processing biomass with conventional fuels has the potential to be a very appealing solution that allows for the realization of full economies of scale while also minimizing issues with product quality. The majority of current co-firing applications include mixing biomass fuels with coal feed, which is frequently used to meet up to 5% of the power plant's energy needs [193].

4. Conversion Technologies Routes

The waste hierarchy advocates for the sustainable reuse and recycling of waste, but untreated biomass feedstocks can be problematic for the direct use as a fuel due to various inherent properties. Low energy density makes the biomass transportation expensive and being a solid fuel limits its potential application. Moreover, high moisture contents can also reduce the net heat available in the direct combustion [194]. However, the energy content of this waste can still be used as a reliable and local energy source. To increase the energy content and make the material more homogeneous, dense and less contaminated, pretreatment of the waste flow is necessary. The objective of the treatment is to sort out the organic fraction, which can simplify the handling and use of the material as an energy source and reduce the handling of byproducts and emissions from the conversion process. Typically, direct combustion or incineration is used in the agroforest sector. The residues generate vapor that consequently produces heat and electricity.

Different ways to produce biofuels from lignocellulosic biomass, such as agro-industrial waste, were studied for decades. These ways can be classified as either biochemical or thermochemical processing. Thermochemical routes include gasification, pyrolysis, lique-

faction, combustion and hydrothermal processes. For instance, the gasification of biomass residues produces syngas that can either be burned in a furnace or transformed into liquid fuels. Thermochemical conversion involves synthesizing the entire biomass into the desired chemical or using it directly. In biochemical conversion, bacteria or enzymes break down biomass molecules into smaller ones. The three primary ways for biochemical conversion are: digestion (anaerobic and aerobic), fermentation and enzymatic or acid hydrolysis [195]. The end products of this process are often methane and carbon dioxide in addition to a solid residue. Interestingly, bacteria obtain oxygen from the biomass itself instead of the surrounding air. A common example is the conversion of sugar cane or agricultural residues such as bagasse and cane straw into ethanol, which is a second-generation biofuel. These methods are expected to play a significant role in generating eco-friendly and renewable fuels for the transportation sector [21]. Multiple studies conducted reviews on the lignocellulosic conversion processes [44,196–198] concluding the advantages of using biomass for energy application. Biomasses contribute significantly less to carbon dioxide emissions when compared to fossil fuels. Many countries have regulations in place to make biomass economically viable, and biomass plants that replace fossil fuels can earn credits for reducing carbon dioxide emissions. These credits can be sold on the market for additional revenue. Moreover, biomass power plants need to source their biomass from within a certain distance. This creates opportunities for associated industries that grow, collect and transport biomass, which can have a positive impact on the local economy. Figure 1 shows the conversion technologies (scenarios) considered in this study, while Table 6 summarizes a comparative experimental recent report of selected biomass residues for the different conversion routes. Most of the published reports referenced Brazilian feedstocks. However, due to lack of literature data in some scenarios, biomasses from other countries were included.

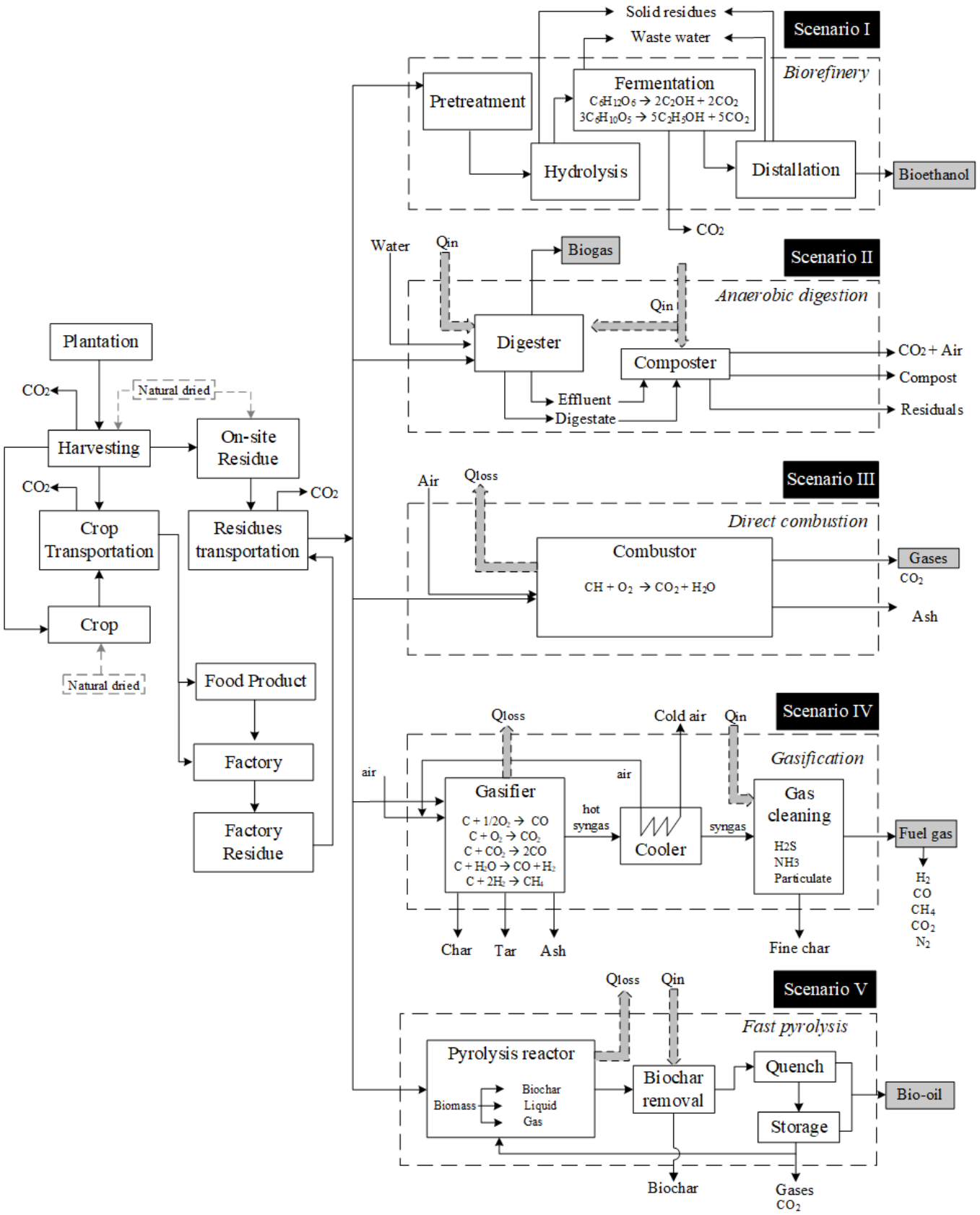

Figure 1. Scenarios of different conversion technologies for biomass utilization.

Table 6. Alternatives for energy generation of the main Brazilian agro-forestry residues.

Feedstock	Source	Operation Parameters	Optimum Obtained Results	Ref.
Scenario I—Bioethanol Production				
Soybean	Waste agro-industrial residue (Brazil)	Hydrolysis conditions: • Temperature [°C]: 127 • Time [min]: 20 • acid/substrate ratio [g/g]: 1:20 • moisture [% w/w]: 90 • H_3PO_4 [% v/v]: 0.3	• Reducing sugars yield [g/kg]: 80.38 • Reducing sugars concentration [g/L]: 6.99 • Sugar concentration [g/L]: 2.01 (glucose); 1.99 (xylose); 0.72 (arabinose) • Inhibitor concentration [g/L]: 0.34 (acetic acid); 0.0 (furfural); 0.2 (5-HMF)	[199]
	Soybean strawfarm residue (Korea)	• Alkaline pretreatment: 0.5~3.0 M NaOH (121 °C, 60 min) • Enzymatic hydrolysis: 42 °C, 200 rpm, 48 h. • Saccharification enzymes: Cellic CTec2 cellulase (contains 206 ± 2.3 g/L glucose and 193.3 ± 0.2 g/L xylose). • Inoculation of a yeast strain: Saccharomyces cerevisiae W303-1A	• For fermentation times between 30–60 h → ethanol concentration of 20–30 g/L; glucose concentration 2–7 g/L and xylose concentration of 7–9 g/L • For cellic CTec2 between 10–50 loading filter paper unit cellulase/g dry soybean straw → enzymatic digestibility 55–90%; concentration of glucose 40–70 g/L; concentration of xylose 5–10 g/L • Effect of NaOH pretreatment (100g soybean straw): For NaOH concentration between 0.5–3.0M → delignification of 34.1–50%	[200]
Rice	Rice huskagro-industrial residue (Brazil)	Hydrolysis conditions • Temperature [°C]: 127 • Time [min]: 60 • acid/substrate ratio [g/g]: 3:20 • moisture [% w/w]: 60 • H_3PO_4 [% v/v]: 5.3	• Reducing sugars yield [g/kg]: 118.16 • Reducing sugars concentration [g/L]: 78.87 • Sugar concentration [g/L]: 2.37 (glucose); 30.10 (xylose); 3.36 (arabinose); 1.86(cellobiose) • Inhibitor concentration [g/L]: 3.48 (acetic acid); 0.51 (furfural); 0.13 (5-HMF)	[199]
	Rice branagro-industrial residue (Brazil)	• Hydrolysis conditions • Temperature [°C]: 127 • Time [min]: 60 • acid/substrate ratio [g/g]: 3:20 • moisture [% w/w]: 60 • H_3PO_4 [% v/v]: 5.3	• Reducing sugars yield [g/kg]: 170.39 • Reducing sugars concentration [g/L]: 42.60 • Sugar concentration [g/L]: 13.78 (glucose); 9.26 (xylose) • Inhibitor concentration [g/L]: 0.82 (acetic acid); 0.69 (furfural); 0.89 (5-HMF)	[199]

Table 6. *Cont.*

Feedstock	Source	Operation Parameters	Optimum Obtained Results	Ref.
Wheat	Waste agro-industrial residue (Brazil)	Hydrolysis conditions • Temperature [°C]: 127 • Time [min]: 20 • acid/substrate ratio [g/g]: 1:20 • moisture [% *w*/*w*]: 90 • H_3PO_4 [% *v*/*v*]: 0.3	• Reducing sugars yield [g/kg]: 228.04 • Reducing sugars concentration [g/L]: 19.83 • Sugar concentration [g/L]: 2.32 (glucose); 4.52 (xylose); 1.83 (arabinose) • Inhibitor concentration [g/L]: 0.18 (acetic acid); 0.01 (furfural); 0.16 (5-HMF)	[199]
	Wheat straw (India)	Pretreatment (100 °C, 2 h—RT overnight): • Pretreatment 1:1.5% *w*/*v* NaOH followed by acid hydrolysis (0.75% *v*/*v* sulfuric acid at 100 °C for 2 h) • Pretreatment 2: 0.75% (*v*/*v*) sulfuric acid at 100 °C for 2 h followed by treatment with 1.5% (*w*/*v*) NaOH • Treated with accellerase 1500 (26 U/g) • Fermentation of the hydrolysate: *Saccharomyces cerevisiae*	• Alkali followed by acid pretreatment: Delignification (70 ± 1%–77 ± 1.7%); sugar loss (0.9 ± 0.26%–0.9 ± 0.36%). • Acid hydrolysate: sugars (9.8 ± 0.15 g/L–10.4 ± 0.55 g/L); Saccharification (11.9 ± 0.62%–12.4 ± 0.26%)Acid followed by alkali pretreatment: Delignification (79.3 ± 0.32%–82.7 ± 0.3%); sugar loss (0.88 ± 0.02%–1.5 ± 0.03%). Acid hydrolysate: sugars (19.6 ± 0.2 g/L); Saccharification (20.8 ± 0.25%) • Highest ethanol concentration at incubation time 36 h: 24.4 g/L ethanol with 0.44 g/g yield.	[201]
Corn	Corn stover collected from field after corn harvest (Brazil)	• Alkali pretreatment: CaO concentration (0.2, 0.4 and 0.6 $g/g_{dry\ biomass}$), 200 rpm, 24 h • Enzymatic hydrolysis (samples conditioned at 200 rpm, 50 °C, 24 h): Cellic Ctec2 (2 wt.% in relation to dry biomass) and Cellic Htec2 (0.5 wt.% in relation to dry biomass) • Fermentation of the hydrolysate: Saccharomyces cerevisiae (PE-2) and wild yeast strain *Wickerhamomyces* sp. (UFFS-CE-3.1.2) • Incubation temperature [°C]: 40, 55 and 70	• Sugar yield after enzymatic hydrolysis: Glucose (0.78 ± 0.01 g/L–20.41 ± 1.59 g/L); xylose (1.17 ± 0.52 g/L–10.05 ± 0.83 g/L); cellobiose (0.48 ± 0.20 g/L–1.10 ± 0.10 g/L); cellulose and hemicellulose converted into fermentable sugars (2.19–52.08%); acetic acid (2.34 ± 0.10 g/L–3.06 ± 0.06 g/L) • Fermentation yield [$g_{etanol}/g_{dry\ biomass}$]: ~0.38 for PE-2 and ~0.34 for UFFS-CE-3.1.2 • Ethanol production started with a concentration of 8.23 g/L glucose, obtaining 2.80 g/L and 3.10 g/L of ethanol for strains UFFS-CE-3.1.2 and PE-2, respectively. 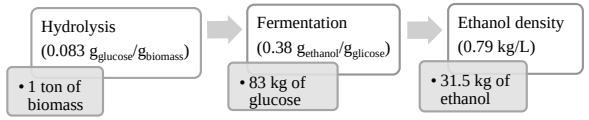	[194]

Table 6. *Cont.*

Feedstock	Source	Operation Parameters	Optimum Obtained Results	Ref.
	Corn stalk agricultural farm (Bangladesh)	• Alkali pretreatment: NaOH solution (concentration 0.5–2.5%), 100 °C, 1 h. • Fermentation: 9 g/L of yeast extract, 0.75 g/L of KH_2PO_4, 0.15 g/L of • $(NH_4)_2SO_4$ and 0.25 g/L $MgSO_4$. organism loading: *Saccharomyces cerevisiae*	• Bioethanol yield: 20.61–24.63 g/L (alkali (0.5–2.5%); 24 h fermentation period) • Bioethanol yield: 31.11 g/L (alkali (2%), 100 °C pretreatment, using *Saccharomyces cerevisiae*, 48 h) • Filtrate of the pretreated corn stalk with 5% inoculum produced 43.8 g/L bioethanol.	[202]
Coffee	• Coffee husk • Ground coffee husk • Aqueous extract from ground coffee husk agricultural farm (Brazil)	• Batch fermentation: 100 rpm; ~13 g of substrate mixed with 100 mL distilled water; time determined based on CO_2 release data. • Organism loading: *Saccharomyces cerevisiae* (Fleischman) (3, 4 and 5 g/L yeast concentration; 25, 30 and 35 °C fermentation temperature)	• Fermentation 4 g/L yeast at 30 °C → Ethanol production [g/100g db]: 7.67 ± 0.15 (coffee husk); 7.19 ± 0.52 (ground coffee husk); 6.43 ± 0.20 (aqueous extract) Theoretical yield [%]: 67.64 ± 1.39 (coffee husk); 62.78 ± 4.56 (ground coffee husk); 48.07 ± 0.96 (aqueous extract) Sugar conversion [%]: 92.10 ± 0.40 (coffee husk); 92.67 ± 0.52(ground coffee husk); 91.43 ± 0.38 (aqueous extract) Productivity [g/L h]: 1.22 ± 0.02 (coffee husk); 1.15 ± 0.08 (ground coffee husk); 1.03 ± 0.03 (aqueous extract)	[203]
	Coffee pulp Semidry processing coffee (Brazil)	• Alkali pretreatment (autoclave 121 °C): • alkali substances (NaOH and $Ca(OH)_2$) • Hydrolysis (50 °C, 150 rpm, 72 h): Enzyme Celluclast 1.5 L; 69.106 FPU/mL; 2 mL of enzyme preparation; 38 mL of 0.05 mol/L citrate buffer (pH 4.8), and 10 g (equivalent to 7% *w*/*v* of dry material per 100 mL of solution) • Fermentation (121 °C, 20 min, autoclave): Supplemented with $(NH_4)_2SO_4$ (1 g/L), K_2HPO_4 (0.1 g/L), and magnesium sulfate heptahydrate (0.2 g/L). Yeast strain *S. cerevisiae.*	• Levels of reducing sugars [g/L]: 24.7–37.97 • Total reducing sugars [g/L]: 26.72–66.15 • Glucose and enzymatic hydrolysis yield [%]: 38.39–60.48 • Fermentation time 24–48 h → glucose: 4.25 ± 0.85–4.17 ± 0.71 g Glucose/L; ethanol: 11.92 ± 0.15–11.99 ± 0.85 g ethanol/L; ethanol yield: 0.40 g ethanol/g glucose	[204]

Table 6. *Cont.*

Feedstock	Source	Operation Parameters	Optimum Obtained Results	Ref.
Banana	Banana leaf waste (India)	Steam, alkali (0.1 N NaOH) and acid pretreatment (0.1 N H_2SO_4) pretreatment [%*w*/*v*]: 1:10 (121 °C, 1 h) Sacharification condition: Cellulase (enzyme): produced by Aspergillus niger JD-11 Enzyme loading [FPU/g]: 5–15 Temperature [°C]: 40, 45 and 50 Substrate [%wt./v]: 2 to 6 Surfactant [%vol]: 0.05–0.15 (Tween 80 and PEG 6000)Time [h]: 70 Fermentation condition: Inoculum: S. cerevisiae (40 g/L reduced sugars, pH 5.5, 30 °C for 30 h)	Pretreatment effect on hydrolysis: Higher reduced sugars[mg/g]: 358.11 (acid pretreatment). Main increase at 40 h Enzyme load effect on hydrolysis: Higher reduced sugars [mg/g]: 397.57 (15 FPU/g). 38% more compared with 5 FPU/g. Temperature effect on hydrolysis: Higher reduced sugars [mg/g]: 455.91 (at 45 °C) Surfactant effect on hydrolysis: Higher reduced sugars [mg/g]: 524.83 (0.15% vol of PEG 6000) Substrate concentration effect on hydrolysis: Higher reduced sugars [mg/g]: 524.83 (2% wt./vol of substrate) Higher ethanol production [g/L]: 15.43Conversion factor reduced sugars to ethanol [g/g]: 0.38 Volumetric productivity [g/L·h]: 1.28 (at 12 h)	[205]
	Banana pulp, peels and pseudostem bagasse (Brazil—Simulation study)	Biomass proportions: 1:2:10 (pulp:peels:pseudestem) Inoculum: S. cerevisiae and Pachysolen tannophilus (ATCC32691). pH fermentation: 5 Fermentation time: 36–48 Hydrolysis Temperature [°C]: 120 Hydrolysis Time [min]: 15	Best ethanol performance at 48 h of fermentation: Reduced sugars before chem pretreatment [g/L]: 151.6 Reduced sugars in hydrolyzed broth [g/L]: 19.5 Ethanol at the beginning of fermentation [g/L]: 0.8 Ethanol at the after fermentation [g/L]: 53.1 Volumetric productivity [g/L·h]: 1.09 Conversion factor reduced sugars to ethanol [g/g]: 0.4	[206]

Table 6. *Cont.*

Feedstock	Source	Operation Parameters	Optimum Obtained Results	Ref.
Orange	Peels (Brazil)	Pretreatment: $Ca(OH)_2$, biomass and destilate water (1:4:20 *w*/*w*/*v*), at 60 °C for 120 min. Enzymatic and dilute acid hydrolysis Enzymes: cellulase and xylanase Acid: HCl	Best cellulose activity [FPU/mL]: 24.08 (ph 4.8, 60 °C) Best xylanase activity [U/kg]:1.99.58 × 10^{-3} (pH 5.2, 50 °C) Acid Hydrolysis effect:Total reduced sugars [mg/g]: 30.15 (acid concentration 3.5%, 55.82 °C, 45 min) Enzymes effect: Total reduced sugars [mg/g]: 99.66 (7.02 PFU/mL of cellulase, 2.5 U/g xylanase, 36 h)	[207]
	Bagasse (Iran)	ABE Production (acetone-butanol-ethanol) Pretreatment: High-pressure reactor: Biomass to water 1:10 (*w*/*w*); T [°C]: 100, 140 and 180; t [min]: 30, 60 and 120 Enzymatic hydrolysis conditions: Cellulase:Hemicellulase 9:1 Cellulase to biomass [FPU/g]: 15; Solid loading [%wt./v]: 5; T [°C]: 45; t [h]: 72 (solid residue from Enzymatic hydrolysis to Anaerobic digestion) Fermentation: C. acetobutylicum NRRL B-591	Pretreatment effect: Best performance at 180 °C and 120 min Solid solubility [%]: 68.2 Hemicellulosic sugar removal [%]: 86.4 Enzymatic hydrolysis: Total sugar concentration [g/L]: 25.7 (23.3 glucose, 2.4 xylose) (Pre: 140 °C, 120 min) Highest ABE production [g/L]: 4.68 (Pre: 140 °C, 30 min) Per kg of Baggase: 42.3 g biobutanol, 33.1 g acetona, 13.4 g ethanol, 104.54 L biohydrogen, 28.3 L biomethane	[208]
Coconut	Husk (Brazil)	Pretreatment: NaOH 5% [mL]: 100, 121 °C, 1 atm for 40 min Enzymatic hydrolysis conditions: Enzyme: Accellerase 1500. Temperature [°C]: 50 Time [h]: 72 Fermentation: PD medium (10 g/L yeast extract; 20 g/L bacteriological peptone, 20 g/L glucose) Time [h]: 18	Reducing sugars yield [g/100 g]: 45.86 Reducing sugars concentration [g/L]: 8.84 Enzymatic conversion [%]: 88.40 Overall enzymatic yield [g/100 g]: 22.71 Ethanol production [g/L·h]: 0.015 Theoretical maximum yield [gEtOH/g biomass]: 0.078	[209]
	Husk (Brazil)	Two way strategies SHF and SSF. Pretreatment: solution NaCl at 10% of the acetic acid.	Highest ethanol yield [L EtOH/ton biomass]: 52.7 (SSF)	[210]

Table 6. *Cont.*

Feedstock	Source	Operation Parameters	Optimum Obtained Results	Ref.
Sugar cane	Bagasse (Brazil)	Ultrasound (US)-assisted enzymatic hydrolysis. Ultrasound parameters: Temperature [°C]: 25, 30, 37.5, 45, 50. Time [s]: 10, 75, 170, 265, 330. Intensity [W/cm^2: 120.6, 150.7, 192.5, 234.4, 263.7 Enzymatic hydrolysis conditions: Enzymes: Celluclast 1.5 L and Cellic CTec2 Temperature [°C]: 50 Time [h]: 24	Reduced sugar concentration (No US) [g/L]: 2.09 (Celluclast 1.5 L) and 3.20 (Cellic CTeC2) Enzyme and US effect on reduced sugars: Celluclast 1.5 L [% Relative RS Concentration]: 189.37 (330 s, 150.7 W/cm^2, 25 °C). Theoretical cellulose yield [%]: 45 (0.487 g/L cellobiose and 3.985 g/L glucose) Cellic CTec2 [% Relative RS Concentration]: 195.39 (75 s, 150.7 W/cm^2, 30 °C) Theoretical cellulose yield [%]: 66.31 (0.487 g/L cellobiose and 3.985 g/L glucose)	[211]
	Bagasse (Brazil)	Hydrolysis conditions: Temperature [°C]: 121, Time [min]: 20, Acid hydrolysis with H_2SO_4: 100 mg/g dry bagasse and solid ratio of 10% Yeast: S. cerevisiae MDS130 immobilized in Ca-alginat Medium: Sugarcane bagasse hemicellulose hydrolysate and molasses Fermentation device: Fixed-bed reactor Operation mode: 20 repeated batches	Ethanol production [g/L·h]: 14.06–22.80 Ethanol yield [gEtOH/gTRS] = 0.36–0.51 Highest ethanol concentration [g/L]: 46.98	[212]
Eucalyptus	Sawdust (Uruguay)	Bioethanol and xylosaccharides Pretreatment: Steam explosion with and without NaOH impregnation (10–20%). T[°C]: 180, 190 and 200; t [min]: 10. Enzymatic hydrolysis: Enzyme loading [FPU/mL]: 125; Solid loading [%wt/w]: 15; T [°C]: 50; t [h]: 96 and 168, pH: 4.85 Fermentation: SHF (separate hydrolysis and fermentation), PSSF (simultaneous saccharification and fermentation) and SSF (simultaneous saccharification and fermentation)	Pretreatment effect: Highest Glucose concentration [g/L]: 105 (200 °C, 0% NaOH); Highest Hydrolysis efficiency [%]: 96 (200 °C, 0% NaOH) Ethanol conversion [%]: 78 (SHF), 82 (PSSF), 83 (SSF) Ethanol production [g/L]: 71.8 (SHF), 70.2 (PSSF), 75.6 (SSF)	[213]

Table 6. *Cont.*

Feedstock	Source	Operation Parameters	Optimum Obtained Results	Ref.
	Bark (Portugal)	Two sequential steps of acid hydrolysis: 1) 0.4 mL of 72% wt. H_2SO_4, T [°C]: room temperature, t [min]: 180 2) 4.4 mL of water was added to obtain a 9% wt. acid solution, T [°C]: 90, 100 and 120	Highest Glucose concentration [%wt.]: 48.6 (100 °C, 2.5 h) Highest Xylose concentration [%wt.]: 15.2 (90 °C—2 h or 120 °C—0.5 h) Hypothetical ethanol yield [L/ton bark]: 248	[214]
Pinus	Sawdust (Mexico)	Two way strategies SHF and SSF. Pretreatment: HNO_3 and NaOH. Concentration [%wt.]: 6 and 12; T [°C]: 100 and 130; t [min]: 30. Enzymatic hydrolysis: Enzyme loading [FPU/g]: 25; t [h]: 72; T [°C]: 48; pH: 4.8 Fermentation: Saccharomyces cerevisiae ITD-00185; pH: 5.5	(SHF) Highest reducing sugar conversion [%]: 98.64 (10.9% HNO_3 at 115 °C and 30 min) Highest ethanol yield [g/L]: 17.1 (40 h) Fermentation yield [%]: 84.1 Hypothetical ethanol yield [L/ton biomass]: 235.3 (SSF) Highest ethanol yield [g/L]: 15.0 Hypothetical ethanol yield [L/ton biomass]: 160	[215]
	Sawdust (Chile)	Two way strategies SHF and SSF. Pretreatment: Soda ethanol Liquor-to-biomass ratio: 5.44:1; T [°C]: 170; t [min]: 60; EtOH:H_2O ratio [%vol]: 35–65 Enzymatic hydrolysis: Enzyme loading [FPU/g]: 30; t [h]: 48; T [°C]: 37; pH: 5 Fermentation: Saccharomyces cerevisiae IMR 1181 (SC 1181)	(SHF): Highest reducing sugar conversion [%]: ~98 Highest bioethanol concentration [g/L]: 3.40 (13 h) Fermentation yield [%]: 89.3 (SSF): Highest bioethanol concentration [g/L]: 5.68 (72 h) Fermentation yield [%]: 100	[216]

Table 6. *Cont.*

Feedstock	Source	Operation Parameters	Optimum Obtained Results	Ref.
Scenario II-Biogas Production				
Soybean	Straw and hull (Brazil)	Subcritical water hydrolysis: Temperature [°C]: 220 Liquid/solid mass ratio: 18 g water/g straw; 15 g water/g hull. Flow rate [mL/min]: 30 Reaction time [min]: 4 (straw); 3 (hull) Fermentation: Yeast: *Wickerhamomyces* sp. UFFS-CE-3.1.2 10 mL of inoculum and 90 mL of hydrolysate Procedure: orbital shaker at 30 °C and 50 rpm. Hydrolysates supplemented with glucose (10 g/L). Biochemical biogas and methane: Starter inoculant: anaerobic sludge treated with swine manure, fresh dairy cattle manure, and anaerobic mesophilic granular sludge from a gelatin manufactory. Temperature [°C]: 37 Procedure: 250 mL glass reactors. 2 g of straw or hull and 30 g for the samples of hydrolysates or fermented hydrolysates were mixed. Inoculum/Substrate ratio: 2	Soybean straw hydrolysate [g/L]: 2.16 (glucose); 1.33 (xylose); 0.08 (arabinose); 4.76 (formic acid); 8.22 (acetic acid); 0.28 (HMF); 0.48 (furfural) Soybean hull hydrolysate [g/L]: 0.96 (glucose); 1.11 (xylose); 0.43 (arabinose); 0.09 (cellobiose); 3.24 (formic acid); 3.14 (acetic acid); 0.16 (HMF); 0.31 (furfural) Fermentation of straw hydrolysate (72h) [g/L]: 0.69 ± 0.06 (ethanol); 2.04 ± 0.17 (glucose); 1.08 ± 0.02 (xylose); 7.35 ± 0.65 (acetic acid); 4.17 ± 0.19 (formic acid); 0.30 ± <0.01 (HMF); 0.30 ± <0.01 (furfural) Fermentation of hull hydrolysate (96 h) [g/L]: 0.72 ± 0.01 (ethanol); 1.02 ± 0.25 (glucose); 0.90 ± 0.04 (xylose); 0.40 ± <0.01 (arabinose); 0.09 ± <0.01 (cellobiose) 2.85 ± 0.05 (acetic acid); 2.96 ± 0.02 (formic acid); 0.19 ± <0.02 (HMF); 0.19 ± <0.04 (furfural) Biogas potential: • Cellulose standard: 94.62 ± 0.3 (Total solid [%m/m]); 94.51 ± 0.9 (volatile solids [%m/m]); 7.92 ± 0.05 (pH initial); 8.06 ± 0.06 (pH final); 634 ± 32 BBP (NmL/g_{Vsad}); 56.4 (CH_4 [%]); 358 ± 18 (BMP [NmL_{CH4}/g_{VSad}]) • New straw: 92.51 ± <0.1 (Total solid [%m/m]); 86.85 ± 5.5 (volatile solids [%m/m]); 7.94 ± 0.12 (pH initial); 8.23 ± 0.10 (pH final); 365 ± 25 BBP (NmL/g_{Vsad}); 58.5 (CH_4 [%]);214 ± 15 (BMP [NmL_{CH4}/g_{VSad}]) • Straw hydrolysate: 8.15 ± 5.6 (Total solid [%m/m]); 7 ± 36.5 (volatile solids [%m/m]); 7.05 ± 0.17 (pH initial); 8.16 ± 0.03 (pH final); 406 ± 8 BBP (NmL/g_{Vsad}); 48.4 (CH_4 [%]); 197 ± 4 (BMP [NmL_{CH4}/g_{VSad}]) • New hull: 92.8 ± 0.2 (Total solid [%m/m]); 87.20 ± 0.5 (volatile solids [%m/m]); 7.91 ± 0.03 (pH initial); 8.25 ± 0.09 (pH final); 542 ± 39 BBP (NmL/g_{Vsad}); 56.7 (CH_4 [%]); 307± 22 (BMP [NmL_{CH4}/g_{VSad}]) • Hull hydrolysate: 8.18 ± 0.3 (Total solid [%m/m]); 6.46 ± 15.9 (volatile solids [%m/m]); 7.21 ± 0.20 (pH initial); 8.21 ± 0.01 (pH final); 677 ± 35 BBP (NmL/g_{Vsad}); 49.2 (CH_4 [%]); 333 ± 17 (BMP [NmL_{CH4}/g_{VSad}])	[217]

Table 6. *Cont.*

Feedstock	Source	Operation Parameters	Optimum Obtained Results	Ref.
	Molasses (Brazil)	Reactor: Lab-scale up-flow anaerobic sludge blanket reactor (UASB) 12 L Organic loads rates [kg COD/m^3d]: 0.28–6.98 Time [days]: 134 Temperature [°C]: 23 ± 1–25 ± 1 pH [-]: 7.3–7.8 Mass of soybean molasses [g]: 17.5–140 Flow rate [L/h]: 0.25–1 Inoculum: 3.5 L of anaerobic granular sludge (28.5 gTS/L and 24.4 gTVS/L) Mesophilic conditions	Characterization raw soybean molasses (dry basis): 50g/kg (crude protein); 250 g/kg (moisture); 150 g/kg (ashes); 5g/kg (fat); 3 g/kg (crude fiber); 5.45 pH; 1.35 g/cm^3 (Density); 9000–14,000 cP (viscosity); 119 g/kg (stachyose); 50g/kg (raffinose); 199 g/kg (sucrose); 25 g/kg (fructose); 4.64 g/100g (galactose); 6 g/kg (glucose); 400 mg/kg (total sugars); 5.32 g/kg (total carbohydrate); 500 mg/kg (sulfite); 5.5 mg/kg (manganese); 100 mg/kg (calcium); 462 mg/kg (iron); 400 mg/kg (sodium); 0.74 mg/kg (cobalt); 1.30 g/kg (magnesium); 4150 mg/kg (phosphorous). OLR [kg COD/m^3d]: 0.28 ± 0.02–6.98 ± 0.35 Biogas production [mL/d]: 12 ± 5–1456 ± 426 Biogas production [mL CH_4/g COD]: 23.3–356.1 Methane [%]: 75.5–82.1	[218]
Rice	Husk (Brazil)	Chernicharo methodology COD monitored between 2016–2017, total of 12 samples. The theoretical production of methane: $COD_{CH4}\left[\frac{kgCOD_4}{d}\right] = Q_{mean}\left[\frac{m^3}{d}\right]\left[(S_0 - S)\left[kg\frac{COD}{m^3}\right]\right.$ $\left. - \left(\left(Y_{obs}\left[Kg\frac{CODsludge}{Kg}CODapplied\right] \times K_{solids}\left[1.42\,kg\frac{COD}{kg}TVS\right]\right) \times (S_0 - S)\right)\right]$	COD [mg/L]: 3968.9–7540.2 Total rice production [tons/year]: 6.4×10^6 Parboiled rice [tons/year]: 2.3×10^6 Effluent flow [m^3/d]: 1.5×10^4 Flow of methane [Nm^3/d]: 1.7×10^4 Chemical energy from husk [MJ/y]: 2.1×10^{10} Parboiling energy demand [MJ/y]: 2.4×10^9 Electrical energy fromCH_4 [KWh/y]: 2.2×10^7 Thermal energy from CH_4 [KWh/y]: 3.1×10^7 Flow of syngas [Nm^3/d]: 9×10^6 Electrical energy from syngas [KWh/y]: 7.3×10^8 Total termal energy from genset and gasifier [KWh/y]: 2×10^9 Total energy [KWh/y]: 2×10^{12}	[219]

Table 6. *Cont.*

Feedstock	Source	Operation Parameters	Optimum Obtained Results	Ref.
	Husk (Brazil)	Biodigester: Flow condition: unsteady Flow regime: laminar Simulation time [s]: 1800 Time Step [s]: 60 Reference pressure [atm]: 1 Inlet [m/s]: 0.18 Temperature [°C]: 25 Feeding: 7 L swine manure—150 g rice husk—400 mL inoculum Anaerobic digestion conducted for 21 days	Generation of biogas [mL/g (VS_{ad})]: 85.5–94.3 Biogas on batch step [mL/g (VS_{ad})]: 14.08–15.52 Biogas on complete process [mL/g (VS_{ad})]: 86.30–71.48 CH_4 on biomass [%v/v]: 33.6 ± 2.4–34.9 ± 5 Methane on complete process [mL/g(VS_{ad})]: 62.3–53.6	[220]
Wheat	Wheat (*Triticum aestivum*) straw (Brazil)	Pretreatment methods to wheat straw: acid; alkaline; thermal; acid+thermal; alkaline+thermal Biodigestor capacity [mL]: 300 Nutrient solution: 200 mL of 2 g/L of yeast extract, 7 g/L of K_2HPO_4, 3 g/L of KH_2PO4. Temperature [°C]: 25 Operation time [days]: 274	Characterization of waste used in bioreactor: Sludge [g/L]: 0.31 (chromium); 1.21 (TKN); 11.27 (TOC); 1.89 (IC); 10.88 (C/N ratio); 34.42% (VS); 7.45 [-] (pH) Leather shavings [%g/g]: 1.14 (chromium); 2.95 (TKN); 32.29 (TOC); 0 (IC); 10.95 (C/N ratio); 90.24% (VS); 4.09 [-] (pH) Wheat straw [%g/g]: 0.60 (TKN); 41.32 (TOC); 0 (IC); 68.87 (C/N ratio); 92.37% (VS); 5.84 [-] (pH) Biogas cumulative volume of VSS added [mL/g]: 4.01–43.15 Methane cumulative volume of VSS [mL/g]: 0.14–10.06 Maximum yield of methane [%]: 7.71–40.61 Days of maximum yield of methane: 161–266	[221]
	Straw (Chile)	Fungi: white rot fungi incubated in agar Petri dishes for 10 d at 30 °C in MEA medium. Inoculum: Industrial anaerobic reactor treating brewery wastewater. Reactor volume [mL]: 250 pH [-]: 7–7.2 Total solids [%]: 18 Substrate/inoculum ratio [gVS/gVS]: 1 Temperature [°C]: 30	0.15 and 30 d of fungal treatment using *Pleurotus ostreatus*: Biogas yield [mLSTP/g VS]: 235 ± 2–337 ± 3 Biogas yield rate [mLSTP/g VSd]: 13.6 ± 0.9–25.8 ± 1.3	[222]

Table 6. *Cont.*

Feedstock	Source	Operation Parameters	Optimum Obtained Results	Ref.
Corn	Vinasse (Brazil)	The vinasse from corn uses the volume of ethanol produced in Brazil in 2019/20 to estimate the bioenergy. Temperature [°C]: 32–37 Reactor: UASB	Corn vinasse: 67.5 kg/m^3 (COD); 87 m^3/kgCOD (ECO_D); 71.25% (CH_4 in biogas); 0.295 m^3 CH_4//kgDQOrem; 25.44 MJ/kg (LHV biogas); 150 days (season period). Biogas flow rate [m^3/h]: 8.52×10^8 Potential power generates from corn biogas [MW/year]: 2.27×10^8 Potential the bioenergy from biogas [MWh/year]: 7.35×10^5 Carbon credits from corm use [tCO_{2eq}/y]: 1.22×10^6–4.29×10^5	[223]
	Stalk (Brazil)	Pretreatment: humid steam in autoclave in the presence of H_2SO_4 and H_2O_2 in an orbital shaker Reactor volume [mL]: 250 pH [-]: 7–7.2 Volatile solids [%]: 10 Substrate/inoculum ratio [gVS/gVS]: 1 Temperature [°C]: 37	Biogas [$L_{Nbiogas}$/kgVS_{ad}]: 650 (Pretreatment with H_2O_2); 550 (not sifted and untreated); 540 (Sifted and untreated); 350 (pretreated with H_2SO_4) Stalk pretreated with H_2O_2 produced about 86% more $L_{Nbiogas}$/kgVS_{ad} when compared to the biomass pretreated with H_2SO_4.	[224]
Coffee	Husk(Brazil)	Ozone pretreatment to generate hydrolysates for biogas Inoculum: mixture of bovine manure and anaerobic sludge (1:1 [*w*/*w*]) Temperature [°C]: 35 Anaerobic digestion: single stage; two stage; single stage with PAC.	Single-stage anaerobic digestion: Maximum methane production [NmL CH_4/g CH]: 36 with hydrolysate (10 mL/g) (LSR); 11 (pH); 18.5 mg O_3/g CH (SAOL); 0.064 kJ/g CH (energy recovery). Two-stage anaerobic digestion: Maximum methane production [NmL CH_4/g CH]: 49, produced 0.26 kJ/g CH (energy recovery).	[225]
	Wastewater (Brazil)	Mesophilic anaerobic biodigestion 4 digestors filled with 1.5 L of substrate Temperature [°C]: 35–40 Reactor volume [L]: 2	Physicochemical parameters of coffee wastewater (INPUT): 3.87–4.50 (pH); 2082–2485 mg/L (COD); 602–1503 mg/L (BOD); 6640–7269 mg/L (TS); 535–1046 mg/L (FS); 6105–6223 mg/L (VS); 11–25 mg/L (TN); 86–92% (VS:TS); 1.39–4.13 (COD:DBO) Biogas composition: 10–38 (Hydraulic Retention Times); 0.2–11.4% (CH_4); 6.4–35.7 (CO_2); 9.1–17.3% (O_2); 54→2000 ppm (CO); 9–1648 ppm (H_2S); 53.1–76.4% (Balance)	[226]

Table 6. *Cont.*

Feedstock	Source	Operation Parameters	Optimum Obtained Results	Ref.
Banana	Peduncle (India)	Pretreatments: Thermal, alkali and extrusion Biomethane potential (BMP): automated methane potential test system II (AMPTS II), Temperature [°C]: 37 Inoculum: Seed sludge	Specific CH_4 yield [mL/g volatile solids]: 527.6 (Thermal 120 °C, 60 min), 298.9 (Alkali 5% NaOH, 1 h) and 248.02 (extruded, twin screw). Optimized Yields [mL/g volatile solids]: 527.6 (thermal 120 °C, 60 min), 298	[227]
	Leaf, stem, and peduncle (Kenya)	Time [day]: 51 Temperature [°C]: 37 Inoculum: digested sludge	CH_4 production [mL_N/g organic dry matter]: 63.34 Net biogas production [ml]: 400 CH_4 yield [m^3/kgoDM]: 0.062 Biogas composition [wt.]: 65.335 (CH_4), 34.665 (CO_2)	[228]
Orange	Peels (Brazil)	Two-stage anaerobic digestion Stage I (acidogenic, pH 5–6), Stage II (methanogenic, pH 7–8) Anaerobic digestion conditions: Temperature [°C]: 35, time [days]: 25.8 Inoculum characteristics: Mesophilic anaerobic sludge, pH: 7.53, TS an VS [%]: 9.07 and 8.03 Reactor mix: [%v/v]: 35 (biomass), 26 (inoculum) and 39 (water)	Highest cumulative CH_4 yield [L/gVS]: 0.79 (in methanogenic stage), 38% more than simple stage reactor. Cumulative biogas volume [cm^3]: 13,000 (stage I), 10,000 (stage II) Total Biogas yield [m^3/ton biomass]: 18.21 Potential electricity generation [MWh/year]: 97.5 × 103 in São Paulo State Potential emission mitigation [tCO_2eq/year]: 7.5 × 103 and 9.05 × 103 in São Paulo State	[229]
	Peels, seeds, bagasse	Treatment: pectin and essential oil extraction. Anaerobic digestion conditions: VDI 4630 procedure, time [h]: 500 Inoculum characteristics: pig manure, VS [g/kg dry matter)]: 45 Inoculum to substrate ratio: 2:1	Highest cumulative CH_4 yield [mL/gVS]: 223 (oils extraction), 222 (pectin extraction), 190 (untreated)	[230]

Table 6. *Cont.*

Feedstock	Source	Operation Parameters	Optimum Obtained Results	Ref.
Coconut	Spent copra (Nigeria)	Pretreatment: Mix with cow urine (CU) at different ratios. CU to copra [mL to g]: 1:15, 1:7, 1:5 Anaerobic digestion conditions: Temperature [°C]: 45, time [days]: 42 Inoculum characteristics: anaerobic digester sludge, pH: 7.1, TS and VS [%]: 9.5 and 5.5	Highest cumulative biogas yield [mL/gVS]: 786 (CU to copra ratio 1:7), 225 (unpretreated copra) Highest cumulative CH_4 yield [mL/gVS]: 648.5 (CU to copra ratio 1:7), 99.9 (unpretreated copra) Highest CH_4 yield [mL/gVS]: 77 (for all pretreatment ratios at day 12), 38 (unpretreated copra at day 24)	[231]
	Shell	Pretreatment: pyrolysis at 600 °C Pyroligneous detoxification: oxidation by H_2O_2: 0–12%, temperature [°C]: 10, time [h]: 4 Anaerobic digestion conditions: Temperature [°C]: 37, time [days]: 4 Inoculum characteristics: Anaerobic granular sludge, pH: 7.74, TS and VS [mg/L]: 13.69 and 9.33 Inoculum to substrate ratio: 3:2	Highest biogas volume [mL]: 1190 ((pretreatment 10% H_2O_2)) Highest CH_4 yield [L/gCOD]: 0.317 (pretreatment 4% H_2O_2)	[232]
Sugar cane	Bagasse (Brazil)	Hydrothermal pretreatment: NaOH [M]: 0.7–2.3, Temperature [°C]: 146.4–213.6, time [min]: 3.2–36.8 Anaerobic co-digestion conditions: Temperature [°C]: 55 time [days]: 52 Inoculum characteristics: from industrial biogas plant Inoculum to substrate [gVS/gVS]: 2:1	Higher CH_4 content in the biogas [%]: 70 (pretreatment conditions of: 200 °C, 2.0 M NaOH, 30 min; 160 °C, 2.0 M, NaOH, 30 min; 180 °C, 2.34 M NaOH, 20 min)	[233]
	Bagasse (Brazil)	Enzymatic pretreatment and two stages anaerobic process Pretreatment (Trametes versicolor laccase): Temperature [°C]: 50, time [min]: 120 Stage I (acidogenic/fermentative): pH: 6.8, Temperature [°C]: 37, time [days]: 8 Inoculum characteristics: Pure *Paraclostridium* sp. isolated from sugarcane bagasse. Stage II (methanogenic): Temperature [°C]: 37, time [day]: 10Inoculum characteristics: Microbial consortium from anaerobic sludge. TVS [g TVS/g]: 0.84.	Stage I: H_2 production rate [mL/L·h]: 3.2 H_2 production [mL/L·h]: 166.8 Stage II: CH_4 production rate [mL/L·h]: 2.31 CH_4 production [mL/L·h]: 870.8	[234]

Table 6. *Cont.*

Feedstock	Source	Operation Parameters	Optimum Obtained Results	Ref.
Eucalyptus	Wood (Colombia)	Alkali pretreatment: solution NaOH (8% wt./v), solid liquid ratio 1:5 (wt./v), Temperature [°C]: 130, time [min]: 60 Anaerobic digestion (Remanent solid): pH: 7, Temperature [°C]: 37, time [days]: 20 Inoculum: sludge form water treatment Inoculum characteristics: TS and VS [%]: 6.4 and 5.7	Highest daily biogas production [mL/gVS.d]: 13.1 Highest cumulative biogas yield [mL/gVS]: 163 Highest cumulative CH_4 yield [ML/gVS]: 87.9	[235]
Pinus	Fresh needles, needle litter, bark and branches (Greece)	Mesophilic anaerobic digestion: Temperature[°C]: 38, time [days]: 30 Inoculum: took from a full-scale digester treating agro-industrial wastes and energy crops. Inoculum characteristics: pH: 7.8, ammonia nitrogen and orthophosphates [mg/L]: 24,411 and 83, TS and VS [g/L]: 34.9 and 22.3	CH_4 yield [mL_N/g VS]: 164 (fresh needles after 26 days), 138 (branches after 30 days), 85 (bark after 30 days), 77 (needle litter after 26 days) CH_4 production potential [Nm^3/km]: 500 (needle litter accumulated on adjacent forest roads)	[236]
	Sawdust (Egypt)	Anaerobic digestion: Temperature [°C]: 30, time [days]: 35 Pretreatment: lignocellulosic degradation microbial consortium (LCDC) from rotten sawdust. Inoculum characteristics: pH: 7.01, total dissolved solids [mg/L]: 910, TS and VS [% db]: 9.33 and 5.68	Highest daily biogas production [L/kgVS.d]: 15.7 (untreated after 19 days) and 15.9 (pretreated after 13 days) Highest significant cumulative biogas yield [L/kgVS]: 248.4 (untreated after 28 days) and 312.0 (pretreated residue after 28 days) Highest significant cumulative CH_4 yield [L/kgVS]: 155.2 (pretreated residue after 28 days), 72.6% more than untreated.	[237]
Scenario III—Combustion				
Rice	Husk (Brazil)	Reactor: atmospheric bubbling fluidized bed pilot Bed material: sand (particle size 0.5 –1 mm) and 95% silica content. Temperature [°C]: 834–877 O_2 [%]: 5–9.9 6% O_2 excess	Main characteristic of the feedstock: high volatile matter (74 wt.%) and medium ash content (12.8 wt.%). Silicon (87.7% as SiO_2), potassium (5.4% as K_2O) and phosphorous (3.7% as P_2O_5). CO_2 [%]: 11.6–14.4 CO [mg/Nm^3]: 1085–1808 NOx [mg/Nm^3]: 100–430 Combustion efficiency [%]: 97.2–98.9	[238]

Table 6. *Cont.*

Feedstock	Source	Operation Parameters	Optimum Obtained Results	Ref.
Wheat	Straw (Brazil)	Technique: TGA curve analysis Isothermal conditions Heating rates [°C/min]: 5–100 Maximum temperature [°C]: 900	Kinetics parameters: 85.4 [kJ/mol] (Activation energy); 3.1×10^6 [1/min] (Pre-exponential factor) Combustion scheme: evolution of volatiles (up to 300 °C); ignition of volatiles (500–650 °C), burning of volatiles (650–800 °C), and burning of char (700–850 °C) Direct combustion at low heating rates is favored with respect to the devolatilization/char burnout schemes. Alkali K_2O crosses the stability regions of CO and CO_2 at a temperature as low as 427 °C.	[239]
Coffee	Husk (Kenya)	Reactor: pilot-scale fluidized bed (FBC) Reactor bed material: quartz sand (0.48 mm) T [°C]: 500–900 Flue gas (O_2) concentration [vol%]: 10–16	Exhaust gas composition (mg/m^3): NOx = 450–525; N_2O = 3–27 N concentration in volatiles [%]: 54.2 (at 500 °C); 52 (at 600 °C); 53.2 (at 700 °C); 60.2 (at 800 °C); 67.6 (at 900 °C) Ash concentration [wt.%]: SiO_2 = 16.6; FeO_3 = 2.4; P_2O_5 = 3.4; Al_2O_3 = 4.5; CaO = 9.8; MgO = 3.7; Na_2O = 0.5; K_2O = 36.9 Note: over 700 °C sintering observed	[240]
Banana	Leaves and stem (Brazil)	Technique: TGA curve analysis Oxidative atmosphere (syntetic air) Comparison between loose and briquetted biomass Heating rate [°C/min]: 10 Operational temperature [°C]: 25–900	Temperature ranges are the same, but there is a lower rate of mass loss in the first stage in loose biomass compared to briquettes First stage temperature range. Leaves: 180–400 °C; Tm [°C]: 280. Stem: 180–360 °C; Tm [°C]: 275 Second stage temperature range: Leaves: 400–580 °C. Stem [°C]: 360–600	[241]
	Leaves (Brazil)	Technique: TGA curve analysis Oxidative atmosphere (syntetic air) Heating rate [°C/min]: 10 Operational temperature [°C]: 22–900 Optical dilatometer at a heating rate [°C/min]: 5 Emissions quantification was carried out in open grill and using a multi flue gas analyzer (5 measurements in 15 min)	Single degradation stage Ti [°C]: ~200; Tm [°C]: ~300; Tb [°C]: ~550 From optical dilatometer: Remaining mass [wt.%]: 98.72 (100 °C); 43.59 (400 °C); 36.32 (899 °C) Max CO_2 release [%]: 0.48 (6 min) Max CO [ppm]: 200 (6 min); 700 (15 min)	[242]

Table 6. *Cont.*

Feedstock	Source	Operation Parameters	Optimum Obtained Results	Ref.
Orange	Bagasse (Greece)	Technique: lab-scale fluidized bed reactor; 2 m height. Reaction time [h]: 4 Minimum fluidization velocity [m/s]: 0.25 Air flow rates [m^3/h]: 4.53–5.94; Excess air ratios [-]: 1.3–1.7 Biomass feed rate [g/min]: 0.84 Bed temperature [°C]: 805–988 Freeboard temperatures [°C]: 810–838	The orange bagasse has a high slagging and fouling tendency. Ash composition [%wt.]: 2.4 (SiO_2); 3.0 (Al_2O_3); 0.2 (Fe_2O_3); 9.4 (MgO); 15.1 (CaO); 4.2 (Na_2O); 37.1 (K_2O); 0.01 (TiO_2); 3.5 (P_2O_5); 0.01 (MnO); 4.7 (SO_3) HHV [MJ/kg]: 16.7 CO heat loses [%]: 1.13 Efficiency [%]: 97.6 Low levels of heavy metals such as Cr, As, Hg and Pb. Toxic elements As, Cd, Hg, Co and Pb ranged from <0.2 ppm to 36 ppm Unburned carbon ashes [%]: 0.50 (bottom ash); 0.70 (fly ash)	[243]
	Bagasse (United Kingdom)	Technique: fixed bed reactor coupled with a mass spectrometer (MS)	EDX orange bagasse [%wt.]: C = 60.2; O = 38.6; K = 0.7; Ca = 0.3; S = 0.2 EDX ashes [%wt.]: C = 35.9; O = 34.5; K = 17.5; Ca = 7.6; P = 1.6: S = 1.4; Mg = 1.0; Cl = 0.4; Si = 0.1 Two stages combustion: 160–370 °C and 440–600 °C Main emissions: N_2O, H_2O, CO_2 and O_2 Low level gas emissions: H_4, H_2, C_2H_6, CH_3CHO, NO and NO_2 Surface area [m^2/g]: 1.89 Pore volume [cm^3/g]: 0.002 Heating rate [°C/min]: 10 Ti [°C]: 260; Tb [°C]: 529; Release heat [W/g]: 1828.6 Heating rate [°C/min]: 20 Ti [°C]: 268; Tb [°C]: 572; Release heat [W/g]: 3294.1 Heating rate [°C/min]: 30 Ti [°C]: 275; Tb [°C]: 632; Release heat [W/g]: 3881.2	[244]

Table 6. *Cont.*

Feedstock	Source	Operation Parameters	Optimum Obtained Results	Ref.
Coconut	Husk	Technique: Lab scale combustion Particle size [μm]: 250–300 Operational temperature [°C]: 650	When Tc (600–750) flue gas main component was HCl (inhibits CO and CO_2 oxidation) When Tc (1000) in flue gas [KCl] 5 times higher than [HCl] Liquid salt solution formation at 600 °C (KCl–NaCle–K_2SO_4–Na_2SO_4) reporting its maximum amount at 720 °C and disappearing at 980 °C Three groups of condensed phases were identified in ash: alkali metal salts (solid and liquid), other solid salts, and solid oxides.	[105]
	Husk-shell (Ghana)	Technique: Pilot scale biochar unit Biomass [kg]: 5 Sample drying time [days]: 3, 6, 9, 12, 15, 18 Direct gas detection from the chimney (no filters)	HHV [MJ/kg]: 11.54 (Uncharred biomass); 21.30 (Charred biomass) CO [ppm](drying time, MC): 9.7 (3 days, 36.4 MC%); 7 (18 days, 10.3 MC%) CO emissions 40% higher than the standard WHO 24-hr AQG (6ppm) Change in smoke color indicates reduction on the volatiles amount and water vapor: thick white (3 days), light smoke (>15 days). PM2.5 [$\mu g/m^3$]: 1200 (3 days); 994 (6–12 days); 1169 (18 days) PM2.5 120% higher than the value indicated by quality guidelines (10 $\mu g/m^3$)	[245]

Table 6. *Cont.*

Feedstock	Source	Operation Parameters	Optimum Obtained Results	Ref.
Sugar cane	Bagasse	Reactor type: Lab-Scale Combustion and gasification Simulator Biomass flow rate [g/h]: 3 Primary air–fuel ration (λ): 0.85 Raw SCB: steam explosion (SE) treated and pelletized Pelletization carried out using a Khal pelletizer 14–175 with a flat-die type AKN1. Grinded pellets size [mm]: 1.0	After steam explosion the SCB ash content increased from 2.2 to 4.7 wt.% SCB (both raw and SE) are primarily composed of Si (35–45 wt.%), K (10–15 wt.%) and Ca, Al, Fe and Mg (5–10 wt.%). SCB slagging propensity is qualified as severe. The slag deposit formed by SE-SCB was less molten and more sintered. SE has positive impact on slagging behavior. Element deposit composition of SCB [wt.%]: 44.3 (O); 29.3 (Si); 7.3 (Fe); 5.5 (Al); 4.6 (K); 2.9 (Ca); 2.6 (C); 1.6 (Ti); 1.2 (Mg) Element deposit composition of SE-SCB [wt.%]: 47.8 (O); 31.8 (Si); 6.4 (Fe); 2.9 (Al); 2.9 (K); 2.5 (Ca); 2.0 (C); 1.6 (Ti); 1.2 (Mg) Specific fouling factor [$(K.m^2)/(W.MJ)$]: 1.66 (SCB); 0.62 (SE-SCB); low fouling factors NOx concentration [g(NO)/GJ fuel]: ~150 (SCB); ~155 (SE-SCB)	[246]
	Bagasse (Chile)	Technique: CFD model. Continuous phase (gas mix): (volatiles, O_2, CO_2, water vapor, CO and N_2) Biomass flow rate [kg/s]: 22.63 at 300 K Air flows [kg/s]: 33.64 at 544 K (primary air); 42.04 at 625 k (secondary air); 7.76 at 544 K (pneumatic air)	Furnace outlet T [°C]: 900 Larger particle size yield a more complete and efficient combustion, but are more likely to reach the rear wall and increase the possibility of slagging. For particle size (1.78 mm): Moisture [%] = 23.50 (grate), 0.00 (exit); Volatiles [%]: 86.60 (grate), 0.11 (exit); Char [%]: 96.67 (grate), 1.67 (exit) Gas flow at furnace exit [g/s]: 5.37 Gas flow components at furnace exit [kg/s]: 7.77 (O_2); 15.27 (CO_2); 18.37 (H_2O); 4.19 (CO); 64.28 (N_2)	[247]

Table 6. *Cont.*

Feedstock	Source	Operation Parameters	Optimum Obtained Results	Ref.
Eucalyptus	Wood and bark (Pakistan)	Technique: TGA curve analysis Heating rate [°C/min]: 25, 35, 45 Operational temperature [°C]: 25–950	Heating rate [25]: Ti [°C]: 260; Tm [°C]: 420; Tb [°C]: 900; CCF: 1.1; Rm [%/s·°C]: 1.9 Heating rate [35]: Ti [°C]: 270; Tm [°C]: 370; Tb [°C]: 930; CCF: 1.5; Rm [%/s·°C]: 3.5 Heating rate [45]: Ti [°C]: 280; Tm [°C]: 540; Tb [°C]: 940; CCF: 1.2; Rm %/s·°C]: 1.8 Insignificant contents of sulfur and nitrogen were detected in the wood, which would reduce the environmental impacts in terms of SOx and NOx emissions. Rm (Mean Reactivity); CCF (Combustion characterization factor)	[248]
	Wood (Chile)	Technique: Combustion in controlled combustion chamber for emissions Wood MC [wt.%]: 0 and 25	Gas pollutants emissions [vol%]: At 0% MC: Max CO_2: 10.66% vol; max CO: 2077 ppm; higher T: 537 °C Combustion efficiency [%]: 93.6 Emissions factor [g/kg]: 38.98 (CO); 1701.62 (CO_2) Emission factor for PM2.5 [g/kg]: 2.01 Emission factors of total PAHs [ng/g]: 5215.47 At 25% MC: Max CO_2: 1.25% vol; max CO: 3742 ppm; higher T: 236 °C Combustion efficiency [%]: 49.3 Emissions factor [g/kg wood): 104.84 (CO); 795.04 (CO_2) Emission factor for PM2.5 [g/kg]: 22.90 Emission factors of total PAHs[ng/g]: 7644.48	[249]

Table 6. *Cont.*

Feedstock	Source	Operation Parameters	Optimum Obtained Results	Ref.
Pinus	Wood (China)	Technique: TGA curve analysis Heating rate [°C/min]: 5 and 40 Operational temperature [°C]: 50–600 Air flow rate [mL/min]: 60	In the study, combustion performance of pine wood was compared with bamboo branches and Lentinus edodes, having the pine wood the best combustion performance. Combustion index [$\times 10^{-7}$%/min^2 K]: 1.97 (5 °C/min), 70.37 (40 °C/min) Flammability index [10^{-4}%/min K2]: 1.12 (5 °C/min), 5.88 (40 °C/min) Ignition index [−2%/min^3]: 0.27 (5 °C/min), 86.70 (40 °C/min) Burn out index [−2%/ min^4]: 0.002 (5 °C/min), 5.296 (40 °C/min)	[250]
	Wood (USA)	Reactor: Integrated Exposure Generation System (platform developed by the authors) Wood MC [%]: 6 and 24 Combustion condition: Flaming (F), Smoldering (S), Incomplete combustion (IC). Final temperature [°C]: 400 (F and IC) and 250 (S), Heating rate [°C/min]: 20 (F, S and IC) O_2 [%vol]: 20.9 (F and S) and 5 (IC)	Bulk inorganic element concentration [wt.%]:0.0468 Relative wood inorganics [%wt.]: 49 (Ca); 15 (K); 14 (Mg); 12 (Al); 4 (S); 2 (Mn); 2 (Na). Gas pollutants: CO emissions [ppm] Moisture effect on [CO ppm]: 63 (6% MC); 49 (24% MC) Combustion condition effect on [CO ppm]: 63 (F); ∼0.3 (S); 13 (IC) VOC emissions [ppb] Moisture effect on [VOC ppb]: 2415 (6% MC); 2436 (24% MC) Combustion condition effect on [VOC ppb]: 2415 (F); 580 (S); 3021 (IC)	[251]
Scenario IV—Gasification				
Soybean	Straw (Brazil)	CFB gasifier in Aspen Plus^{TM} Assumptions: zero-dimensional; steady-state; isothermal conditions; drying and pyrolysis occur instantaneously; inert ashes; char is 100% carbon; fuel-bound N, S, and Cl are converted into NH_3, H_2S, and HCl, respectively; heat loss neglected; thermodynamic model: Peng-Robinson with Boston-Mathias (PR-BM); feedstock particle size and density not influence; gasifier operated below the ash melting point. Temperature [°C]: 779–920.71	Syngas composition [%vol]: 14.07–45.24 (H_2); 5.68–20.88 (CO); 20.58–37.29 (CO_2); 13.12–40.97 (CH_4) HHV syngas [MJ/m^3]: 13.13–18.33 Flow rate syngas [kg/h]: 19.62–21.69 Heat duty gasifier [MJ/kg]: 4.59–8.82 H_2/CO: 1.44–3.92 The cold gas efficiency [%]: 68.46–77.22	[252]

Table 6. *Cont.*

Feedstock	Source	Operation Parameters	Optimum Obtained Results	Ref.
	Straw (Canada)	Fixed bed tubular batch reactor Conditions: subcritical water (300 °C) and supercritical water (400 and 500 °C). Biomass-to-water ratio: 1:5 and 1:10 Biomass particle size [mm]: 0.13 and 0.8 Residence time [min]: 30–60 Pressure range [MPa]: 22–25 Hydrothermal gasification process using Aspen Plus program.	Maximum H_2 yield [mmol/g]: 6.62 Total gas yields [mmol/g]: 14.91 Carbon gasification efficiency [%]: 20.2 Lower heating value [kJ/Nm^3]: 1592 Hydrogen selectivity [%]: 63.0 Product yield [wt.%]: 6.28 ± 0.33–8.13 ± 0.30 (Solid product); 57.92 ± 1.41–75.46 ± 0.64 (Liquid product); 3.14 ± 0.16–4.54 ± 0.01 (gas product). ratio of the experimental yield to the equilibrium yield values of CH_4, CO_2 and H_2 yields for the non-catalytic gasification of soybean straw at 500 °C were 17.9%, 27% and 57.6%.	[57]
Rice	Husk (Brazil)	CFB gasifier in Aspen Plus™ Temperature [°C]: 779–920.71	Syngas composition [%vol]: 15.72–47.72 (H_2); 4.26–19.93 (CO); 21.31–39.57 (CO_2); 11.23–39.19 (CH_4) HHV syngas [MJ/m^3]: 12.42–17.94 Flow rate syngas [kg/h]: 17.03–19.58 Heat duty gasifier [MJ/kg]: 3.46–7.36 H_2/CO: 1.65–4.48 The cold gas efficiency [%]: 66.55–76.29	[252]
	Husk (Indonesia)	Fixed bed downdraft reactor Air at equivalence ratio: 0.15, 0.20, 0.25 Air flows [m^3/h] = 1.07, 1.43, 1.79 Temperature [°C] = 600–800 Reaction time [1/min]: 10–30	Syngas composition; H_2 (8.05%,), CO (15.41%,), CH_4 (<2%). Cold gas efficiency of the gasifier = 72.73% gas yield: 4.33 Nm^3/gas. Tar formed from 5.8 to 53.3 g/Nm^3	[253]
Wheat	Straw (Brazil)	CFB gasifier in Aspen Plus™ Temperature [°C]: 779–920.71	Syngas composition [%vol]: 11.16–41.95 (H_2); 4.70–22.95 (CO); 19.51–38.51 (CO_2); 16.29–43.82 (CH_4) HHV syngas [MJ/m^3]: 13.97–19.50 Flow rate syngas [kg/h]: 20.96–23.03 Heat duty gasifier [MJ/kg]: 8.22–12.91 H_2/CO: 1.00–3.25 The cold gas efficiency [%]: 71.57–81.41	[252]

Table 6. *Cont.*

Feedstock	Source	Operation Parameters	Optimum Obtained Results	Ref.
Corn	Straw (Brazil)	CFB gasifier in Aspen Plus™ Temperature [°C]: 779–920.71	Syngas composition [%vol]: 13.88–44.68 (H_2); 4.51–21.24 (CO); 22.52–42.02 (CO_2); 11.81–37.04 (CH_4) HHV syngas [MJ/m^3]: 12.34–17.27 Flow rate syngas [kg/h]: 19.37–21.78 Heat duty gasifier [MJ/kg]: 3.14–7.08 H_2/CO: 1.38–3.82 The cold gas efficiency [%]: 68.09–77.29	[252]
Coffee	Husk	Reactor type: Fluidized bed gasifier T [°C]: 790 Airrate/Biomassadmission [kg/h/$Nm^{3/}$h]: 0.48	Syngas Composition (vol%): H_2 = 12.4; CO = 11.4; CH_4 = 1.6; CO_2 = 18.7; N_2 = 52.3; C_2H_4 = ~4.36; C_2H_6 = ~1.01; C_2H_2 = ~3.86. HHV (MJ·Nm−3): 3.34	[254]
Banana	Stem	Reactor type: pilot-scale plant Operational temperature [°C]: 368 Biomass [g]: 11.75 Particle size [mm]: 1.84 Atmospheric pressure Catalyzer: Ni/Al_2O_3 [Ni% *w*/*w*]: 1.5, 2.5 and 5 Fluidization agent: superheated water vapor	Gas composition [% molar]: Ni [0%]: 25.79 (H_2); 47.15 (CO_2); 3.87 (CO); 20.32 (C_2H_4); 2.21 (CH_4). HHV [kcal/kg]: 3342.5, LHV [kcal/kg]: 3077.4 Best hydrogen yield: Ni [2.5%]: 51.78 (H_2); 22.54 (CO_2); 0 (CO); 25.01 (C_2H_4); 0.44 (CH_4). HHV [kcal/kg]: 5057.0, LHV [kcal/kg]: 4604.0	[255]
	Peel	Reactor type: fixed bed Heating rate [°C/min]: 10 Gasification agent: Steam (200 °C) Biomass [g]: 1 Operational temperature [°C]: 650–850 Operational time [h]: 2	Ash composition: 3.5 (Ca); 67.3 (K); 2.4 (Na); 2.8 (Si); 21.8 (Cl); 2.2 (other) 50% weight loss (T50) [°C]: 386.1 Best hydrogen yield at 850 °C Carbo conversion efficiency increase as temperature increase having a max near to 70% at 850 °C	[48]

Table 6. *Cont.*

Feedstock	Source	Operation Parameters	Optimum Obtained Results	Ref.
Orange	Bagasse (USA)	Technique: Gasification under TGA curve analysis For gasification: (1) the pyrolysis step at 20 K/min to 800 °C, (2) isothermal step of 15 min to stabilize the weight in the TGA Gasifying agent: 100% CO_2 Particle size [mm]: 0.6–0.8	Reactivity [min^{-1}]: ~0.15 The high reactivity of orange peel char is attributed to its high potassium content (catalytic role) Ash content and inorganic elements [%]: ~3 (ash feed basis); 12 (ash char basis); 0.68 (Ca); 0.007 (Fe); 3.8 (K); 0.11 (Mg); 0.005 (Al); 0.23 (P); 0.14 (S); 0.07 (Si) Inorganic index: 3.65 Time for 95% conversion [min]: 3	[256]
	Bagasse (Italy)	Reactor type: bench-scale fluidized bed reactor Operational temperature [°C]: 700, 750 and 850 Steam to biomass [wt/wt]: 0.5, 0.75, 1 and 1.25 Particle size [mm]: 0.4–1 Biomass flow rate [g/min]: 0.3–2 Gasifying agent: air-steam	Syngas composition and H_2 yields [Nm^3/kgbiom] are function of (S/B) and T. Max H_2 concentration [%vol]: 26.5 (S/B: 1.5; T: 750 °C) Max H_2 yield [Nm^3/kgbiom]: 0.69 (S/B: 1.5; T: 750 °C) Max syngas yield [Nm^3/kgbiom]: 2.45 (S/B: 1.5; T: 750 °C) At 750 °C, as the S/B increases from 0.5 to 1.25, the N_2% vol decreases from 44% to 41% Max carbon efficiency: ~ 0.90 (S/B: 0.5; T: 850 °C) Max cold gas efficiency: 0.64 (S/B: 0.5; T: 850 °C)	[257]
Coconut	Shell (India)	Reactor type: fixed bed downdraft reactor Gasifying medium: air Equivalence ratio (ER): 0.1–0.45	Gas composition: CO [%]: ~11 (ER: 0.1) to ~18 (ER:0.35) H_2 [%]: ~11 (practically constant throughout the process) CH_4 [%]: ~10 (ER: 0.1) to ~ 4 (ER: 0.35) Max HHV [MJ/Nm^3]: 4.229 (ER: 0.35) Specific gas generation [m^3 of gas/kg of fuel]: 2.1 (ER: 0.1); 3.05 (ER: 0.45) Max cold gas efficiency [%]: 72.47 (ER: 0.35) Max hot gas efficiency [%]: 78.37 (ER: 0.35) Optimun operational T [°C]: 900 (ER: 0.35) Tar in gas at optimum operational condition [g/m^3]: 0.62; Particle matter in gas at optimum operational condition [g/m^3]: 0.215	[258]

Table 6. *Cont.*

Feedstock	Source	Operation Parameters	Optimum Obtained Results	Ref.
	Husk (India)	Reactor type: packed bed gasification column Biomass [g]: 20 Particle size [mm]: 0.25, 0.72, 2 and 3 Operational temperature [°C]: 700–850 Heating rate [°C/min]: 50 Gasifying medium: air Air relative humidity [%]: 55–95 Equivalence ratio (ER): 0.1–0.4	Gasification started after 700 °C T effect (p.s: 0.72, ER: 0.1): Max H_2 in flue gas [mole]: 7.67 (800–850 °C) Max CO in flue gas [mole]: ~16 (850 °C) Max CH_4 in flue gas [mole]: 7.17 (700 °C); Max GY [Nm^3/kg]: 0.78 Max carbon conversion (C-conv) [%]: 22.18 Max HHV [MJ/Nm^3]: 4.9 (850 °C) ER effect (p,s: 0.72, T: 800 °C): Max H_2 in flue gas [mole]: ~ 8 (0.1 ER) Max CO in flue gas [mole]: ~18 (0.2 ER) Max CH_4 in flue gas [mole]: 7.41 (0.3 ER); Max GY [Nm^3/kg]: 2.89 Max carbon conversion (C-conv)[%]: 77.53 Max HHV [MJ/Nm^3]: ~5.4 (0.2–0.3) RH effect (p.s: 0.72, T: 800 °C, ER: 0.1): Max H_2 in flue gas [mole]: 10.26 (0.1 ER) Max CO in flue gas [mole]: ~18 (0.2 ER) Max CH_4 in flue gas [mole]: 13.13 (0.3 ER); Max GY [Nm^3/kg]: 1 Max carbon conversion (C-conv)[%]: 42.56 Max HHV [MJ/Nm^3]: 8.81 (95% RH) Biochar specific surface [m^2/g]: 173.42 Total pore vol [cm^3/g]: 0.074733	[259]

Table 6. *Cont.*

Feedstock	Source	Operation Parameters	Optimum Obtained Results	Ref.
Sugarcane	Bagasse	Technique: Simulation in ASPEN Gasification process divided in four steps: heating and drying, pyrolysis, gas–solid reactions, and gas phase reactions. Zero-dimensional and time independent reactions were considered. The model is considered in thermodynamic equilibrium, it is not necessary the use of reaction kinetics or hydrodynamics of the reactor. Gasification temperature [°C]: 100–1000Steam to biomass [wt/wt]: 0.3–1	The higher the steam temperature, the higher the LHV [MJ/kg]: ~14.8 (100 °C); ~15.0 (600 °C); ~15.2 (1000 °C) The higher the air temperature, the higher the LHV [MJ/kg]:~14.55 (10 °C); ~15.0 (40 °C); ~15.3 (60 °C) The higher the gasification temperature, the higher the LHV [MJ/kg]: ~14.38 (600 °C); ~14.85 (600 °C); ~15.1 (1200 °C) Max LHV as a function of S/B between 0.5 and 0.6: ~15.05 Average LHV [MJ/kg]: 14.9 Syngas composition [%]: 45–40 (CO_2); 31–35 (CO); 16–19 (CH_4); 3–6 (H_2); 0.3 (N_2) Dry flue gas composition [%]: 69.24 (N_2); 19.61 (CO_2); 11.15 (H_2O)	[260]
	Bagasse	Technique: Simulation (tri-generation system) The biomass was assumed free of ash, dry, N and S and comprising C, H and O. Biomasses are gasified into the gasifier using the waste heat of the Homogenous Charge Compression Ignition (HCCI) engine Operational temperature [°C]: 600 LHV [kJ/mole]: 467 Q_{in}. Gasification [kW]: 2.33	Syngas composition [%wt.]: 48.08 (H_2); 18.86 (CO); 24.29 (CO_2); 8.77 (CH_4) Cold gas efficiency [%]: 73 Hydrogen efficiency [%]: 34 Exergy efficiency of gasifier [%]: 90 Exergy results [kW]: 3538 (biomass); 83.51 (steam); 1.536 (gasifier inlet heat); 3243 (syngas)	[261]
Eucalyptus	Wood	Reactor: Batch using $NiFe_2O_4$ as a catalyzer Operational temperature [°C]: 400, 450 and 500 Residence time [min]: 30, 40 and 60 Catalyst amount (Cat) [g]: 0, 1 and 2 Gasification agent: Super critical water (SCW)	Under same T, as increase the catalyst increase the GY Rx (450 °C, 30 min): best GY[wt.%]: 58.28 (1 g cat); best conversion[%]: 89.12 (2 g cat] Rx (450 °C, 40 min): best GY[wt.%]: 52.57 (1 g cat); best conversion[%]: 92.84 (2 g cat] Rx (450 °C, 60 min): best GY[wt.%]: 48.19 (1 g cat); best conversion[%]: 95.49 (2 g cat] Highest GY [wt.%]: 65.94 (60 min, 500 °C, 2 g cat) Highest H_2 [mol%]: 22.69 (60 min, 450 °C, 2 g cat) HGE (60 min, 450 °C) [%]: 11.1 (0 g cat); 30.62 (2 g cat) CGE (60 min, 450 °C) [%]: 69.6 (0 g cat); 97.03 (2 g cat)	[248]
	Wood	Reactor: pilot scale bubbling fluidized bed Biomass flow rate (bfr) [kg/h]: 57.8 to 94 Bed reactor temperature [°C]: 700–900 Gasification agent: air	Highest H_2 [mol%]: 14.7 (94 kg/h bfr, 764 °C) Highest cold gas efficiency [%]: 0.74 (64.5 kg/h bfr, 846 °C) Highest CGE [%]: 0.94 (kg/h bfr, 887 °C) Highest syngas LHV [MJ/m^3): 5.9 (95.5 kg/h bfr, 795 °C)	[262]

Table 6. *Cont.*

Feedstock	Source	Operation Parameters	Optimum Obtained Results	Ref.
Pinus	Wood	Technique: Aspen Plus simulation Operational temperature [°C]: 700, 750, 800, 850 and 900 Particle size [mesh]: 60, 80, 100 Steam-to-biomass mass (S/B): 0, 0.7, 1.4, 2.1 and 2.8 Gasification agent: Steam (200 °C) Biomass flow rate [g/min]: 3	Syngas composition [%vol] at 900 °C: 100 mesh: 25.24 (CO); 32.74 (H_2); 2.28 (CH_4); 12.12 (CO_2) 80 mesh: 52.83 (CO); 30.53 (H_2); 1.95 (CH_4); 14.69 (CO_2). Best performance 60 mesh: 54.49 (CO); 25.89 (H_2); 1.79 (CH_4); 16.96 (CO_2) Temperature effect at mesh 80 (700 to 900 °C): CO and CH_4 decreases by 4.17% and 6.95%, respectively. H_2 and CO_2 increased by 5.43% and 5.69%, respectively. Optimal T [°C]: 850. S/B effect at mesh 80 and 850°C (0.7 to 2.8): CO and CH4 decreases by 19.52% and 1.9%, respectively. H_2 and CO_2 increased by 6.78% and 13.74%, respectively. Optimal S/B: 1.4	[263]
	Wood (Brazil)	Reactor: downdraft gasifier and combustion engine coupled to a power generator. Not SteadyState entirely operation Particle size [cm]:1–2.5	Syngas composition [%wt.]: 12.72 (H_2); 24.78 (CO); 11.1 (CO_2); 2.1 (CH_4). LHV [MJ/kg]: 5.51 1 kg of produced gas requires about 0.64 kg of air. Average E/R: 0.26 Average Cold gas efficiency [%]: 69.4 (18% lower than manufacturer announcement)	[264]
Scenario V—Fast Pyrolysis (Substitutes for Fuel Oil)				
Soybean	Hull (Brazil)	Reactor: fluidized bed reactor Reactor loaded with 800 g of inert material (sand) Temperature [°C]: 550 Velocity of the fluidizing gas (nitrogen) [cm/s]: 150 Biomass feeding rate [kg/h]: 40	Average yield [%]: 45 (bio-oil); 33 (char); 22 (non-condensable gases). In the organic phase, the three main compounds identified in soybean hull bio-oil were: phenol (14.88%), 2-methylphenol (7.59%) and 4-methylphenol (12.55%). Bio-oil organic: 64.66 wt.% (C); 6.68 wt.% (H); 5.80 wt.% (N); 1.17 wt.% (S); 21.69 wt.% (O); 24.28 MJ/kg (HHV); 22.83 MJ/kg (LHV) Bio-oil aqueous: 13.31 wt.% (C); 2.15 wt.% (H); 3.01 wt.% (N); 0.42 wt.% (S); 81.11 wt.% (O); 6.89MJ/kg (HHV); 6.42 MJ/kg (LHV)	[265]
	Straw	Bubbling fluidized bed reactor Temperature [°C]: 500	Average yield [%]: 67 (biooil); 28.5 (biochar); 4.25 (syngas) Bio-oil organic: 67.24 wt.% (C); 47.37 wt.% (H); 50.34 wt.% (O)	[266]

Table 6. *Cont.*

Feedstock	Source	Operation Parameters	Optimum Obtained Results	Ref.
Rice	Husk (Brazil)	Reactor: Laboratory-scale fluidized bed with a SiC bed. Feed rates [g/L]: 875 Carrier gas to biomass ratio [wt/wt]: 0.8 Temperatures [°C]: 450, 525, and 600 SiC bed heights [cm]: 4.9 and 6.5	Product yield: 43% (max liquid); 31% (organics); 12% (water); 32% (solids); 25% (gas and losses).	[267]
Corn	Stalk (USA)	Temperature [°C]: 400–450 Acid pretreated and untreated corn stalks were pyrolyzed Feed rate [kg/h]: 1–2.5	Average yield [%]: 35–46 (biooil); 20.4–29 (biochar); 4.4–32 (syngas) Elemental analysis untreated stalk bio-oil: 19.05% C, 9.31% H, 0.17% N, 71.46% remaining. Acid-treated stalk bio-oil: 24.88% C, 5.33% H, 0% N, 69.79% remaining	[268]
Coffee	Husk (Brazil)	Biomass in [g]: 100 g Stirring rate [rpm]: 64 Heating rate [°C/min]: 20 T [°C]: 500	Yield [%]: SY (26.2–28.7); LY (47.5–56.5); NCGY (18.6–24.8) Biochar composition [% db]: C (73.75 ± 0.5); H (1.99 ± 0.1); N (1.90 ± 0.2); O (6.00 ± 0.3) HHV biochar [MJ/kg]: 24.6 ± 0.28 LHV biochar [MJ/kg]: 23.16 ± 0.26 Proximate analysis biochar [wt.% db]: VM (9.5 ± 1.18); FC (73.5 ± 1.48); AC (17 ± 0.63) MC [wt.% wb]: 1.89 ± 0.14 Apparent density biochar [kg/m^3]: 401 ± 6 Specific density biochar [kg/m^3]: 770 ± 10 Porosity biochar [−]: 0.48 Moisture aqueous phase (at different temperature ranges) [%wb]: 82.05 ± 0.24 (25–200 °C); 77.22 ± 0.22 (200–250 °C); 61.09 ± 0.29 (250–300 °C); 55.31 ± 0.37 (300–350 °C); 29.55 ± 0.23(350–400 °C); 22.76 ± 0.22 (400–500 °C) HHV aqueous phase (at different temperature ranges) [MJ/kg]: 16.77 ± 0.45 (25–200 °C); 17.17 ± 0.40 (200–250 °C); 21.75 ± 0.33 (250–300 °C); 27.87 ± 0.38 (300–350 °C); 30.63 ± 0.42(350–400 °C); 33.51 ± 0.29 (400–500 °C) pH aqueous phase (at different temperature ranges) [−]: 3.63 ± 0.01 (25–200 °C); 4.12 ± 0.01 (200–250 °C); 4.74 ± 0.01 (250–300 °C); 6.44 ± 0.01 (300–350 °C); 7.87 ± 0.01 (350–400 °C); 8.19 ± 0.01 (400–500 °C)	[269]

Table 6. *Cont.*

Feedstock	Source	Operation Parameters	Optimum Obtained Results	Ref.
Banana	Leaves (India)	Technique: TGA curve analysis Particle size [µm]: 250 Heating rate [°C/min]: 10, 20, 30 Operational temperature [°C]: 22–900	Heating rate [10]: Ti [°C]: 151.5; Tb [°C]: 493; Tm [°C]: 297 Max mass decomposition [µg/min]: 437 Heating rate [20]: Ti [°C]: 159; Tb [°C]: 499; Tm [°C]: 304 Max mass decomposition [µg/min]: 652 Heating rate [30]: Ti [°C]: 163; Tb [°C]: 506; Tm [°C]: 316 Max mass decomposition [µg/min]: 1131	[270]
	Leaves (Brazil)	Reactor type: pilot-scale plant Fluidization agent: air Flow gas rate [Nm^3/h]: 15 Operational temperature [°C]: 500 Biomass feed rate [kg/h]: 0.84	Tm [°C]: 340 LY [wt.%]: 27; SY [wt.%]: 23.3; GY [wt.%]: 49.6 Bio-oil: two phases (light and heavy) Heavy oil composition [%]: 55.9 (CO_2); 7.8 (H_2); 0.87 (N_2); 0.08 (S); 35.3 (O_2). HHV [MJ/kg]: 25.0 Light oil composition [%]: 16.9 (CO_2); 8.8 (H_2); (N_2); 0.01 (S); 74.3 (O_2). HHV [MJ/kg]: 1.2 Biochar: Proximate analysis [wt.%]: 1.68 (MC); 53.2 (VM); 23.2 (FC); 23.5 (AC) Ultimate analysis [wt.%]: 48.0 (C); 3.2 (H); 1.2 (N); 0.33 (S)HHV [MJ/kg]: 18.2 Total process energy consumption: 5.58 kWh	[271]
Orange	Bagasse	Reactor type: Conical Spouted Bed Reactor. Residence time[min]: 50 min Specifications: Reactor, cyclone and filter are located in a hot box heated to 290 C to avoid condensation of heavy compounds. Particle size [µm]: 1000 Biomass flow rate [$g.min^{-1}$]: 1 N_2 flow rate [$L.min^{-1}$]: 7 Operational temperature [°C]: 425, 500 and 600	SY [wt%]: 33 (425 °C); 29 (500 °C); 27 (600 °C); LY [wt%]: 54.6 (425 °C); 54.9 (500 °C); 49 (600 °C) GY [wt%]: 12 (425 °C); 16 (500°); 24 (600 °C); Gas: Composition (vol%): Mainly CO_2 and CO (45–80%); C1-C4, H_2 and CH_4 (detected but not specified). LHV [$MJ.m^{-3}$]: 8.5 (600 °C). Bio-oil (500 °C): Composition [%wt]: Alcohols = 4.74; Ketone = 13.98; Furans = 21.47; Phenols = 1.71; Saccharides = 2.88; Nitrogenous compounds = 0.51; Hydrocarbons = 0.02; Unidentified = 7.2; Water = 40.81 Bio-char (600 °C): Composition [wt%]: C= 72.9; H= 2.6; N= 1.4; O= 12.2; Proximate analysis [wt%]: VM= 26.9; FC= 72.2; AC= 10.9. HHV [MJ/kg]: 27.5 Surface area [m^2/g]: 4.8 Pore volume [m^3/g]: 0.003	[158]

Table 6. *Cont.*

Feedstock	Source	Operation Parameters	Optimum Obtained Results	Ref.
Bagasse		Reactor type: Pyrex glass semi-batch. Specifications: Ice cold water is feed directly to the straight condenser using a miniature submersible pump to condense the pyrolysis vapors into liquid. Three different batches were performed, varying final temperature, heat rate and gas flow rate. Particle size [μm]: 425 Biomass [g]: 30 Operational temperature [°C]: 350, 375, 400, 425, 450, 475, 500, 525, 550, 575 and 600 Heating rate [°C/min]: 25, 50, 75 and 100 N_2 flow rate [L/min]: 0.1, 0.2, 0.3, 0.4 and 0.5	Batch 1: highest pyrolysis oil yield of 28.04 wt% at 525 °C, heating rate of 25 °C/min and N_2 gas flow rate of 0.1 L/min. T [350–600 °C]: SY [wt%]: 56.71–28.26; LY [wt%]: 16.38–26.20; GY [wt%]: 20.76–37.83 Mass loss [wt%]: 1.2–3.24 Pyrolysis-gas: H_2/C molar ratio: 0.04; Flow rate [L/min]: 0.09; Volume [mL]: 2030; GCV [MJ/m^3]: 5.19 Batch 2: highest pyrolysis oil yield of 34.03 wt% at 75 °C/min, constant temperature of 525 °C and N_2 gas flow rate of 0.1 L/min Heating rate [25–100 °C/min]: SY [wt%]: 33.02–24.87; LY [wt%]: 28.04–33.62; GY [wt%]: 31.37–34.89 Mass loss [wt%]: 2.61–3.11 Pyrolysis-gas: H_2/C molar ratio: 0.04; Flow rate [L/min]: 0.12; Volume [ml]: 2270; GCV [MJ/m^3]: 5.47 Batch 3: highest pyrolysis oil yield of 35.53 wt% at N_2 gas flow rate of 0.2 L/min at 525 °C and heating rate of 75 °C/min N_2 flow rate [0.1–0.5 °C/min]: SY [wt%]: 22.66–22.37; LY [wt%]: 34.03–30.41; GY [wt%]: 31.90–39.58 Mass loss [wt%]: 2.94–4.96 Pyrolysis-gas: H_2/C molar ratio: 0.04; Flow rate [L/min]: 0.15; Volume [mL]: 2360; GCV [MJ/m^3]: 5.49 Bio-char: Composition [wt%]: C = 70.13; H = 4.26; N = 0.61; O = 24.97; S = 0.03; proximate analysis [wt%]: MC = 2.14; VM = 41.26; FC = 53.58; AC = 3.02. HHV [MJ/kg]: 27.67 Molecular weight [g/mol]: 13.13; Surface area [m^2/g]: 23.17; Pore Volume [m^3/g]: 1.52×10^{-5} Other elements [%wt]: Si = 1.01; Mn = 0.82; Fe = 0.36; Co = 0.05; Al = 78.76 Bio-oil: Composition [wt%]: C = 54.20; H = 5.99; N = 0.02; O = 39.75; S = 0.04; AC = 1.31 HHV [MJ/kg]: 21.72. Molecular weight [g/mol]: 22.79; Total Acid Number [mgKOH/mL]: 24.73; pH = 3.21; Water content [%wt] = 21.30; Kinematic viscosity [40 °C, cSt] = 23.58; Kinematic viscosity [100 °C, cSt] = 10.11; Density [gm/cc, 15 °C] = 0.98; Flash point [°C] = 71; Fire point [°C] = 91; IBP [°C] = 93; FBP [°C] = 321	[102]

Table 6. *Cont.*

Feedstock	Source	Operation Parameters	Optimum Obtained Results	Ref.
Coconut	Shell (China)	Reactors: microwave and fixed-bed reactor Catalyst (cat): Conventional ZSM-5 zeolites and ZSM-5 (25) @SBA-15	LY [%]: 42 (ZSM-5), 68 (ZSM-5 (25)@SBA-15) Hydrocarbon yield [%]: 146 (ZSM-5), 200 (ZSM-5 (25)@SBA-15) The phenol selectivity was greater than 70% of the area, regardless of the catalyst. Microwave reactor enhanced the conversion of phenols to hydrocarbons For phenolic-rich bio-oil (14.3 wt.%) is recommended the combination of the fixed-bed reactor and core–shell hierarchical ZSM-5@SBA-15. For hydrocarbon-rich bio-oil (6 wt.%) is recommended the combination of microwave reactor and core–shell hierarchical ZSM-5@SBA-15.	[272]
	Shell (Iran)	Reactor type: fixed-bed reactor Particle size [μm]: <150 Heating rate [°C.min-1]: 100 Flow gas rate (Ar) [mL/min]: 30 Operational temperature [°C]: 500 Reaction time [min]: 30	Tm [°C]: 333 LY [wt%]: 50.25; SY [wt%]: 29.0; GY [wt%]: 20.75 Gas product composition [vol%]: 58.0 (CO_2); 18.5 (CO); 10.9 (H_2); 9.9 (CH_4); 2.7 (C2–C4) Gas product LHV [MJ/Nm^3]: 8.85; H^2/CO ratio [-]: 0.59 Bio-oil relative components concentration [%]: 23.5 (hydrocarbon); 6.1 (alcohol); 4.2 (acid); 35.3 (phenol); 10.7 (ketone); 7.1 (ester); 5 (ether); 3.5 (furfural) Biochar specific surface [$m^{2/}$g]: 26.22 Av pore diameter [nm]: 9.35 Total pore vol [cm^3/g]: 0.084	[273]
Sugarcane	Bagasse	Type: reaction (semi batch reactor) Operational temperature [°C]: 500–700 Heating rate [°C/min]: 10 Particle size [mm]: 0.5 N_2 flow rate [ml/min]: 200	Best oil characteristics performance at 700 °C Density [kg/m^3]: 988 Viscosity [cSt]: 9.4 Acid number [mg KO/g]: 44.7 pH: 3 Flash point [°C]: 130 Heating value [MJ/kg]: 4.3 Total phenol content [%]: 58.89	[274]

Table 6. *Cont.*

Feedstock	Source	Operation Parameters	Optimum Obtained Results	Ref.
Eucalyptus	Bagasse	Type: reaction (semi batch reactor) Operational temperature [°C]: 350–650 Heating rate [°C/min]: 10 and 50 Particle size [mm]: <0.25–1.7 N_2 flow rate [cm^3/min]	Heating rate [°C/min]: 10 Ti [°C]: 160; Tb [°C]: 500; Tm [°C]: 311 (peak 1); 440 (peak 2); LY [wt.%]: 29.41 (350 °C); 42.29 (500 °C); 38.82 (650 °C) SY [wt.%]:49.45 (350 °C); 23.47 (650 °C) GY [wt.%]: 21.14 (350 °C); 37.71 (650 °C) Heating rate [°C/min]: 10 LY [wt.%]: 31.25 (350 °C); 45.23 (500 °C); 40.39 (650 °C) SY [wt.%]:47.41 (350 °C); 24.88 (650 °C) GY [wt.%]: 21.34 (350 °C); 34.73 (650 °C) Max LY[wt.%]:45.23 (500 °C, 50 °C/min); 45.03 (particle size 0.5 mm); 44.95 (N_2 flow 100 cm^3/min) Bio-oil composition [wt.%]: 65.64 (C); 26.67 (O); 6.97 (H); 0.96 (N); 0.03 (S) Bio-oil density [kg/m^3]: 1039 Bio-oil kinetic viscosity [cSt, 40 °C]: 14.20 HHV [MJ/kg]: 27.75	[275]
	Wood	Microwave-assisted pyrolysis (for high nitrogen-containing compounds (NCCs)) Catalyst (cat): MoO_3 Cat ratios (Wood/MoO3): 1/1, 2/1 and 3/1 Operational temperature [°C]: 550	Raw wood yields [wt%]: LY: 34.12; SY: 23.78; GY: 42.1. HHV [MJ/kg]: 17.4. NCCs in bio-oil [%]: 7.81 (raw); 15.32 (1/1); Highest LY [wt%]: 41.66 (2/1) Highest GY [wt%]: 54.37 (1/1)	[276]
	Wood (Brazil)	Pilot scale: fluidized bed Biomass flow rate [kg/h]: 20 Poor O_2 atmosphere Operational temperature [°C]: 500 Fluidization gas flow [Nm^3/h]: 15	SY [wt%]: 14. Composition [wt%]: 0.38 (N_2), 67.18 (C), 3.86 (H_2). HHV [MJ/kg]: 26.38 LY [wt%]: 53. Composition [wt%]: 0.17 (N_2), 53.63 (C), 7.37 (H_2). HHV [MJ/kg]: 22.39 Bio-oil properties: 30% heavy fraction and 22% light fraction. Sulfur content [mg.kg-1]: 85. Density (at 20) [kg/m^3]: 1225.6. pH: 3.3. Water content [wt%]: 14.2 Volatile organic compounds [wt%]: 0.40 (methanol), 0.27 (ethanol), 0.04 (acetone), 11.22 (acetic acid), 0.01 (furfural)	[277]

Table 6. *Cont.*

Feedstock	Source	Operation Parameters	Optimum Obtained Results	Ref.
	Wood (Brazil)	Auto-thermal SDB-20 pilot-scale plant Feed rate [kg/h]: 15.06 Temperature [°C]: 480 ± 8 Fluidization agent: Air supplied by a blower at 13 Nm^3/h, and recirculation gases, supplied by a fan at 7 Nm^3/h. Quartz sand (Quartzo Brasil Minas 403/050) of 1300 kg/m^3	Heavy bio-oil energy yield of 30% and 21.4 MJ kg^{-1} lower heating value	[278]
Pinus	Wood	Reactor: fixed bed reactor Operational temperature [°C]: 500 Fluidization agent: N_2, H_2, CO_2 and CH_4 Biomass [g]: 5 Particle size [μm]: >125 Heat rate [°C·min^{-1}]: 10	Fluidization agents: CH_4: Highest biomass conversion (76.90%). CO content of 93.58% H_2: Promote non-condensable gases formation but lower LY CH_4 and CO_2: LY of 27.77 wt% N_2: Max HHV of 22.62 MJ/kg	[279]
	Wood	Pilot scale. Thermomechanical pretreatment. Pretreatment: wood heated at 173 °C, for 3, 24, and 72 min, impregnated or not with acid citric (CA) solution 1.5 wt% Pyrolysis: Reactor: bubbling fluidized bed Biomass flow rate [kg/h]:0.4–0.7 Operational temperature [°C]: 450	Raw wood yields [wt%]: LY: 54.70; SY: 17.18; GY: 19.18. HHV [MJ·kg^{-1}]: 17.4 Highest LYs [wt%]: 60.56 (72 min, no CA), HHV [MJ/kg]: 18.6; 61.62 (3 min + CA), HHV [MJ/kg]: 18.1 highest HHV [MJ/kg]: 18.9 (24 min + CA)	[270]

RT—retention time; SHF—separate hydrolysis and fermentation, PSSF—simultaneous saccharification and fermentation; SSF—simultaneous saccharification and fermentation; BBP—Biogas potential; BMP—methane potential; OLR—Organic loads rates; VSS—volatile suspended solids; VDS—volatile dissolved solids; TOC—total organic carbon.

5. Carbon Potential

Five scenarios for carbon release or carbon sequestration potentials were evaluated:

(I) Biomass to bioethanol to replace gasoline;
(II) Anaerobic digestion for biogas production;
(III) Direct combustion for power generation;
(IV) Gasification to replace natural gas;
(V) Fast pyrolysis for bio-oil production as substitutes for fuel oil.

The established scenarios aim to sequester the CO_2 emissions by reducing the fossil fuel utilization.

To calculate the carbon potential by each scenario, Equation (8) was applied, based on the methodology described in the literature [280].

$$TC_{scenario} = C^{fossil\ fuel}_{renewable\ fuel} \cdot \sum_{i=1}^{n} y_i \cdot P_i \cdot Y_i \quad (8)$$

where $TC_{scenario}$ is the total carbon potential, y_i is the yield of renewable fuel production from associated biomass in a specific scenario, P_i is the annual production of the crop, Y_i is the equivalent fuel reference described in each scenario considerations and $C^{fossil\ fuel}_{renewable\ fuel}$ is the carbon potential ratio of the renewable fuel to fossil fuel.

Approximately 276 Tg was the overall carbon content, from the studied agro-forest residues with a potential of 1014 Tg CO_2 production by uncontrolled burning. The carbon sequestration potential for each scenario and biomass is shown in Table 7. According to the Intergovernmental Panel on Climate Change (ICPP) [281], open burning can also generate significant amounts of NOx that, if not treated, will produce environmental damage. The global warming effect of N_2O is nearly 300 times greater than that of CO_2. Another important concern is related to the waste remaining in cultivation area until they are broken down by microorganisms that produce greenhouse gases such as methane. By utilizing these remains for energy generation, not only does it eliminate them from the field and decrease environmental contamination, but it also adds value to the waste.

Table 7. Carbon potential analysis.

	Agricultural Residues									Wood Residues	
	Soybean	**Corn**	**Sugarcane**	**Rice**	**Wheat**	**Coffee**	**Banana**	**Orange**	**Coconut**	**Eucalyptus**	**Pinus**
Carbon content (Tg)	84.8	6.0	163.7	7.8	4.1	0.4	8.3	0.9	0.6	74.3	16.9
Carbon sequestration (Tg-CO_2)	310.9	22.2	599.8	28.7	15.0	1.5	30.4	3.4	2.4	273	61.9
Scenario I—Bioethanol production											
Biothanol potential (v/w%)	29.27	35.04	40.15	33.65	37.43	37.06	24.43	15.58	31.47	39.7	38.9
Ethanol (GL)	56.01	4.74	143.69	5.91	3.59	0.33	5.25	0.34	0.39	60.0	13.9
Equivalent gasoline (GL)	40.27	3.41	103.31	4.25	2.58	0.24	3.77	0.24	0.28	43.1	10.0
CO_2 emission from biethanol production	5.60	0.47	14.37	0.59	0.36	0.03	0.52	0.03	0.04	6.0	1.4
Carbon sequestration (Tg-CO_2)	85.37	7.23	219.02	9.01	5.47	0.51	8.00	0.52	0.59	91.4	21.1
Scenario II—biogas production											
Biogas potential (Gm^3)	105.2	7.6	226.4	9.0	5.8	0.6	12.4	4.8	0.8	91.6	21.6
Equivalent energy (PJ)	2240.0	162.5	4821.9	191.9	122.6	11.8	264.3	102.3	18.0	1950	460
Carbon sequestration (Tg CO_2-eq)	136.6	9.9	294.1	11.7	7.5	0.7	16.1	6.2	1.1	119	28.1
Scenario III—Combustion											
Heat value (MJ/kg)	16.9	17.2	16.3	16.6	14.6	16.9	15.5	15.5	17.8	17.8	17.8
Harvested Energy (PJ)	3230.5	232.3	5814.9	290.7	140.0	15.1	333.8	33.6	21.8	2694	636
Equivalent Coal (Tg)	125.7	9.0	226.3	11.3	5.4	0.6	13.0	1.3	0.8	105	24.7
Carbon sequestration (Tg CO_2)	289.1	20.8	520.4	26.0	12.5	1.4	29.9	3.0	2.0	241	56.9
Scenario IV—Gasification (ar)											
Heat value of gas (MJ/Nm^3)	6.0	6.0	6.0	6.0	6.0	6.0	6.0	6.0	6.0	6.00	6.00
Harvested Energy (PJ)	2295.9	162.5	4294.1	210.8	115.0	10.8	257.7	26.1	14.7	1813	428
Equivalent Natural gas (Nm^3)	62.1	4.4	116.1	5.7	3.1	0.3	7.0	0.7	0.4	49.0	11.6
Carbon sequestration (Tg)	133.4	9.4	249.5	12.2	6.7	0.6	15.0	1.5	0.9	105	24.9
Scenario V—fast-pyrolysis (substitutes for fuel oil)											
Heat value of bio-oil (MJ/kg)	20.0	20.0	20.0	20.0	20.0	20.0	20.0	20.0	20.0	20.0	20.0
Harvested Energy (PJ)	1913.3	135.4	3578.4	175.6	95.9	9.0	214.7	21.7	12.2	1511	357
Equivalent fuel oil (Tg)	44.5	3.1	83.2	4.1	2.2	0.2	5.0	0.5	0.3	35.1	8.3
Carbon sequestration (Tg) (fuel oil)	133.4	9.4	249.4	12.2	6.7	0.6	15.0	1.5	0.9	105	24.8

In the first scenario, the following considerations were established. The type of the biomass, the process parameters, including enzyme loading and medium acidity, have a significant impact on bioethanol production yield [282]. Moreover, it was estimated that the CO_2 emissions required to create 1 GL of bioethanol are approximately 0.1 Tg, as stated by Hudiburg et al. [283], and that the volumetric energy density of ethanol is roughly 72% higher than that of gasoline. As a result, about 64 Tg of CO_2 emission from the conversion of biomass to bioethanol from the residual biomasses was calculated.

The average pure biogas production yield of 0.7 m^3 from each kg of volatile solids [284] and LHV of 21.3 MJ/m^3 [285] was considered in the scenario II. To calculate mass and energy yield produced by the biogas, the results were combined with the biomass volatile matter. As a result,, the biogas production from main Brazilian agro-forest residues was around 67 Gm^3, and the potential energy production was 7935 PJ/yr and 2663 PJ/yr for agricultural and wood residues, respectively. The emission rate for natural gas of 61 g CO_2-eq for each produced MJ [280,284] was considered to calculate the biomass total carbon sequestration. Approximately 484 Tg/yr and 825 Tg/yr of total biogas carbon potential was calculated for agricultural and wood residues.

In scenario III, an average generation of 26 MJ energy per kg of coal [286] that leads to the emission of 2.3 kg CO_2 (90.5 g CO_2/MJ) was assumed [287]. Coal is one of the most important sources of energy worldwide with an increasing market. At the same time, the CO_2 emissions from coal-fired power facilities account for over 28% [286]. Biomass co-firing can be integrated to coal-fired power plants without the need for high investment to reduce cost and GHG emissions [288]. Similarly, biomass co-firing was used in the residential sector, mainly in the form of bio-coal briquettes combustion [289,290]. Approximately 3639 Tg/yr of CO_2-eq from the studied biomasses for co-combustion with coal in power plants was determined.

Gasification is one of the most attractive options for converting biomass into high-quality synthetic liquid and gaseous fuels [210]. For scenario IV, it was assumed that 1 Nm^3 of natural gas produce on average 37 MJ energy [289] and leads to the emission of 1.86 kg CO_2-eq (53.06 g CO_2/MJ) [280]. From the studied samples, the total carbon sequestration potential by gasification was approximately1229 Tg CO_2eq. As gasification, pyrolysis is one of the most researched processes for thermochemical biomass conversion. Fuel oil can be replaced with liquid fuel from pyrolysis in any application requiring static heating or electricity generation. In scenario V, the average bio-oil production yield was assumed to range from 26% to 75% [193,290,291]. As a result,, bio-oil production from studied biomass residues was around 410 Tg bio-oil, with LHV of bio-oil from 16 to 22.95 MJ/kg [138,193,290]. According to EPA [280], the emission factor for fuel-oil combustion is about 69.7 g CO_2-eq per MJ. Thus, approximately 1228 Tg CO_2eq total carbon potential given a fuel–oil average energy content of 43 MJ/kg [289].

Brazil has historically had a robust sugar cane production industry and the ethanol production expanded enormously largely due to strong governmental incentives and pro-ethanol legislation. However, bio-oil technologies and production in Brazil are still far from the ethanol ones. It will require more time, incentives and regulations for production and use. Research is needed to reduce the costs of production of biomass-based fuels in Brazil.

6. Summary, Conclusions and Outline

Brazil is one of the world's major agro-forest producers and activities arising from harvesting and processing agro-forest products result in large biomass residual generation. Brazil produces over 679.5 million tons of agricultural residues with an energy potential of 1257 PJ, mainly from sugarcane, soybean and banana crop residues. Additionally, to wood residues—*Eucalyptus* sp. and *Pinus* sp., with 3098 and 6200 PJ/yr, respectively.

The biomass data were used to determine the CO_2 potential from biomasses in renewable energy practices such as bioethanol production, anaerobic digestion, direct combustion, gasification and fast pyrolysis as substitutes for fossil fuel utilization. The total carbon content from agricultural residues was about 276 Tg, which has the potential to generate approximately 1014 Tg of CO_2 by uncontrolled burning. For wood residues, the carbon contents were calculated to be 151 Tg/yr for *Eucalyptus* and 35.6 Tg/yr for *Pine*. The studied Brazilian biomasses have high potential to be used in renewable energy practices for sustainable development.

Author Contributions: Conceptualization, E.P.R.A. and C.M.-M.; methodology, E.P.R.A., O.S.-P., J.N. and C.M.-M.; writing—original draft preparation, E.P.R.A., O.S.-P., J.N. and C.M.-M.; writing—review and editing, E.P.R.A., O.S.-P., J.N., S.E. and C.M.-M.; visualization, E.P.R.A., O.S.-P., J.N., S.E.; supervision, C.M.-M. All authors have read and agreed to the published version of the manuscript.

Funding: The authors gratefully acknowledge the funding from the Academy of Finland for the project "Role of forest industry transformation in energy efficiency improvement and reducing CO_2 emissions", grant number 315019.

Data Availability Statement: Data are contained within the article: sources for utilized data are given in this article.

Conflicts of Interest: The authors declare no conflict of interest.

References

1. IEA. *International Energy Agency—Data and Statistics*; IEA: Paris, France, 2022.
2. Zou, C.; Xiong, B.; Xue, H.; Zheng, D.; Ge, Z.; Wang, Y.; Jiang, L.; Pan, S.; Wu, S. The role of new energy in carbon neutral. *Pet. Explor. Dev.* **2021**, *48*, 480–491. [CrossRef]
3. Antar, M.; Lyu, D.; Nazari, M.; Shah, A.; Zhou, X.; Smith, D.L. Biomass for a sustainable bioeconomy: An overview of world biomass production and utilization. *Renew. Sustain. Energy Rev.* **2021**, *139*, 110691. [CrossRef]
4. Kim, S.H.; Kumar, G.; Chen, W.H.; Khanal, S.K. Renewable hydrogen production from biomass and wastes (ReBioH2-2020). *Bioresour. Technol.* **2021**, *331*, 125024. [CrossRef]
5. Edenhofer, O.; Madruga, R.P.; Sokona, Y.; Seyboth, K.; Matschoss, P.; Kadner, S.; Zwickel, T.; Eickemeier, P.; Hansen, G.; Schlömer, S.; et al. *Renewable Energy Sources and Climate Change Mitigation: Special Report of the Intergovernmental Panel on Climate Change*; Cambridge University Press: Cambridge, UK, 2011. [CrossRef]
6. Agência Nacional de Energia Elétrica, Sistema de Informações de Geração da ANEEL-SIGA. 2023. Available online: https://www.gov.br/aneel/pt-br/ (accessed on 24 April 2023).
7. Mendoza Martinez, C.L.; Alves Rocha, E.P.; Oliveira Carneiro, A.D.C.; Borges Gomes, F.J.; Ribas Batalha, L.A.; Vakkilainen, E.; Cardozo, M. Characterization of residual biomasses from the coffee production chain and assessment the potential for energy purposes. *Biomass Bioenergy* **2019**, *120*, 68–76. [CrossRef]
8. Climate Watch. Historical GHG Emissions. 2021. Available online: https://www.climatewatchdata.org/ (accessed on 25 April 2023).
9. *Building an Environmental Powerhouse Brazil 2045—Volume 1—Environmental Policy Proposals for 2023–2024; Observatorio Do Clima: Rio de Janeiro*. 2022. Available online: https://www.oc.eco.br/wp-content/uploads/2022/05/2045-EN%E2%80%94VF.pdf (accessed on 24 April 2023).
10. Mapbiomas Brasil. Available online: https://mapbiomas.org/ (accessed on 24 April 2023).
11. Tišma, M.; Bucić-Kojić, A.; Planinić, M. Bio-based Products from Lignocellulosic Waste Biomas. *Chem. Biochem. Eng. Q* **2021**, *35*, 139–156. [CrossRef]
12. Usmani, Z.; Sharma, M.; Karpichev, Y.; Pandey, A.; Chandra Kuhad, R.; Bhat, R.; Punia, R.; Aghbashlo, M.; Tabatabaei, M.; Gupta, V.K. Advancement in valorization technologies to improve utilization of bio-based waste in bioeconomy context. *Renew. Sustain. Energy Rev.* **2020**, *131*, 109965. [CrossRef]
13. Oasmaa, A.; Fonts, I.; Pelaez-Samaniego, M.R.; Garcia-Perez, M.E.; Garcia-Perez, M. Pyrolysis Oil Multiphase Behavior and Phase Stability: A Review. *Energy Fuels* **2016**, *30*, 6179–6200. [CrossRef]
14. Anex, R.P.; Aden, A.; Kazi, F.K.; Fortman, J.; Swanson, R.M.; Wright, M.M.; Satrio, J.A.; Brown, R.C.; Daugaard, D.E.; Platon, A. Techno-economic comparison of biomass-to-transportation fuels via pyrolysis, gasification, and biochemical pathways. *Fuel* **2010**, *89*, S29–S35. [CrossRef]
15. Statista. *Agricultural Sector's Share of GDP in Brazil 2020*. 2022. Available online: https://www.statista.com/statistics/1075019/brazil-agriculture-share-gdp/ (accessed on 24 April 2023).
16. IBÁ. *Annual Report 2020 Brazilian Tree Industry*; IBÁ: Sao Paulo, Brazil, 2020.
17. IBA. *Brazilian Tree Industry-Annual Report, Brazilian Tree Industry*; IBÁ: Sao Paulo, Brazil, 2016.

18. IBGE. *Average Yield, per Harvest Year and Crop Yield*; IBGE: Rio de Janeiro, Brazil, 2022. Available online: https://www.ibge.gov.br/ (accessed on 24 April 2023). (In Portuguese)
19. FAOSTAT. *Crops and Livestock Products*. 2022. Available online: https://www.fao.org/faostat/en/#data/ (accessed on 24 April 2023).
20. IBGE. *Agriculture and Livestock Census 2017*; IBGE: Rio de Janeiro, Brazil, 2018. Available online: https://www.ibge.gov.br/ (accessed on 24 April 2023).
21. Ullah, K.; Kumar Sharma, V.; Dhingra, S.; Braccio, G.; Ahmad, M.; Sofia, S. Assessing the lignocellulosic biomass resources potential in developing countries: A critical review. *Renew. Sustain. Energy Rev.* **2015**, *51*, 682–698. [CrossRef]
22. Singh, J.; Panesar, B.S.; Sharma, S.K. Energy potential through agricultural biomass using geographical information system—A case study of Punjab. *Biomass Bioenergy* **2008**, *32*, 301–307. [CrossRef]
23. CONAB. *Brazilian Grain Harvest*; Ministry of Agriculture, Livestock and Supply: Manaus, Brazil, 2021.
24. Sruamsiri, S. Agricultural wastes as dairy feed in Chiang Mai. *Anim. Sci. J.* **2007**, *78*, 335–341. [CrossRef]
25. Roozen, A. *Availability of Sustainable Lignocellulosic Biomass Residues in Brazil for Export to the EU*; Universiteit Utrecht: Utrecht, The Netherlands, 2015.
26. Ferreira-Leitao, V.; Gottschalk, L.M.F.; Ferrara, M.A.; Nepomuceno, A.L.; Molinari, H.B.C.; Bon, E.P.S. Biomass residues in Brazil: Availability and potential uses. *Waste Biomass Valorization* **2010**, *1*, 65–76. [CrossRef]
27. Meena, S.K.; Sahu, R.; Ayothiraman, R. Utilization of Waste Wheat Straw Fibers for Improving the Strength Characteristics of Clay. *J. Nat. Fibers* **2019**, *18*, 1404–1418. [CrossRef]
28. CONAB. *Brazilian Coffee Harvest*; Ministry of Agriculture, Livestock and Supply: Manaus, Brazil, 2021.
29. De Castro Pereira Brainer, M.S. Coconut: Production and market. *Cad Setorial ETENE* **2021**, *206*, 1–13. (In Portuguese)
30. CONAB. *Brazilian Sugarcane Harvest*; Ministry of Agriculture, Livestock and Supply: Manaus, Brazil, 2021.
31. IBGE. *Systematic Survey of Agricultural Production*; IBGE: Rio de Janeiro, Brazil, 2022. Available online: https://www.ibge.gov.br/ (accessed on 24 April 2023).
32. Wadhwa, M.; Bakshi, M.P.S.; Makkar, H.P.S. Waste to worth: Fruit wastes and by-products as animal feed. *CAB Rev.* **2015**, *2015*, 10. [CrossRef]
33. CitrusBR. *Brazilian Orange Juice: En Route to Sustainability*; CitrusBR: São Paulo, Brazil, 2012. Available online: https://issuu.com/citrusbr/docs/folder_citrus__ingles_vers_o_site (accessed on 25 April 2023).
34. Bundhoo, Z.M.A. Potential of bio-hydrogen production from dark fermentation of crop residues: A review. *Int. J. Hydrog. Energy* **2019**, *44*, 17346–17362. [CrossRef]
35. World Agricultural production. *World Rice Production by Country 2022/2023*. 2022. Available online: http://www.worldagriculturalproduction.com/crops/rice.aspx/ (accessed on 5 February 2023).
36. Ahmad, S.; Zhu, X.; Wei, X.; Zhang, S. Influence of process parameters on hydrothermal modification of soybean residue: Insight into the nutrient, solid biofuel, and thermal properties of hydrochars. *J. Environ. Manag.* **2021**, *283*, 111981. [CrossRef]
37. USDA. *Production, Supply and Distribution—Market and Trade Data*; USDA: Washington, D.C., USA, 2023.
38. Ratna, A.S.; Ghosh, A.; Mukhopadhyay, S. Advances and prospects of corn husk as a sustainable material in composites and other technical applications. *J. Clean. Prod.* **2022**, *371*, 133563. [CrossRef]
39. Aghaei, S.; Karimi Alavijeh, M.; Shafiei, M.; Karimi, K. A comprehensive review on bioethanol production from corn stover: Worldwide potential, environmental importance, and perspectives. *Biomass Bioenergy* **2022**, *161*, 106447. [CrossRef]
40. Zhao, Y.; Damgaard, A.; Christensen, T.H. Bioethanol from corn stover—A review and technical assessment of alternative biotechnologies. *Prog. Energy Combust. Sci.* **2018**, *67*, 275–291. [CrossRef]
41. FAO. Land use in agriculture by the numbers. Sustainable Food and Agriculture. Food and Agriculture Organization of the United Nations. Available online: https://www.fao.org/faostat/en/#data/ (accessed on 24 April 2023).
42. Pighinelli, A.L.M.T.; Boateng, A.A.; Mullen, C.A.; Elkasabi, Y. Evaluation of Brazilian biomasses as feedstocks for fuel production via fast pyrolysis. *Energy Sustain. Dev.* **2014**, *21*, 42–50. [CrossRef]
43. ANP. *Oil, Natural Gas and Biofuels Statistical Yearbook 2022—Português (Brasil)*; ANP: Brasilia, DF, Brazil, 2022.
44. Mendoza Martinez, C.L.; Saari, J.; Melo, Y.; Cardoso, M.; de Almeida, G.M.; Vakkilainen, E. Evaluation of thermochemical routes for the valorization of solid coffee residues to produce biofuels: A Brazilian case. *Renew. Sustain. Energy Rev.* **2021**, *137*, 110585. [CrossRef]
45. Pereira, B.S.; de Freitas, C.; Vieira, R.M.; Brienzo, M. Brazilian banana, guava, and orange fruit and waste production as a potential biorefinery feedstock. *J. Mater. Cycles Waste Manag.* **2022**, *24*, 2126–2140. [CrossRef]
46. Mendes, F.B.; Delmondes, K.L.; Hassan, D.; Barros, J.H.T. Economic, Social and Environmental Perspectives on Organic Residues from Brazilian Amazonian Fruits (Acre). In Proceedings of the World Congress on Engineering and Computer Science, San Francisco, CA, USA, 22–24 October 2019.
47. Redondo-Gómez, C.; Quesada, M.R.; Astúa, S.V.; Zamora, J.P.M.; Lopretti, M.; Vega-Baudrit, J.R. Biorefinery of Biomass of Agro-Industrial Banana Waste to Obtain High-Value Biopolymers. *Molecules* **2020**, *25*, 3829. [CrossRef]
48. Anniwaer, A.; Chaihad, N.; Zhang, M.; Wang, C.; Yu, T.; Kasai, Y.; Abudala, A.; Guan, G. Hydrogen-rich gas production from steam co-gasification of banana peel with agricultural residues and woody biomass. *Waste Manag.* **2021**, *125*, 204–214. [CrossRef]
49. Sawarkar, A.N.; Kirti, N.; Tagade, A.; Tekade, S.P. Bioethanol from various types of banana waste: A review. *Bioresour. Technol. Rep.* **2022**, *18*, 101092. [CrossRef]

50. Prastuti, O.P.; Septiani, E.L.; Kurniati, Y.; Widiyastuti, S.H. Banana Peel Activated Carbon in Removal of Dyes and Metals Ion in Textile Industrial Waste. *Mater. Sci. Forum* **2019**, *966*, 204–209. [CrossRef]
51. Umaru, I.J.; Umaru, H.A.; Umaru, K.I. Extraction of essential oils from coconut agro-industrial waste. In *Extraction of Natural Products from Agro-industrial Wastes*, 1st ed.; Elservier: New Delhi, India, 2023; pp. 303–318. [CrossRef]
52. De la Torre, I.; Martin-Dominguez, V.; Acedos, M.G.; Esteban, J.; Santos, V.E.; Ladero, M. Utilisation/upgrading of orange peel waste from a biological biorefinery perspective. *Appl. Microbiol. Biotechnol.* **2019**, *103*, 5975–5991. [CrossRef]
53. Biel-Nielsen, T.L.; Li, K.; Sørensen, S.O.; Sejberg, J.J.P.; Meyer, A.S.; Holck, J. Utilization of industrial citrus pectin side streams for enzymatic production of human milk oligosaccharides. *Carbohydr. Res.* **2022**, *519*, 108627. [CrossRef]
54. Christofi, A.; Tsipiras, D.; Malamis, D.; Moustakas, K.; Mai, S.; Barampouti, E.M. Biofuels production from orange juice industrial waste within a circular economy vision. *J. Water Process. Eng.* **2022**, *49*, 103028. [CrossRef]
55. Simões, L.M.S.; Setter, C.; Sousa, N.G.; Cardoso, C.R.; de Oliveira, T.J.P. Biomass to biofuel densification of coconut fibers: Kinetic triplet and thermodynamic evaluation. *Biomass Convers. Biorefinery* **2022**, *12*, 1–18. [CrossRef]
56. Brookes, G. Farm income and production impacts from the use of genetically modified (GM) crop technology 1996-2020. *GM Crops Food* **2022**, *13*, 171–195. [CrossRef]
57. Okolie, J.A.; Nanda, S.; Dalai, A.K.; Kozinski, J.A. Hydrothermal gasification of soybean straw and flax straw for hydrogen-rich syngas production: Experimental and thermodynamic modeling. *Energy Convers. Manag.* **2020**, *208*, 112545. [CrossRef]
58. Xian, S.; Xu, Q.; Feng, Y. Simultaneously remove organic pollutants and improve pyrolysis gas quality during the co-pyrolysis of soybean straw and oil shale. *J. Anal. Appl. Pyrolysis* **2022**, *167*, 105665. [CrossRef]
59. Chen, D.; Cen, K.; Gan, Z.; Zhuang, X.; Ba, Y. Comparative study of electric-heating torrefaction and solar-driven torrefaction of biomass: Characterization of property variation and energy usage with torrefaction severity. *Appl. Energy Combust. Sci.* **2022**, *9*, 100051. [CrossRef]
60. Leng, S.; Li, W.; Han, C.; Chen, L.; Chen, J.; Fan, L.; Lu, Q.; Li, J.; Leng, L.; Zhou, W. Aqueous phase recirculation during hydrothermal carbonization of microalgae and soybean straw: A comparison study. *Bioresour. Technol.* **2020**, *298*, 122502. [CrossRef]
61. Jiang, Y.; Havrysh, V.; Klymchuk, O.; Nitsenko, V.; Balezentis, T.; Streimikiene, D. Utilization of Crop Residue for Power Generation: The Case of Ukraine. *Sustainability* **2019**, *11*, 7004. [CrossRef]
62. Namsaraev, Z.B.; Gotovtsev, P.M.; Komova, A.V.; Vasilov, R.G. Current status and potential of bioenergy in the Russian Federation. *Renew. Sustain. Energy Rev.* **2018**, *81*, 625–634. [CrossRef]
63. Vijay, V.; Kapoor, R.; Singh, P.; Hiloidhari, M.; Ghosh, P. Sustainable utilization of biomass resources for decentralized energy generation and climate change mitigation: A regional case study in India. *Environ. Res.* **2022**, *212*, 113257. [CrossRef]
64. Krička, T.; Matin, A.; Voća, N.; Pospišil, A.; Grubor, M.; Šaronja, I.; Jurišić, V. Changes in nutritional and energy properties of soybean seed and hull after roasting. *Res. Agric. Eng.* **2018**, *64*, 96–103. [CrossRef]
65. Toro-Trochez, J.L.; DE Haro Del Río, D.A.; Sandoval-Rangel, L.; Bustos-Martínez, D.; García-Mateos, F.J.; Ruiz-Rosas, R.; Rodríguez-Mirasol, J.; Cordero, T.; Carrillo-Pedraza, E.S. Catalytic fast pyrolysis of soybean hulls: Focus on the products. *J. Anal. Appl. Pyrolysis* **2022**, *163*, 105492. [CrossRef]
66. Fitri Faradilla, R.H.; Lucia, L.; Hakovirta, M. Hydrothermal carbonization of soybean hulls for the generation of hydrochar: A promising valorization pathway for low value biomass. *Environ Nanotechnology. Monit. Manag.* **2021**, *16*, 100571. [CrossRef]
67. Huang, Y.F.; Chen, W.R.; Chiueh, P.T.; Kuan, W.H.; Lo, S.L. Microwave torrefaction of rice straw and pennisetum. *Bioresour. Technol.* **2012**, *123*, 1–7. [CrossRef] [PubMed]
68. Zhang, C.; Yang, W.; Chen, W.H.; Ho, S.H.; Pétrissans, A.; Pétrissans, M. Effect of torrefaction on the structure and reactivity of rice straw as well as life cycle assessment of torrefaction process. *Energy* **2022**, *240*, 122470. [CrossRef]
69. Kai, X.; Meng, Y.; Yang, T.; Li, B.; Xing, W. Effect of torrefaction on rice straw physicochemical characteristics and particulate matter emission behavior during combustion. *Bioresour. Technol.* **2019**, *278*, 122730. [CrossRef]
70. Chen, C.; Qu, B.; Wang, W.; Wang, W.; Ji, G.; Li, A. Rice husk and rice straw torrefaction: Properties and pyrolysis kinetics of raw and torrefied biomass. *Environ. Technol. Innov.* **2021**, *24*, 101872. [CrossRef]
71. Chen, D.; Chen, F.; Cen, K.; Cao, X.; Zhang, J.; Zhou, J. Upgrading rice husk via oxidative torrefaction: Characterization of solid, liquid, gaseous products and a comparison with non-oxidative torrefaction. *Fuel* **2020**, *275*, 117936. [CrossRef]
72. Naqvi, M.; Yan, J.; Dahlquist, E.; Naqvi, S.R. Off-grid electricity generation using mixed biomass compost: A scenario-based study with sensitivity analysis. *Appl. Energy* **2017**, *201*, 363–370. [CrossRef]
73. Cheng, X.; Huang, Z.; Wang, Z.; Ma, C.; Chen, S. A novel on-site wheat straw pretreatment method: Enclosed torrefaction. *Bioresour. Technol.* **2019**, *281*, 48–55. [CrossRef]
74. Bai, X.; Wang, G.; Sun, Y.; Yu, Y.; Liu, J.; Wang, D.; Wang, Z. Effects of combined pretreatment with rod-milled and torrefaction on physicochemical and fuel characteristics of wheat straw. *Bioresour. Technol.* **2018**, *267*, 38–45. [CrossRef]
75. Gao, X.; Zhou, Z.; Coward, B.; Wang, J.; Tian, H.; Yin, Y.; Cheng, Y. Improvement of wheat (T. aestivum) straw catalytic fast pyrolysis for valuable chemicals production by coupling pretreatment of acid washing and torrefaction. *Ind. Crop. Prod.* **2022**, *187*, 115475. [CrossRef]
76. Biswas, B.; Pandey, N.; Bisht, Y.; Singh, R.; Kumar, J.; Bhaskar, T. Pyrolysis of agricultural biomass residues: Comparative study of corn cob, wheat straw, rice straw and rice husk. *Bioresour. Technol.* **2017**, *237*, 57–63. [CrossRef] [PubMed]

77. Suman, S.; Gautam, S. Physicochemical Performance of Wood Chips Char and Wheat Husk Char for Utilisation as an Alternate Source of Energy. *Int. J. Recent Technol. Eng.* **2020**, *8*, 2876–2880. [CrossRef]
78. Rajkumar, P.; Murugavelh, S. Co-pyrolysis of wheat husk and residual tyre: Techno-economic analysis, performance and emission characteristics of pyro oil in a diesel engine. *Bioresour. Technol. Rep.* **2022**, *19*, 101164. [CrossRef]
79. Brlek, T.; Bodroza-Solarov, M.; Vuckovic, J.; Levic, J. Utilization of Spelt Wheat Hull as a Renewable Energy Source by Pelleting758 Agricultural Academy. *Bulg. J. Agric. Sci.* **2012**, *18*, 752.
80. Santos, J.; Ouadi, M.; Jahangiri, H.; Hornung, A. Integrated intermediate catalytic pyrolysis of wheat husk. *Food Bioprod. Process.* **2019**, *114*, 23–30. [CrossRef]
81. Han, S.; Bai, L.; Chi, M.; Xu, X.; Chen, Z.; Yu, K. Conversion of Waste Corn Straw to Value-Added Fuel via Hydrothermal Carbonization after Acid Washing. *Energies* **2022**, *15*, 1828. [CrossRef]
82. Liu, Y.; Rokni, E.; Yang, R.; Ren, X.; Sun, R.; Levendis, Y.A. Torrefaction of corn straw in oxygen and carbon dioxide containing gases: Mass/energy yields and evolution of gaseous species. *Fuel* **2021**, *285*, 119044. [CrossRef]
83. Wang, Q.; Sun, S.; Zhang, X.; Liu, H.; Sun, B.; Guo, S. Influence of air oxidative and non-oxidative torrefaction on the chemical properties of corn stalk. *Bioresour. Technol.* **2021**, *332*, 125120. [CrossRef]
84. Chen, D.; Cen, K.; Cao, X.; Li, Y.; Zhang, Y.; Ma, H. Restudy on torrefaction of corn stalk from the point of view of deoxygenation and decarbonization. *J. Anal. Appl. Pyrolysis* **2018**, *135*, 85–93. [CrossRef]
85. Maj, G.; Szyszlak-Bargłowicz, J.; Zajac, G.; Słowik, T.; Krzaczek, P.; Piekarski, W. Energy and Emission Characteristics of Biowaste from the Corn Grain Drying Process. *Energies* **2019**, *12*, 4383. [CrossRef]
86. Walmsley, T.G.; Varbanov, P.S.; Su, R.; Klemeš, J.J.; Tippayawong, N.; Rerkkriangkrai, P.; Aggarangsi, P.; Pattiya, A. Characterization of Biochar from Pyrolysis of Corn Residues in a Semi-continuous Carbonizer. *Chem. Eng. Trans.* **2018**, 70. [CrossRef]
87. Klaas, M.; Greenhalf, C.; Ouadi, M.; Jahangiri, H.; Hornung, A.; Briens, C.; Aggarangsi, P.; Pattiya, A. The effect of torrefaction pre-treatment on the pyrolysis of corn cobs. *Results Eng.* **2020**, *7*, 100165. [CrossRef]
88. Phuakpunk, K.; Chalermsinsuwan, B.; Assabumrungrat, S. Comparison of chemical reaction kinetic models for corn cob pyrolysis. *Energy Rep.* **2020**, *6*, 168–178. [CrossRef]
89. Setter, C.; Silva, F.T.M.; Assis, M.R.; Ataíde, C.H.; Trugilho, P.F.; Oliveira, T.J.P. Slow pyrolysis of coffee husk briquettes: Characterization of the solid and liquid fractions. *Fuel* **2020**, *261*, 116420. [CrossRef]
90. Mukherjee, A.; Okolie, J.A.; Niu, C.; Dalai, A.K. Experimental and Modeling Studies of Torrefaction of Spent Coffee Grounds and Coffee Husk: Effects on Surface Chemistry and Carbon Dioxide Capture Performance. *ACS Omega* **2022**, *7*, 638–653. [CrossRef]
91. Tadesse, Y.; Kassahun, S.K.; Kiflie, Z. Effects of operational parameters on torrefaction performance of coffee husk and cotton stalk mixed biomass: A surface response methodology approach. *Biomass. Convers. Biorefinery* **2021**, *2021*, 1–16. [CrossRef]
92. Singh, R.K.; Pandey, D.; Patil, T.; Sawarkar, A.N. Pyrolysis of banana leaves biomass: Physico-chemical characterization, thermal decomposition behavior, kinetic and thermodynamic analyses. *Bioresour. Technol.* **2020**, *310*, 123464. [CrossRef]
93. Alves, J.L.F.; da Silva, J.C.G.; Sellin, N.; de Prá, F.B.; Sapelini, C.; Souza, O.; Marangoni, C. Upgrading of banana leaf waste to produce solid biofuel by torrefaction: Physicochemical properties, combustion behaviors, and potential emissions. *Environ. Sci. Pollut. Res.* **2021**, *29*, 25733–25747. [CrossRef]
94. Mosqueda, A.; Medrano, K.; Gonzales, H.; Takahashi, F.; Yoshikawa, K. Hydrothermal treatment of banana leaves for solid fuel combustion. *Biofuels* **2019**, *12*, 1123–1129. [CrossRef]
95. Espinosa, E.; Tarrés, Q.; Domínguez-Robles, J.; Delgado-Aguilar, M.; Mutjé, P.; Rodríguez, A. Recycled fibers for fluting production: The role of lignocellulosic micro/nanofibers of banana leaves. *J. Clean Prod.* **2018**, *172*, 233–238. [CrossRef]
96. Taib, R.M.; Abdullah, N.; Aziz, N.S.M. Bio-oil derived from banana pseudo-stem via fast pyrolysis process. *Biomass Bioenergy* **2021**, *148*, 106034. [CrossRef]
97. Rambo, M.K.D.; Schmidt, F.L.; Ferreira, M.M.C. Analysis of the lignocellulosic components of biomass residues for biorefinery opportunities. *Talanta* **2015**, *144*, 696–703. [CrossRef] [PubMed]
98. Li, C.; Liu, G.; Nges, I.A.; Deng, L.; Nistor, M.; Liu, J. Fresh banana pseudo-stems as a tropical lignocellulosic feedstock for methane production. *Energy Sustain. Soc.* **2016**, *6*, 27. [CrossRef]
99. Prawisudha, P.; Azka, G.R.; Triyono, B.; Pasek, A.D. Multi-production of solid fuel and liquid fertilizer from organic waste by employing wet torrefaction process. *AIP Conf. Proc.* **2018**, *1984*, 30008. [CrossRef]
100. Virmond, E.; De Sena, R.F.; Albrecht, W.; Althoff, C.A.; Moreira, R.F.P.M.; José, H.J. Characterisation of agroindustrial solid residues as biofuels and potential application in thermochemical processes. *Waste Manag.* **2012**, *32*, 1952–1961. [CrossRef]
101. Alves, J.L.F.; da Trindade, E.O.; da Silva, J.C.G.; Mumbach, G.D.; Alves, R.F.; Barbosa Filho, J.M.; De Athayde-Filho, P.F.; De Sena, R.F. Lignocellulosic Residues from the Brazilian Juice Processing Industry as Novel Sustainable Sources for Bioenergy Production: Preliminary Assessment Using Physicochemical Characteristics. *J. Braz. Chem. Soc.* **2020**, *31*, 1939–1948. [CrossRef]
102. Bhattacharjee, N.; Biswas, A.B. Pyrolysis of orange bagasse: Comparative study and parametric influence on the product yield and their characterization. *J. Environ. Chem. Eng.* **2019**, *7*, 102903. [CrossRef]
103. Bhattacharjee, N.; Biswas, A.B. Physicochemical analysis and kinetic study of orange bagasse at higher heating rates. *Fuel* **2020**, *271*, 117642. [CrossRef]
104. Bardone, E.; Bravi, M.; Keshavarz, T.; Zanella, K.; Gonçalves, J.L.; Taranto, O.P. Charcoal Briquette Production Using Orange Bagasse and Corn Starch. *Chem. Eng. Trans.* **2016**, *49*, 313–318. [CrossRef]

105. Jerzak, W.; Kuźnia, M. Examination of inorganic gaseous species and condensed phases during coconut husk combustion based on thermodynamic equilibrium predictions. *Renew. Energy* **2021**, *167*, 497–507. [CrossRef]
106. Nakason, K.; Pathomrotsakun, J.; Kraithong, W.; Khemthong, P.; Panyapinyopol, B. Torrefaction of Agricultural Wastes: Influence of Lignocellulosic Types and Treatment Temperature on Fuel Properties of Biochar. *Int. Energy J.* **2019**, *19*, 253–266.
107. Wang, Q.; Sarkar, J. Pyrolysis behaviors of waste coconut shell and husk biomasses. *Int. J. Energy Prod. Manag.* **2018**, *3*, 34–43. [CrossRef]
108. Lee, Y.T.; Ng, H.K.; Gan, S.; Jourabchi, S.A. Thermochemical upgrading of coconut husk and rubber seed to coal co-firing feedstock via torrefaction. *IOP Conf. Ser. Earth Environ. Sci.* **2019**, *354*, 12074. [CrossRef]
109. Meriño Stand, L.; Valencia Ochoa, G.; Duarte Forero, J. Energy and exergy assessment of a combined supercritical Brayton cycle-orc hybrid system using solar radiation and coconut shell biomass as energy source. *Renew. Energy* **2021**, *175*, 119–142. [CrossRef]
110. Ahmad, R.; Ahmahdi, S.M.; Mohamed, A.R.; Abidin, C.Z.A.; Kasim, N.N. Pretreatment of Coconut Shell by Torrefaction for Pyrolysis Conversion. *IOP Conf. Ser. Earth Environ. Sci.* **2021**, *920*, 12002. [CrossRef]
111. Da Silva, J.C.G.; Alves, J.L.F.; de Araujo Galdino, W.V.; de Sena, R.F.; Andersen, S.L.F. Pyrolysis kinetics and physicochemical characteristics of skin, husk, and shell from green coconut wastes. *Energy Ecol. Environ.* **2019**, *4*, 125–132. [CrossRef]
112. Akogun, O.A.; Waheed, M.A. Property Upgrades of Some Raw Nigerian Biomass through Torrefaction Pre-Treatment- A Review. *J. Phys. Conf. Ser.* **2019**, *1378*, 32026. [CrossRef]
113. Nanda, S.; Isen, J.; Dalai, A.K.; Kozinski, J.A. Gasification of fruit wastes and agro-food residues in supercritical water. *Energy Convers. Manag.* **2016**, *110*, 296–306. [CrossRef]
114. Toscano Miranda, N.; Lopes Motta, I.; Maciel Filho, R.; Wolf Maciel, M.R. Sugarcane bagasse pyrolysis: A review of operating conditions and products properties. *Renew. Sustain. Energy Rev.* **2021**, *149*, 111394. [CrossRef]
115. Canettieri, E.V.; da Silva, V.P.; Neto, T.G.S.; Hernández-Pérez, A.F.; da Silva, D.D.V.; Dussán, K.J.; Maria de Carvalho, J.A. Physicochemical and thermal characteristics of sugarcane straw and its cellulignin. *J. Braz. Soc. Mech. Sci. Eng.* **2018**, *40*, 416. [CrossRef]
116. dos Reis Ferreira, R.A.; da Silva Meireles, C.; Assunção, R.M.N.; Reis Soares, R. Heat required and kinetics of sugarcane straw pyrolysis by TG and DSC analysis in different atmospheres. *J. Therm. Anal. Calorim.* **2018**, *132*, 1535–1544. [CrossRef]
117. Halder, P.; Kundu, S.; Patel, S.; Parthasarathy, R.; Pramanik, B.; Paz-Ferreiro, J.; Maria de Carvalho, J.A. TGA-FTIR study on the slow pyrolysis of lignin and cellulose-rich fractions derived from imidazolium-based ionic liquid pre-treatment of sugarcane straw. *Energy Convers. Manag.* **2019**, *200*, 112067. [CrossRef]
118. Schmitt, C.C.; Moreira, R.; Neves, R.C.; Richter, D.; Funke, A.; Raffelt, K.; Shah, K. From agriculture residue to upgraded product: The thermochemical conversion of sugarcane bagasse for fuel and chemical products. *Fuel Process Technol.* **2020**, *197*, 106199. [CrossRef]
119. Kanwal, S.; Chaudhry, N.; Munir, S.; Sana, H. Effect of torrefaction conditions on the physicochemical characterization of agricultural waste (sugarcane bagasse). *Waste Manag* **2019**, *88*, 280–290. [CrossRef] [PubMed]
120. Manatura, K. Inert torrefaction of sugarcane bagasse to improve its fuel properties. *Case Stud. Therm. Eng.* **2020**, *19*, 100623. [CrossRef]
121. Da Veiga, P.A.S.; Cerqueira, M.H.; Gonçalves, M.G.; da Matos, T.T.S.; Pantano, G.; Schultz, J.; De Andrade, J.D.; Mangrich, A.S. Upgrading from batch to continuous flow process for the pyrolysis of sugarcane bagasse: Structural characterization of the biochars produced. *J. Environ. Manag.* **2021**, *285*, 112145. [CrossRef]
122. Pena-Vergara, G.; Castro, L.R.; Gasparetto, C.A.; Bizzo, W.A. Energy from planted forest and its residues characterization in Brazil. *Energy* **2022**, *239*, 122243. [CrossRef]
123. Rocha, E.P.A.; Gomes, F.J.B.; Sermyagina, E.; Cardoso, M.; Colodette, J.L. Analysis of Brazilian Biomass Focusing on Thermochemical Conversion for Energy Production. *Energy Fuels* **2015**, *29*, 7975–7984. [CrossRef]
124. Silva, F.T.M.; Ataíde, C.H. Valorization of eucalyptus urograndis wood via carbonization: Product yields and characterization. *Energy* **2019**, *172*, 509–516. [CrossRef]
125. Sette, C.R.; Hansted, A.L.S.; Novaes, E.; Lima, P.A.F.; Rodrigues, A.C.; de Santos, D.R.S.; Yamaji, F.M. Energy enhancement of the eucalyptus bark by briquette production. *Ind. Crop. Prod.* **2018**, *122*, 209–213. [CrossRef]
126. de Paula Protásio, T.; Scatolino, M.V.; de Araújo, A.C.C.; de Oliveira, A.F.C.F.; de Figueiredo, I.C.R.; de Assis, M.R.; Trugilho, P.M. Assessing Proximate Composition, Extractive Concentration, and Lignin Quality to Determine Appropriate Parameters for Selection of Superior Eucalyptus Firewood. *BioEnergy Res.* **2019**, *12*, 626–641. [CrossRef]
127. Loxley, T.A. *Within-Tree Fuel Quality of Loblolly Pine (Pinus taeda)*; Auburn University: Auburn, AL, USA, 2018.
128. Acquah, G.E.; Via, B.K.; Gallagher, T.; Billor, N.; Fasina, O.O.; Eckhardt, L.G. High Throughput Screening of Elite Loblolly Pine Families for Chemical and Bioenergy Traits with Near Infrared Spectroscopy. *Forests* **2018**, *9*, 418. [CrossRef]
129. Park, J.; Hung, I.; Gan, Z.; Rojas, O.J.; Lim, K.H.; Park, S. Activated carbon from biochar: Influence of its physicochemical properties on the sorption characteristics of phenanthrene. *Bioresour. Technol.* **2013**, *149*, 383–389. [CrossRef]
130. Pacheco, J.M.; Lima, R.; Sehgal, D.; Anderson, R.; Mangueira, F.; Coelho, S.T.; Filho, A.F. Quantification analysis unravels significance of residual biomass of Pinus taeda L. *Aust. J. Basic Appl. Sci.* **2020**, *14*, 1–9. [CrossRef]
131. Tanger, P.; Field, J.L.; Jahn, C.E.; DeFoort, M.W.; Leach, J.E. Biomass for thermochemical conversion: Targets and challenges. *Front. Plant Sci.* **2013**, *4*, 218. [CrossRef]

132. Demirbas, A. Thermochemical Conversion Processes. In *Green Energy Technologies*, 1st ed.; Springe: London, UK, 2009; pp. 261–304. [CrossRef]
133. Brito, F.M.S.; Paes, J.B.; da Oliveira, J.T.S.; Arantes, M.D.C.; Neto, H.F. Anatomical and Physical Characterization of the Giant Bamboo (Dendrocalamus giganteus Munro) (In Portuguese). *Floresta Ambient* **2015**, *22*, 559–566. [CrossRef]
134. Leoncio Paiva, H.; Neutzling Bierhals, A.; dos Santos Guimarrães, V.; Carlos Marafon, A.; Dias Santiago, A.; Felipe Câmara Amaral, A. Drying of elephant grass biomass for direct combustion. (In Portuguese). In Proceedings of the Congresso Acadêmico Integrado de Inovação e Tecnologia—CAIITE, Alagoas, Brazil, 8–10 November 2016.
135. dos Santos, G.R.V.; Jankowsky, I.P.; de Andrade, A. Characteristic drying curve for Eucalyptus grandis lumber. *Sci. For.* **2003**, *63*, 214–220.
136. Fernandes, E.R.K.; Marangoni, C.; Souza, O.; Sellin, N. Thermochemical characterization of banana leaves as a potential energy source. *Energy Convers. Manag.* **2013**, *75*, 603–608. [CrossRef]
137. Mendoza Martinez, C.L.; Sermyagina, E.; Saari, J.; Silva de Jesus, M.; Cardoso, M.; Matheus de Almeida, G.; Vakkilainen, E. Hydrothermal carbonization of lignocellulosic agro-forest based biomass residues. *Biomass Bioenergy* **2021**, *147*, 106004. [CrossRef]
138. Van Swaaij, W.P.; Kersten, S.R.; Palz, W. *Biomass Power for the World*; CRC Press: Boca Raton, FL, USA, 2015.
139. Heinek, S.; Polanz, S.; Huber, M.B.; Hofmann, A.; Monthaler, G.; Fuchs, H.P.; Larch, C.; Giovannini, A. Biomass Conditioning Degradation Of Biomass During The Storage Of Woodchips. In Proceedings of the 21st European Biomass Conference and Exhibition, Copenhagen, Denmark, 3–7 June 2013.
140. Obernberger, I.; Brunner, T.; Bärnthaler, G. Chemical properties of solid biofuels—Significance and impact. *Biomass Bioenergy* **2006**, *30*, 973–982. [CrossRef]
141. Wzorek, M. Solar drying of granulated waste blends for dry biofuel production. *Environ. Sci. Pollut. Res.* **2021**, *28*, 34290–34299. [CrossRef] [PubMed]
142. Saravanan, A.; Senthil Kumar, P.; Jeevanantham, S.; Karishma, S.; Vo, D.V.N. Recent advances and sustainable development of biofuels production from lignocellulosic biomass. *Bioresour. Technol.* **2022**, *344*, 126203. [CrossRef] [PubMed]
143. Vedovatto, F.; Ugalde, G.; Bonatto, C.; Bazoti, S.F.; Treichel, H.; Mazutti, M.A.; Zabot, G.L.; Tres, M.V. Subcritical water hydrolysis of soybean residues for obtaining fermentable sugars. *J. Supercrit. Fluids* **2021**, *167*, 105043. [CrossRef]
144. Šelo, G.; Planinić, M.; Tišma, M.; Tomas, S.; Koceva Komlenić, D.; Bucić-Kojić, A. A Comprehensive Review on Valorization of Agro-Food Industrial Residues by Solid-State Fermentation. *Foods* **2021**, *10*, 927. [CrossRef]
145. Robles Barros, P.J.; Ramirez Ascheri, D.P.; Siqueira Santos, M.L.; Morais, C.C.; Ramirez Ascheri, J.L.; Signini, R.; dos Santos, D.M.; de Campos, A.J.; Alessandro Devilla, I. Soybean hulls: Optimization of the pulping and bleaching processes and carboxymethyl cellulose synthesis. *Int. J. Biol. Macromol.* **2020**, *144*, 208–218. [CrossRef]
146. Debiagi, F.; Faria-Tischer, P.C.S.; Mali, S. Nanofibrillated cellulose obtained from soybean hull using simple and eco-friendly processes based on reactive extrusion. *Cellul* **2019**, *27*, 1975–1988. [CrossRef]
147. Toro-Trochez, J.L.; Carrillo-Pedraza, E.S.; Bustos-Martínez, D.; García-Mateos, F.J.; Ruiz-Rosas, R.R.; Rodríguez-Mirasol, J.; Cordero, T. Thermogravimetric characterization and pyrolysis of soybean hulls. *Bioresour. Technol. Rep.* **2019**, *6*, 183–189. [CrossRef]
148. Osorio, L.L.D.R.; Flórez-López, E.; David Grande-Tovar, C.; Flórez-López, E.; Grande-Tovar, C.D.; Trombetta, D. The Potential of Selected Agri-Food Loss and Waste to Contribute to a Circular Economy: Applications in the Food, Cosmetic and Pharmaceutical Industries. *Molecules* **2021**, *26*, 515. [CrossRef]
149. da Silva Vilar, D.; Cruz, I.A.; Torres, N.H.; Figueiredo, R.T.; de Melo, L.; de Resende, I.T.F.; Eguiluz, K.I.B.; Bharagava, R.N.; Ferreira, L.F.R. Agro-industrial Wastes: Environmental Toxicology, Risks, and Biological Treatment Approaches. In *Microorganisms for Sustainability*; Bharagava, R., Ed.; Springer: Berlin/Heidelberg, Germany, 2019; pp. 1–23. [CrossRef]
150. Romaní, A.; Rocha, C.M.R.; Michelin, M.; Domingues, L.; Teixeira, J.A. Valorization of Lignocellulosic-Based Wastes. In *Current Developments in Biotechnology and Bioengineering: Resource Recovery from Wastes*; Elservier: Amsterdam, The Netherlands, 2020; pp. 383–410. [CrossRef]
151. Bledzki, A.K.; Mamun, A.A.; Volk, J. Physical, chemical and surface properties of wheat husk, rye husk and soft wood and their polypropylene composites. *Compos. Part A Appl. Sci. Manuf.* **2010**, *41*, 480–488. [CrossRef]
152. Sobhy, M.S.; Tammam, M.T. The influence of fiber length and concentration on the physical properties of wheat husk fibers rubber composites. *Int. J. Polym. Sci.* **2010**, *2010*, 528173. [CrossRef]
153. Terzioğlu, P.; Yücel, S.; Kuş, Ç. Review on a novel biosilica source for production of advanced silica-based materials: Wheat husk. *Asia-Pac. J. Chem. Eng.* **2019**, *14*, e2262. [CrossRef]
154. Ahmad, S.; Iqbal, Y.; Muhammad, R. Effects of coal and wheat husk additives on the physical, thermal and mechanical properties of clay bricks. *Boletín Soc Española Cerámica Vidr.* **2017**, *56*, 131–138. [CrossRef]
155. Wang, P.; Liu, C.; Chang, J.; Yin, Q.; Huang, W.; Liu, Y.; Dang, X.; Gao, T.; Lu, F. Effect of physicochemical pretreatments plus enzymatic hydrolysis on the composition and morphologic structure of corn straw. *Renew. Energy* **2019**, *138*, 502–508. [CrossRef]
156. Othman, S.H.; Najhah Tarmiti, N.A.; Shapi'i, R.A.; Mohd Zahiruddin, S.M.; Amin Tawakkal, I.S.M.; Basha, R.K. Starch/banana pseudostem biocomposite films for potential food packaging applications. *BioResources* **2020**, *15*, 3984–3998. [CrossRef]
157. Mohamad, N.A.N.; Jai, J. Response surface methodology for optimization of cellulose extraction from banana stem using NaOH-EDTA for pulp and papermaking. *Heliyon* **2022**, *8*, e09114. [CrossRef]

158. Alvarez, J.; Hooshdaran, B.; Cortazar, M.; Amutio, M.; Lopez, G.; Freire, F.B.; Haghshenasfard, M.; Hosseini, S.H.; Olazar, M. Valorization of citrus wastes by fast pyrolysis in a conical spouted bed reactor. *Fuel* **2018**, *224*, 111–120. [CrossRef]
159. Mantovan, J.; Yamashita, F.; Mali, S. Modification of Orange Bagasse with Reactive Extrusion to Obtain Cellulose-Based Materials. *Polysaccharides* **2022**, *3*, 401–410. [CrossRef]
160. Gonçalves, F.A.; Ruiz, H.A.; Nogueira, C.D.C.; dos Santos, E.S.; Teixeira, J.A.; De Macedo, G.R. Comparison of delignified coconuts waste and cactus for fuel-ethanol production by the simultaneous and semi-simultaneous saccharification and fermentation strategies. *Fuel* **2014**, *131*, 66–76. [CrossRef]
161. Azeta, O.; Ayeni, A.O.; Agboola, O.; Elehinafe, F.B. A review on the sustainable energy generation from the pyrolysis of coconut biomass. *Sci. Afr.* **2021**, *13*, e00909. [CrossRef]
162. Batista, G.; Souza, R.B.A.; Pratto, B.; dos Santos-Rocha, M.S.R.; Cruz, A.J.G. Effect of severity factor on the hydrothermal pretreatment of sugarcane straw. *Bioresour. Technol.* **2019**, *275*, 321–327. [CrossRef]
163. Halysh, V.; Sevastyanova, O.; de Carvalho, D.M.; Riazanova, A.V.; Lindström, M.E.; Gomelya, M. Effect of oxidative treatment on composition and properties of sorbents prepared from sugarcane residues. *Ind. Crop. Prod.* **2019**, *139*, 111566. [CrossRef]
164. Formann, S.; Hahn, A.; Janke, L.; Stinner, W.; Sträuber, H.; Logroño, W.; Nikolausz, M. Beyond Sugar and Ethanol Production: Value Generation Opportunities Through Sugarcane Residues. *Front. Energy Res.* **2020**, *8*, 267. [CrossRef]
165. Loaiza, J.M.; Palma, A.; Díaz, M.J.; Ruiz-Montoya, M.; García, M.T.; García, J.C. Effect of autohydrolysis on hemicellulose extraction and pyrolytic hydrogen production from Eucalyptus urograndis. *Biomass Convers. Biorefinery* **2020**, *12*, 4021–4030. [CrossRef]
166. da Silva Morais, A.P.; Sansígolo, C.A.; de Oliveira Neto, M. Effects of autohydrolysis of Eucalyptus urograndis and Eucalyptus grandis on influence of chemical components and crystallinity index. *Bioresour. Technol.* **2016**, *214*, 623–628. [CrossRef] [PubMed]
167. Negrão, D.R.; da Silva, T.A.Ô.F., Jr.; de Passos, J.R.S.; Sansígolo, C.A.; de Minhoni, M.T.A.; Furtado, E.L. Biodegradation of eucalyptus urograndis wood by fungi. *Int. Biodeterior. Biodegrad.* **2014**, *89*, 95–102. [CrossRef]
168. de Medeiros, L.C.D.; Pimenta, A.S.; Braga, R.M.; de Carnaval, T.K.A.; Neto, P.N.M.; de Melo, D.M.A. Effect of pyrolysis heating rate on the chemical composition of wood vinegar from Eucalyptus Urograndis and Mimosa Tenuiflora. *Rev. Árvore* **2019**, *43*, 1–11. [CrossRef]
169. Kandhola, G.; Djioleu, A.; Rajan, K.; Labbé, N.; Sakon, J.; Carrier, D.J.; Kim, J.W. Maximizing production of cellulose nanocrystals and nanofibers from pre-extracted loblolly pine kraft pulp: A response surface approach. *Bioresour. Bioprocess* **2020**, *7*, 19. [CrossRef]
170. Huang, F.; Ragauskas, A. Extraction of hemicellulose from loblolly pine woodchips and subsequent kraft pulping. *Ind. Eng. Chem. Res.* **2013**, *52*, 1743–1749. [CrossRef]
171. Lengowski, E.C.; De Muñiz, G.I.B.; Klock, U.; Nisgoski, S. Potential use of NIR and visible spectroscopy to analyze chemical properties of thermally treated wood. *Maderas Cienc Tecnol* **2018**, *20*, 627–640. [CrossRef]
172. de Morais, S.A.L.; do Nascimento, E.A.; de Melo, D.C. Chemical analysis of Pinus oocarpa wood part I: Quantification of macromolecular components and volatile extractives. *Rev. Árvore* **2005**, *29*, 461–470. [CrossRef]
173. Rajan, K.; Djioleu, A.; Kandhola, G.; Labbé, N.; Sakon, J.; Carrier, D.J.; Kim, J.W. Investigating the effects of hemicellulose pre-extraction on the production and characterization of loblolly pine nanocellulose. *Cellul* **2020**, *27*, 3693–3706. [CrossRef]
174. Febrero, L.; Granada, E.; Regueiro, A.; Míguez, J.L. Influence of Combustion Parameters on Fouling Composition after Wood Pellet Burning in a Lab-Scale Low-Power Boiler. *Energies* **2015**, *8*, 9794–9816. [CrossRef]
175. Pronobis, M. Evaluation of the influence of biomass co-combustion on boiler furnace slagging by means of fusibility correlations. *Biomass Bioenergy* **2005**, *28*, 375–383. [CrossRef]
176. Teixeira, P.; Lopes, H.; Gulyurtlu, I.; Lapa, N.; Abelha, P. Evaluation of slagging and fouling tendency during biomass co-firing with coal in a fluidized bed. *Biomass Bioenergy* **2012**, *39*, 192–203. [CrossRef]
177. Yin, H.B.; Yao, M. Analysis of the nonuniform slag film, mold friction, and the new cracking criterion for round billet continuous casting. *Metall. Mater. Trans. B* **2005**, *36*, 857–864. [CrossRef]
178. Zhou, C.; Liu, G.; Xu, Z.; Sun, H.; Lam, P.K.S. The retention mechanism, transformation behavior and environmental implication of trace element during co-combustion coal gangue with soybean stalk. *Fuel* **2017**, *189*, 32–38. [CrossRef]
179. Seckler, D.; Dea, C.M.; Rios, E.A.M.; de Godoi, M.; da Rampon, D.S.; D'Oca, M.G.M.; D'Oca, C.R.M. Rice straw ash extract/glycerol: An efficient sustainable approach for Knoevenagel condensation. *New. J. Chem.* **2022**, *46*, 4570–4578. [CrossRef]
180. Shen, X.; Zeng, J. Prediction of rice straw ash fusion behaviors and improving its ash fusion properties by layer manure addition. *J. Mater. Cycles Waste Manag.* **2020**, *22*, 965–974. [CrossRef]
181. Kwan, W.H.; Wong, Y.S. Acid leached rice husk ash (ARHA) in concrete: A review. *Mater. Sci. Energy Technol.* **2020**, *3*, 501–507. [CrossRef]
182. Vassilev, S.V.; Vassileva, C.G.; Song, Y.C.; Li, W.Y.; Feng, J. Ash contents and ash-forming elements of biomass and their significance for solid biofuel combustion. *Fuel* **2017**, *208*, 377–409. [CrossRef]
183. Wang, Y.; Tan, H.; Wang, X.; Du, W.; Mikulčić, H.; Duić, N. Study on extracting available salt from straw/woody biomass ashes and predicting its slagging/fouling tendency. *J. Clean. Prod.* **2017**, *155*, 164–171. [CrossRef]
184. Ma, Q.; Han, L.; Huang, G. Evaluation of different water-washing treatments effects on wheat straw combustion properties. *Bioresour. Technol.* **2017**, *245*, 1075–1083. [CrossRef]

185. Sharma, V.; Rathore, P.K.; Sharma, A. Soil Stabilization by Using Wheat Husk Ash. *J. Civ. Eng. Environ. Technol.* **2018**, *5*, 31–35.
186. Song, X.; Lin, Z.; Bie, R.; Wang, W. Effects of Additives Blended in Corn Straw to Control Agglomeration and Slagging in Combustion. *BioResources* **2019**, *14*, 8963–8972. [CrossRef]
187. Atahu, M.K.; Saathoff, F.; Gebissa, A. Strength and compressibility behaviors of expansive soil treated with coffee husk ash. *J. Rock. Mech. Geotech. Eng.* **2019**, *11*, 337–348. [CrossRef]
188. Kanning, R.C.; Portella, K.F.; Bragança, M.O.G.P.; Bonato, M.M.; Dos Santos, J.C.M. Banana leaves ashes as pozzolan for concrete and mortar of Portland cement. *Constr. Build. Mater.* **2014**, *54*, 460–465. [CrossRef]
189. Yathushan, V.; Puswewala, U.G.A. Effectiveness of Pozzolanic Leaf Ashes and Plastics on Geotechnical Characteristics. *Int. J. Eng. Technol. Innov.* **2022**, *12*, 155–166. [CrossRef]
190. Torres de Sande, V.; Sadique, M.; Pineda, P.; Bras, A.; Atherton, W.; Riley, M. Potential use of sugar cane bagasse ash as sand replacement for durable concrete. *J. Build. Eng.* **2021**, *39*, 102277. [CrossRef]
191. Rizvi, T.; Xing, P.; Pourkashanian, M.; Darvell, L.I.; Jones, J.M.; Nimmo, W. Prediction of biomass ash fusion behaviour by the use of detailed characterisation methods coupled with thermodynamic analysis. *Fuel* **2015**, *141*, 275–284. [CrossRef]
192. Birley, R.I.; Jones, J.M.; Darvell, L.I.; Williams, A.; Waldron, D.J.; Levendis, Y.A.; Rokni, E.; Panahi, A. Fuel flexible power stations: Utilisation of ash co-products as additives for NOx emissions control. *Fuel* **2019**, *251*, 800–807. [CrossRef]
193. Bridgwater, A.V. Review of fast pyrolysis of biomass and product upgrading. *Biomass Bioenergy* **2012**, *38*, 68–94. [CrossRef]
194. Bohn, L.R.; Dresch, A.P.; Cavali, M.; Vargas, A.C.G.; Führ, J.F.; Tironi, S.P.; Fogolari, O.; Mibielli, G.M.; Alves Jr, S.L.; Bender, J.P. Alkaline pretreatment and enzymatic hydrolysis of corn stover for bioethanol production. *Res. Soc. Dev.* **2021**, *10*, e149101118914. [CrossRef]
195. Chen, H.; Wang, L. *Technologies for Biochemical Conversion of Biomass*; Elsevier Inc.: Amsterdam, The Netherlands, 2017.
196. Nanda, S.; Kozinski, J.A.; Dalai, A.K. Lignocellulosic Biomass: A Review of Conversion Technologies and Fuel Products. *Curr. Biochem. Eng.* **2016**, *3*, 24–36. [CrossRef]
197. McKendry, P. Energy production from biomass (part 2): Conversion technologies. *Bioresour. Technol.* **2002**, *83*, 47–54. [CrossRef]
198. Adams, P.; Bridgwater, T.; Lea-Langton, A.; Ross, A.; Watson, I. *Biomass Conversion Technologies. Greenh Gas. Balanc. Bioenergy Syst.*, 1st ed.; Elservier: London, UK, 2018; pp. 107–139. [CrossRef]
199. Soares, J.F.; Confortin, T.C.; Todero, I.; Luft, L.; Ugalde, G.A.; Tovar, L.P.; Mayer, F.D.; Mazutti, M.A. Estimation of Bioethanol, Biohydrogen, and Chemicals Production from Biomass Wastes in Brazil. *Clean—Soil Air Water* **2022**, *50*, 2200155. [CrossRef]
200. Kim, S. Evaluation of Alkali-Pretreated Soybean Straw for Lignocellulosic Bioethanol Production. *Int. J. Polym. Sci.* **2018**, *2018*, 5241748. [CrossRef]
201. Govumoni, S.P.; Koti, S.; Kothagouni, S.Y.; Venkateshwar, S.; Linga, V.R. Evaluation of pretreatment methods for enzymatic saccharification of wheat straw for bioethanol production. *Carbohydr. Polym.* **2013**, *91*, 646–650. [CrossRef]
202. Rabeya, T.; Jehadin, F.; Asad, M.A.; Ayodele, O.O.; Adekunle, A.E.; Islam, M.S. Alkali Intensified Heat Treat. *Corn Stalk Bioethanol Production. Sugar Tech.* **2020**, *23*, 643–650. [CrossRef]
203. Gouvea, B.M.; Torres, C.; Franca, A.S.; Oliveira, L.S.; Oliveira, E.S. Feasibility of ethanol production from coffee husks. *Biotechnol. Lett.* **2009**, *31*, 1315–1319. [CrossRef]
204. Menezes, E.G.T.; do Carmo, J.R.; Alves, J.G.L.F.; Menezes, A.G.T.; Guimarães, I.C.; Queiroz, F.; Pimenta, C.J. Optimization of alkaline pretreatment of coffee pulp for production of bioethanol. *Biotechnol. Prog.* **2014**, *30*, 451–462. [CrossRef] [PubMed]
205. Suhag, M.; Kumar, A.; Singh, J. Saccharification and fermentation of pretreated banana leaf waste for ethanol production. *SN Appl. Sci.* **2020**, *2*, 1448. [CrossRef]
206. Uchôa, P.Z.; Porto, R.C.T.; Battisti, R.; Marangoni, C.; Sellin, N.; Souza, O. Ethanol from residual biomass of banana harvest and commercialization: A three-waste simultaneous fermentation approach and a logistic-economic assessment of the process scaling-up towards a sustainable biorefinery in Brazil. *Ind. Crop. Prod.* **2021**, *174*, 114170. [CrossRef]
207. Nogueira, D.P.; Ferreira-Rosa, P.R.; Seolatto, A.A.; Galeano-Suarez, C.A.; Ferreira-Freitas, F. Sacarificación de bagazo de naranja pretratado con hidroxido de calcio usando un cóctel enzimático y acido diluido. *Rev. ION* **2019**, *32*, 75–85. [CrossRef]
208. Saadatinavaz, F.; Karimi, K.; Denayer, J.F.M. Hydrothermal pretreatment: An efficient process for improvement of biobutanol, biohydrogen, and biogas production from orange waste via a biorefinery approach. *Bioresour. Technol.* **2021**, *341*, 125834. [CrossRef] [PubMed]
209. Cabral, M.M.S.; de Abud, A.K.S.; de Silva, C.E.F.; Almeida, R.M.R.G. Bioethanol production from coconut husk fiber. *Ciência Rural* **2016**, *46*, 1872–1877. [CrossRef]
210. Bronzato, G.R.F.; dos Reis, V.A.C.A.; Borro, J.A.; Leão, A.L.; Cesarino, I. Second generation ethanol made from coir husk under the biomass Cascade approach. *Mol. Cryst. Liq. Cryst.* **2020**, *693*, 107–114. [CrossRef]
211. de Carvalho Silvello, M.A.; Martínez, J.; Goldbeck, R. Increase of reducing sugars release by enzymatic hydrolysis of sugarcane bagasse intensified by ultrasonic treatment. *Biomass Bioenergy* **2019**, *122*, 481–489. [CrossRef]
212. Perez, C.L.; Pereira, L.P.R.d.C.; Milessi, T.S.; Sandri, J.P.; Demeke, M.; Foulquié-Moreno, M.R.; Thevelein, J.M.; Zangirolami, T.C. Towards a practical industrial 2G ethanol production process based on immobilized recombinant S. cerevisiae: Medium and strain selection for robust integrated fixed-bed reactor operation. *Renew. Energy* **2022**, *185*, 363–375. [CrossRef]

213. Rochón, E.; Cabrera, M.N.; Scutari, V.; Cagno, M.; Guibaud, A.; Martínez, S.; Böthig, S.; Guchin, N.; Ferrari, M.D.; Lareo, C. Co-production of bioethanol and xylosaccharides from steam-exploded eucalyptus sawdust using high solid loads in enzymatic hydrolysis: Effect of alkaline impregnation. *Ind. Crop. Prod.* **2022**, *175*, 114253. [CrossRef]
214. Oliveira, R.J.; Santos, B.; Mota, M.J.; Pereira, S.R.; Branco, P.C.; Pinto, P.C.R. The impact of acid hydrolysis conditions on carbohydrate determination in lignocellulosic materials: A case study with Eucalyptus globulus bark. *Holzforschung* **2021**, *75*, 957–967. [CrossRef]
215. Farías-Sánchez, J.C.; Velázquez-Valadez, U.; Pineda-Pimentel, M.G.; López-Miranda, J.; Castro-Montoya, A.J.; Carrillo-Parra, A.; Vargas-Santillán, A.; Rutiaga-Quiñones, J.G. Simultaneous saccharification and fermentation of pine sawdust (Pinus pseudostrobus L.) pretreated with nitric acid and sodium hydroxide for bioethanol production. *BioResources* **2017**, *12*, 1052–1063. [CrossRef]
216. Carrillo-Varela, I.; Vidal, C.; Vidaurre, S.; Parra, C.; Machuca, A.; Briones, R.; Mendonça, R.T. Alkalization of Kraft Pulps from Pine and Eucalyptus and Its Effect on Enzymatic Saccharification and Viscosity Control of Cellulose. *Polymers* **2022**, *14*, 3127. [CrossRef] [PubMed]
217. Vedovatto, F.; Bonatto, C.; Bazoti, S.F.; Venturin, B.; Alves, S.L.; Kunz, A.; Steinmetz, R.L.R.; Treichel, H.; Mazutti, M.A.; Zabot, G.L.; et al. Production of biofuels from soybean straw and hull hydrolysates obtained by subcritical water hydrolysis. *Bioresour. Technol.* **2021**, *328*, 124837. [CrossRef]
218. Rodrigues, B.C.G.; De Mello, B.S.; Gonsales Da Costa Araujo, M.L.; Ribeiro Da Silva, G.H.; Sarti, A. Soybean molasses as feedstock for sustainable generation of biomethane using high-rate anaerobic reactor. *J. Environ. Chem. Eng.* **2021**, *9*, 105226. [CrossRef]
219. Nadaleti, W.C. Utilization of residues from rice parboiling industries in southern Brazil for biogas and hydrogen-syngas generation: Heat, electricity and energy planning. *Renew. Energy* **2019**, *131*, 55–72. [CrossRef]
220. Leite, S.A.F.; Leite, B.S.; Ferreira, D.J.O.; Baêta, B.E.L.; Dangelo, J.V.H. The effects of agitation in anaerobic biodigesters operating with substrates from swine manure and rice husk. *Chem. Eng. J.* **2023**, *451*, 138533. [CrossRef]
221. Simioni, T.; Agustini, C.B.; Dettmer, A.; Gutterres, M. Enhancement of biogas production by anaerobic co-digestion of leather waste with raw and pretreated wheat straw. *Energy* **2022**, *253*, 124051. [CrossRef]
222. Albornoz, S.; Wyman, V.; Palma, C.; Carvajal, A. Understanding of the contribution of the fungal treatment conditions in a wheat straw biorefinery that produces enzymes and biogas. *Biochem. Eng. J.* **2018**, *140*, 140–147. [CrossRef]
223. Vaz, A.; Mattos, A.P.; Nascimento, A.; Ana, V.; Mattos, P. Energy and carbon credits generation from the production of biogas from the ethanol stillage of corn and sugar cane. In Proceedings of the 18th Brazilian Congress of Thermal Science and Engineering, Online Event, Brazil, 8–10 December 2020.
224. Venturin, B.; Frumi Camargo, A.; Scapini, T.; Mulinari, J.; Bonatto, C.; Bazoti, S.; Pereira-Siqueira, D.; Maria-Colla, L.; Alves, S.L.; Paulo-Bender, J.; et al. Effect of pretreatments on corn stalk chemical properties for biogas production purposes. *Bioresour. Technol.* **2018**, *266*, 116–124. [CrossRef]
225. dos Santos, L.C.; Adarme, O.F.H.; Baêta, B.E.L.; Gurgel, L.V.A.; de Aquino, S.F. Production of biogas (methane and hydrogen) from anaerobic digestion of hemicellulosic hydrolysate generated in the oxidative pretreatment of coffee husks. *Bioresour. Technol.* **2018**, *263*, 601–612. [CrossRef] [PubMed]
226. Da Pin, B.V.R.; Barros, R.M.; Silva Lora, E.E.; Almazan del Olmo, O.; Silva dos Santos, I.F.; Ribeiro, E.M.; Victor de Freitas Rocha, J. Energetic use of biogas from the anaerobic digestion of coffee wastewater in southern Minas Gerais, Brazil. *Renew. Energy* **2020**, *146*, 2084–2094. [CrossRef]
227. Benish, P.M.R.; Mozhiarasi, V.; Nagabalaji, V.; Weichgrebe, D.; Srinivasan, S.V. Optimization of process parameters for enhanced methane production from banana peduncle by thermal pretreatment. *Biomass Convers. Biorefinery* **2022**, *12*, 1–15. [CrossRef]
228. Oyaro, D.K.; Oonge, Z.I.; Odira, P.M. Anaerobic Digestion of Banana Wastes for Biogas Production. *J. Civ. Environ. Eng.* **2020**, *10*, 3. [CrossRef]
229. Jiménez-Castro, M.P.; Buller, L.S.; Zoffreo, A.; Timko, M.T.; Forster-Carneiro, T. Two-stage anaerobic digestion of orange peel without pre-treatment: Experimental evaluation and application to São Paulo state. *J. Environ. Chem. Eng.* **2020**, *8*, 104035. [CrossRef]
230. Echeverri, A.; Forero-Rojas, L.F.; Durán-Aranguren, D.; Carazzone, C.; Sierra, R. A Biorefinery for the Valorization of Orange Residues. In Proceedings of the 29th, European Biomass Conference and Exhibition, Online Event, 26–29 April 2021.
231. Ndubuisi-Nnaji, U.U.; Ofon, U.A.; Offiong, N.A.O. Anaerobic co-digestion of spent coconut copra with cow urine for enhanced biogas production. *Waste Manag. Res.* **2020**, *39*, 594–600. [CrossRef]
232. Cheng, J.R.; Liu, X.M.; Chen, Z.Y.; Zhang, Y.S.; Zhang, Y.H. A Novel Mesophilic Anaerobic Digestion System for Biogas Production and In Situ Methane Enrichment from Coconut Shell Pyroligneous. *Appl. Biochem. Biotechnol.* **2016**, *178*, 1303–1314. [CrossRef]
233. Soares, L.A.; Solano, M.G.; Lindeboom, R.E.F.; van Lier, J.B.; Silva, E.L.; Varesche, M.B.A. Valorization of sugarcane bagasse through biofuel and value-added soluble metabolites production: Optimization of alkaline hydrothermal pretreatment. *Biomass Bioenergy* **2022**, *165*, 106564. [CrossRef]
234. Silva Rabelo, C.A.B.; Camargo, F.P.; Sakamoto, I.K.; Varesche, M.B.A. Metataxonomic characterization of an autochthonous and allochthonous microbial consortium involved in a two-stage anaerobic batch reactor applied to hydrogen and methane production from sugarcane bagasse. *Enzym. Microb. Technol.* **2023**, *162*, 110119. [CrossRef]
235. Poveda-Giraldo, J.A.; Cardona Alzate, C.A. Biorefinery potential of eucalyptus grandis to produce phenolic compounds and biogas. *Can. J. Res.* **2021**, *51*, 89–100. [CrossRef]

236. Eftaxias, A.; Passa, E.A.; Michailidis, C.; Daoutis, C.; Kantartzis, A.; Diamantis, V. Residual Forest Biomass in Pinus Stands: Accumulation and Biogas Production Potential. *Energies* **2022**, *15*, 5233. [CrossRef]
237. Ali, S.S.; Abomohra, A.E.F.; Sun, J. Effective bio-pretreatment of sawdust waste with a novel microbial consortium for enhanced biomethanation. *Bioresour. Technol.* **2017**, *238*, 425–432. [CrossRef]
238. Armesto, L.; Bahillo, A.; Veijonen, K.; Cabanillas, A.; Otero, J. Combustion behaviour of rice husk in a bubbling fluidised bed. *Biomass Bioenergy* **2002**, *23*, 171–179. [CrossRef]
239. Pottmaier, D.; Melo, C.R.; Sartor, M.N.; Kuester, S.; Amadio, T.M.; Fernandes, C.A.H.; Marinha, D.; Alarcon, O.E. The Brazilian energy matrix: From a materials science and engineering perspective. *Renew. Sustain. Energy Rev.* **2013**, *19*, 678–691. [CrossRef]
240. Saenger, M.; Hartge, E.U.; Werther, J.; Ogada, T.; Siagi, Z. Combustion of coffee husks. *Renew. Energy* **2001**, *23*, 103–121. [CrossRef]
241. de Oliveira Maia, B.G.; de Oliveira, A.P.N.; de Oliveira, T.M.N.; Marangoni, C.; Souza, O.; Sellin, N. Characterization and production of banana crop and rice processing waste briquettes. *Environ. Prog. Sustain. Energy* **2018**, *37*, 1266–1273. [CrossRef]
242. De Oliveira Maia, B.G.; Souza, O.; Marangoni, C.; Hotza, D.; De Oliveira, A.P.N.; Sellin, N. Production and Characterization of Fuel Briquettes from Banana Leaves Waste. *Chem. Eng. Trans.* **2014**, *37*, 439–444. [CrossRef]
243. Vamvuka, D.; Trikouvertis, M.; Pentari, D.; Alevizos, G. Evaluation of ashes produced from fluidized bed combustion of residues from oranges' plantations and processing. *Renew. Energy* **2014**, *72*, 336–343. [CrossRef]
244. Osman, A.I. Mass spectrometry study of lignocellulosic biomass combustion and pyrolysis with NOx removal. *Renew. Energy* **2020**, *146*, 484–496. [CrossRef]
245. Obeng, G.Y.; Amoah, D.Y.; Opoku, R.; Sekyere, C.K.K.; Adjei, E.A.; Mensah, E. Coconut Wastes as Bioresource for Sustainable Energy: Quantifying Wastes, Calorific Values and Emissions in Ghana. *Energies* **2020**, *13*, 2178. [CrossRef]
246. Abelha, P.; Leiser, S.; Pels, J.R.; Cieplik, M.K. Combustion properties of upgraded alternative biomasses by washing and steam explosion for complete coal replacement in coal-designed power plant applications. *Energy* **2022**, *248*, 123546. [CrossRef]
247. Centeno-González, F.O.; Silva Lora, E.E.; Villa Nova, H.F.; Mendes Neto, L.J.; Martínez Reyes, A.M.; Ratner, A.; Ghamari, M. CFD modeling of combustion of sugarcane bagasse in an industrial boiler. *Fuel* **2017**, *193*, 31–38. [CrossRef]
248. Aziz, I.; Bin Babar, Z.; Haider, R.; Saleem, M.; Munir, S.; Sattar, H. A comparative study of thermal and combustion kinetics for raw and bio-chars of eucalyptus wood and bark. *Energy Sources Part A Recovery Util. Environ. Eff.* **2022**, *44*, 3313–3329. [CrossRef]
249. Guerrero, F.; Yáñez, K.; Vidal, V.; Cereceda-Balic, F. Effects of wood moisture on emission factors for PM2.5, particle numbers and particulate-phase PAHs from Eucalyptus globulus combustion using a controlled combustion chamber for emissions. *Sci. Total Environ.* **2019**, *648*, 737–744. [CrossRef]
250. Xu, X.; Pan, R.; Chen, R. Combustion Characteristics, Kinetics, and Thermodynamics of Pine Wood Through Thermogravimetric Analysis. *Appl. Biochem. Biotechnol.* **2021**, *193*, 1427–1446. [CrossRef]
251. Singh, D.; Tassew, D.D.; Nelson, J.; Chalbot, M.C.G.; Kavouras, I.G.; Demokritou, P.; Tesfaigzi, Y. Development of an Integrated Platform to Assess the Physicochemical and Toxicological Properties of Wood Combustion Particulate Matter. *Chem. Res. Toxicol.* **2022**, *35*, 1541–1557. [CrossRef]
252. Motta, I.L.; Marchesan, A.N.; Maciel Filho, R.; Wolf Maciel, M.R. Correlating biomass properties, gasification performance, and syngas applications of Brazilian feedstocks via simulation and multivariate analysis. *Ind. Crop. Prod.* **2022**, *181*, 114808. [CrossRef]
253. Susastriawan, A.A.P.; Saptoadi, H.; Purnomo. Comparison of the gasification performance in the downdraft fixed-bed gasifier fed by different feedstocks: Rice husk, sawdust, and their mixture. *Sustain. Energy Technol. Assess.* **2019**, *34*, 27–34. [CrossRef]
254. Ismail, T.M.; Abd El-Salam, M.; Monteiro, E.; Rouboa, A. Eulerian—Eulerian CFD model on fluidized bed gasifier using coffee husks as fuel. *Appl Therm. Eng* **2016**, *106*, 1391–1402. [CrossRef]
255. Tacuri, D.; Andrade, C.; Álvarez, P.; Abril-González, M.; Pinos-Vélez, V.; Jara, L.; Montero-Izquierdo, A.; Zalamea, S. Design and Development of a Catalytic Fixed-Bed Reactor for Gasification of Banana Biomass in Hydrogen Production. *Catalysts* **2022**, *12*, 395. [CrossRef]
256. Aluri, S.; Syed, A.; Flick, D.W.; Muzzy, J.D.; Sievers, C.; Agrawal, P.K. Pyrolysis and gasification studies of model refuse derived fuel (RDF) using thermogravimetric analysis. *Fuel Process Technol.* **2018**, *179*, 154–166. [CrossRef]
257. Prestipino, M.; Chiodo, V.; Maisano, S.; Zafarana, G.; Urbani, F.; Galvagno, A. Hydrogen rich syngas production by air-steam gasification of citrus peel residues from citrus juice manufacturing: Experimental and simulation activities. *Int. J. Hydrog. Energy* **2017**, *42*, 26816–26827. [CrossRef]
258. Arun, K.; Venkata Ramanan, M.; Mohanasutan, S. Comparative studies and analysis on gasification of coconut shells and corn cobs in a perforated fixed bed downdraft reactor by admitting air through equally spaced conduits. *Biomass Convers. Biorefinery* **2022**, *12*, 1257–1269. [CrossRef]
259. Ram, M.; Mondal, M.K. Conversion of unripe coconut husk into refined products using humidified air in packed bed gasification column. *Biomass Convers. Biorefinery* **2020**, *10*, 409–421. [CrossRef]
260. Shukla, A.; Sudhir, D.; Kumar, Y. A Comparative study of Sugarcane Bagasse gasification and Direct Combustion. *Int. J. Appl. Eng. Res.* **2017**, *12*, 14739–14745.
261. Parsa, S.; Jafarmadar, S.; Neshat, E.; Javani, N. Thermodynamic analysis of a novel biomass-driven trigeneration system using different biomass resources. *Biomass Convers. Biorefinery* **2022**, *12*, 1–17. [CrossRef]
262. Parrillo, F.; Ardolino, F.; Calì, G.; Marotto, D.; Pettinau, A.; Arena, U. Fluidized bed gasification of eucalyptus chips: Axial profiles of syngas composition in a pilot scale reactor. *Energy* **2021**, *219*, 119604. [CrossRef]

263. Huang, F.; Jin, S. Investigation of biomass (pine wood) gasification: Experiments and Aspen Plus simulation. *Energy Sci. Eng.* **2019**, *7*, 1178–1187. [CrossRef]
264. Soares, J.; Oliveira, A.C. Experimental assessment of pine wood chips gasification at steady and part-load performance. *Biomass Bioenergy* **2020**, *139*, 105625. [CrossRef]
265. Oliveira, T.J.P.; Cardoso, C.R.; Ataíde, C.H. Fast pyrolysis of soybean hulls: Analysis of bio-oil produced in a fluidized bed reactor and of vapor obtained in analytical pyrolysis. *J. Therm. Anal. Calorim.* **2015**, *120*, 427–438. [CrossRef]
266. Boateng, A.A.; Mullen, C.A.; Goldberg, N.M.; Hicks, K.B.; Devine, T.E.; Lima, I.M.; McMurtrey, J.E. Sustainable production of bioenergy and biochar from the straw of high-biomass soybean lines via fast pyrolysis. *Environ. Prog. Sustain. Energy* **2010**, *29*, 175–183. [CrossRef]
267. Raymundo, L.M.; Espindola, J.S.; Borges, F.C.; Lazzari, E.; Trierweiler, J.O.; Trierweiler, L.F. Continuous fast pyrolysis of rice husk in a fluidized bed reactor with high feed rates. *Chem. Eng. Commun.* **2020**, *208*, 1553–1563. [CrossRef]
268. Pittman, C.U.; Mohan, D.; Eseyin, A.; Li, Q.; Ingram, L.; Hassan, E.B.M.; Mitchell, B.; Guo, H.; Steele, P.H. Characterization of Bio-oils Produced from Fast Pyrolysis of Corn Stalks in an Auger Reactor. *Energy Fuels* **2012**, *26*, 3816–3825. [CrossRef]
269. da Silva, J.P. *Caracterização da Casca de Café (coffea arábica L.) in Natura, e de seus Produtos Obtidos pelo Processo de Pirólise em Reator Mecanicamente Agitado*; Universidade Estadual de Campinas: Campinas, SP, Brazil, 2012.
270. Singh, R.K.; Patil, T.; Pandey, D.; Tekade, S.P.; Sawarkar, A.N. Co-pyrolysis of petroleum coke and banana leaves biomass: Kinetics, reaction mechanism, and thermodynamic analysis. *J. Environ. Manag.* **2022**, *301*, 113854. [CrossRef] [PubMed]
271. Sellin, N.; Krohl, D.R.; Marangoni, C.; Souza, O. Oxidative fast pyrolysis of banana leaves in fluidized bed reactor. *Renew. Energy* **2016**, *96*, 56–64. [CrossRef]
272. Wei, X.; Xue, X.; Wu, L.; Yu, H.; Liang, J.; Sun, Y. High-grade bio-oil produced from coconut shell: A comparative study of microwave reactor and core-shell catalyst. *Energy* **2020**, *212*, 118692. [CrossRef]
273. Babatabar, M.A.; Yousefian, F.; Mousavi, M.V.; Hosseini, M.; Tavasoli, A. Pyrolysis of lignocellulosic and algal biomasses in a fixed-bed reactor: A comparative study on the composition and application potential of bioproducts. *Int. J. Energy Res.* **2022**, *46*, 9836–9850. [CrossRef]
274. Fardhyanti, D.S.; Megawati, C.A.; Prasetiawan, H.; Raharjo, P.T.; Habibah, U.; Abasaeed, A.E. Production of bio-oil from sugarcane bagasse by fast pyrolysis and removal of phenolic compounds. *Biomass Convers. Biorefinery* **2022**, *12*, 1–11. [CrossRef]
275. Varma, A.K.; Mondal, P. Pyrolysis of sugarcane bagasse in semi batch reactor: Effects of process parameters on product yields and characterization of products. *Ind. Crop. Prod.* **2017**, *95*, 704–717. [CrossRef]
276. Li, M.; Yu, Z.; Bin, Y.; Huang, Z.; He, H.; Liao, Y.; Zheng, A.; Ma, X. Microwave-assisted pyrolysis of eucalyptus wood with MoO3 and different nitrogen sources for coproducing nitrogen-rich bio-oil and char. *J. Anal. Appl. Pyrolysis* **2022**, *167*, 105666. [CrossRef]
277. Matos, M.; Mattos, B.D.; de Cademartori, P.H.G.; Lourençon, T.V.; Hansel, F.A.; Zanoni, P.R.S.; Yamamoto, C.I.; Magalhães, W.L.E. Pilot-Scaled Fast-Pyrolysis Conversion of Eucalyptus Wood Fines into Products: Discussion Toward Possible Applications in Biofuels, Materials, and Precursors. *Bioenergy Res.* **2020**, *13*, 411–422. [CrossRef]
278. Xu, B.; Argyle, M.D.; Shi, X.; Goroncy, A.K.; Rony, A.H.; Tan, G.; Fan, M. Effects of mixture of CO2 /CH4 as pyrolysis atmosphere on pine wood pyrolysis products. *Renew. Energy* **2020**, *162*, 1243–1254. [CrossRef]
279. Torr, K.M.; De Miguel Mercader, F.; Murton, K.D.; Harbers, T.J.M.; Cooke-Willis, M.H.; Van De Pas, D.J.; Suckling, I.D. Fast Pyrolysis of Pine Wood Pretreated by Large Pilot-Scale Thermomechanical Refining for Biochemical Production. *Ind. Eng. Chem. Res.* **2020**, *59*, 21294–21304. [CrossRef]
280. EPA Center for Corporate Climate Leadership. Greenhouse Gas Inventory Guidance: Direct Emissions from Stationary Combustion Sources, December 2020. Available online: https://www.epa.gov/sites/default/files/2020-12/documents/stationaryemissions.pdf/ (accessed on 2 April 2023).
281. Metz, B.; Davidson, O.R.; Bosch, P.R.; Dave, R.; Meyer, L.A. Contribution of working group III to the fourth assessment report of the intergovernmental panel on climate change. *IPCC Fourth Assess Rep.* **2007**. Available online: https://archive.ipcc.ch/publications_and_data/publications_ipcc_fourth_assessment_report_wg3_report_mitigation_of_climate_change.htm/ (accessed on 3 April 2023).
282. Zhu, J.Y.; Zhuang, X.S. Conceptual net energy output for biofuel production from lignocellulosic biomass through biorefining. *Prog. Energy Combust. Sci.* **2012**, *38*, 583–598. [CrossRef]
283. Hudiburg, T.W.; Wang, W.; Khanna, M.; Long, S.P.; Dwivedi, P.; Parton, W.J.; Hartman, M.; Delucia, E.H. Impacts of a 32-billion-gallon bioenergy landscape on land and fossil fuel use in the US. *Nat. Energy* **2016**, *1*, 15005. [CrossRef]
284. Rana, R.; Ingrao, C.; Lombardi, M.; Tricase, C. Greenhouse gas emissions of an agro-biogas energy system: Estimation under the Renewable Energy Directive. *Sci. Total Environ.* **2016**, *550*, 1182–1195. [CrossRef]
285. IPEA. *Diagnóstico dos Resíduos Orgânicos do Setor Agrossilvopastoril e Agroindústrias Associadas*; IPEA: Brasilia, Brazil, 2012. Available online: https://repositorio.ipea.gov.br/bitstream/11058/7687/1/RP_Diagn%C3%B3stico_2012.pdf (accessed on 24 April 2023).
286. Board CIA. *Power Generation from Coal: Measuring and Reporting Efficiency Performance and CO2 Emissions*; CIAB International Energy Agency; Rep OECD/IEA2010 2010:1–114; Board CIA: Paris, France, 2010.
287. FAO. *Food and Agricultural Commodities Production. Countries by Commodity, Sugarcane*; FAO: Rome, Italy, 2018.
288. Basu, P.; Butler, J.; Leon, M.A. Biomass co-firing options on the emission reduction and electricity generation costs in coal-fired power plants. *Renew. Energy* **2011**, *36*, 282–288. [CrossRef]

289. World Nuclear Association. *Heat Values of Various Fuels*; World Nuclear Association: London, UK, 2018.
290. Kersten, S.; Garcia-Perez, M. Recent developments in fast pyrolysis of ligno-cellulosic materials. *Curr. Opin. Biotechnol.* **2013**, *24*, 414–420. [CrossRef]
291. Mesa-Pérez, J.M.; Rocha, J.D.; Barbosa-Cortez, L.A.; Penedo-Medina, M.; Luengo, C.A.; Cascarosa, E. Fast oxidative pyrolysis of sugar cane straw in a fluidized bed reactor. *Appl. Therm. Eng* **2013**, *56*, 167–175. [CrossRef]